Development of a Novel Rheometric Device for the Determination of Pressure Dependent Viscosity of non-Newtonian Fluids

by

Salma Akhter, B.Sc. Eng.

M.Eng. 2000

Development of a Novel Rheometric Device for the Determination of Pressure Dependent Viscosity of non-Newtonian Fluids

by

Salma Akhter, B.Sc. Eng.

This thesis is submitted to Dublin City University as the fulfilment of the requirement for the award of the degree of

Master of Engineering

Supervisor: Professor M.S.J. Hashmi, Ph.D, D.Sc.

School of Mechanical and Manufacturing Engineering
Dublin City University

February, 2000

DECLARATION

I hereby certify that this material, which I now submit for assessment on the programme of study leading to the award of *Master of Engineering*, is entirely my own work and has not been taken from the work of others save and to the extent that such work has been cited and acknowledged within the text of my work

Singed S Akhter ID No 96971509

Salma Akhter

Date February 2000

Dedication

This thesis is dedicated to my parents who took all the troubles in the world with smile for the advancement of their children's knowledge and to my husband and daughter

Acknowledgements

I would like to express my sincere thanks and gratitude to Prof M S J Hashmi my supervisor and Head of School of Mechanical and Manufacturing Engineering of Dublin City University for his kind supervision, guidance, encouragement and advice throughout the course of this work The author would like to thank Professor Hashmi for offering the opportunity to do research work at the School of Mechanical and Manufacturing Engineering School, Dublin City University

Special thanks to Mr Liam Domican and Mr Michael Tyrell for their technical assistance at various stages of this work I would also like to thank all the technicians of the workshop of the School of Mechanical and Manufacturing Engineering for their help and co-operation during the manufacturing of the rig

I would also like to thank Michelle Considine for her co-operation in relation to various correspondence, and documentation during the work

The author would also like to thank her brothers and sister for encouraging her during this work

The author also acknowledges her parents who always cared and encouraged her from the childhood to advance her knowledge Also the author acknowledges her father-in-law for his encouragement

The author is grateful for the many sacrifices made by her husband and daughter so that this work might be completed

Finally, all praise to God almighty for enabling me to complete this work

Salma Akhter

Notation

p_1	Pressure gradient in the first section of the unit
p_2	Pressure gradient in the second part of the unit
τ_1	Shear stress in the fluid in the first part of unit
τ_2	Shear stress in the fluid in the second part of unit
K	Non-Newtonian factor
τc_1	Shear stress on the shaft in the first section of the unit
τc_2	Shear stress on the shaft in the second section of the unit
τca	Critical shear stress
μ_0	Initial viscosity of polymer melt
a	Viscosity constant
b	Pressure coefficient of viscosity
V	Velocity of the shaft
Q_1	Flow of fluid in the first section of the unit
Q_2	Flow of fluid in the second section of the unit
U_1	Velocity of polymer in the first section of the unit
U_1	Velocity of polymer in the second section of the unit
P_m	Maximum pressure in the step
h_1	Radial gap in the first section of the unit
h_2	Radial gap in the second section of the unit
L_1	Length of the first section of the unit
L_1	Length of the second section of the unit

Development of a Novel Rheometric Device for the Determination of Pressure Dependent Viscosity of non-Newtonian Fluids

Salma Akhter, BSc Eng

ABSTRACT

A new type of Rheometer has been designed based on hydrodynamic principles Hydrodynamic pressure technique is a relatively new and innovative technique for rheological studies of viscous non-Newtonian fluids These principles have been extensively used for the last ten years for drawing and coating of strips and wires The Rheometric Device consists of a rotating inner cylinder (shaft) in a fixed hollow outer cylinder The complex geometry gap between the two cylinders is filled with a viscous non-Newtonian fluid When the surface of the shaft is rotating inside the hollow cylinder filled with a viscous fluid, shearing takes place and hydrodynamic pressure develops the magnitude of which is dependent on the shape of the surfaces, the viscosity of the fluid as well as the shear rate i e the speed with which the inner solid cylinder is rotated The Rheometer has been developed to determine the Rheological properties of viscous fluid at pressures of up to 100 bar and a shear rate range of 500 to 4000 sec ^{1}

Experimental procedure and methods have been outlined and a number of experiments have been carried out to determine the effects of pressure and shear rate on viscosity Included in the work are measurements of the pressure with variation of the shearing speed and inserts Three different non-Newtonian fluids, glycerine, and silicon with two different viscosities were used as the pressure medium The experimental works were undertaken with glycerine keeping temperature at $18 \pm 1^{\circ}$ C and silicon at $25 \pm 1^{\circ}$ C for shearing speeds of between 0 25 m/sec-2 0 m/sec In the present study, theoretical models have been developed based on the non-Newtonian characteristics and a shear rate viscosity relationship was determined using the rheometer at different pressures by comparing the calculated theoretical pressure distribution with the experimental results

Additional experimental work has been carried out using a Brookfield viscometer to determine the effect of shear rate on viscosity at lower shear rates The Newtonian or non-Newtonian, characteristics of glycerine, silicon was investigated by using this viscometer Using the theoretical model the viscosity of the fluid was determined at lower shear rates at atmospheric pressure Results from the new Rheometric Device and the Brookfield viscometer have been presented graphically and new type of equations have been developed based on the experimental results using BDV and new Rheometer at the shear rates between 0-4000 Sec^{1} and only at atmospheric pressure

Determination of Pressure Dependent Viscosity of non-Newtonian Fluids Using a Novel Rheometric Device

Contents

	Page
Acknowledgements	i
Notation	ii
Abstract	iii
Contents	v
List of Figures and Plates	ix
List of Tables	xvi
1 Introduction and Literature Review	1
1 Introduction	1
1 1 Hydrodynamic phenomena	1
1 2 Rheology of non-Newtonian fluids	2
1 3 Variables which affect viscosity	3
1 3 1 Effect of pressure on viscosity	3
1 3 2 Effect of shear rate	5
1 3 3 Effect of temperature	6
1 3 4 Effect of flow characteristics	9
1 3 5 Critical Shear Stress	9

1 4 Literature Review 10

1 4 1 Background literature of hydrodynamic phenomena in drawing process 10

1 4 2 Background literature of polymer melts as a lubricant in drawing process 12

1 4 3 Background literature of Rheometers and Rheological research 14

1 5 Present Project and its aim 17

1 6 Overview of the Project 19

2 Hydrodynamic Analysis 36

2 1 Introduction 36

2 2 Theoretical Analysis 37

2 2 1 Determination of the Pressure and the Coefficents of Viscosity Equation of non-Newtonian fluids 38

3 Designing and Commissioning of the Rheometric Device and Test Procedure 47

3 1 General description 47

3 2 Instrumentation 48

3 2 1 Pressure Transducers 48

3 2 2 Digital Magnetic Pickup 49

3 2 3 Thermocouple 49

3 2 4 The Variable Speed Motor 49

3 2 5 Digital Tachometer 50

3 2 6 RDP Machine 50

3 3 Design of the Rheometric Device 51

3 3 1 Insert 1 51

3 3 2 Insert 2 52

3 3 3 Shaft 52

3 3 4 Pressure End plate 53

3 3 5 Shaft End Plate 53

3 4 Design of the Electrical Installation 53

3 5 Test procedure with the Novel Rheometric Device 54

4 Experimental Equipment, Test Procedure, Material 68

4 1 The High Pressure Rheometric Device and Test Procedure 63

4 2 Working Principle of the Device 69

4 3 Pressure fluid 71

4 4 BROOKFIELD DIGITAL VISCOMETER 71

4 5 Test Procedure with the viscometer 72

4 5 1 Autozero 72

4 5 2 Spindle Selection 72

4 5 3 Speed Selection and Setting 73

5 Results and Discussions 76

5 1 Introduction 76

5 2 Results of Pressure 76

5 2 1 Results of the Pressure distribution 77

5 2 2 Results of Maximum Pressure Vs Speed 80

5 3 Determination of the Rheology

(Values of the coefficient 'a' and 'b') 81

5 4 Effect of Pressure on Viscosity 83

5 5 Effect of Shear Rate on Viscosity 84

5 6 Discussions 125

5 6 1 Introduction 125

5 6 2 Discussion on the Test Procedure and the Experimental Work 125

5 6 2 Discussions on the Analysis and the Theoretical Results 127

5 6 3 Error Analysis 128

6 Conclusion and Suggestions for Further 130

6 1 Introduction 130

6 2 Conclusion 130

6 3 Suggestions For the Future Work 131

References 133

Appendix A 142

Appendix B 147

Appendix C 149

LIST OF FIGURES

Chapter Number		*Page*
Chapter One		
Fig 1 1	Flow Curves for 0 92 polyethylene at 130° C	20
Fig 1 2	Viscosity vs Pressure for different shear rates (0 92 Polyethylene	21
Fig 1 3	Flow Curve for ALKATHENE WVG23	22
Fig 1 4	Flow curve for POLYPROPYLENE KM61	23
Fig 1 5	Flow curves for RIGIDEX	24
Fig 1 6	Flow curves for POLYSTYRENE	25
Fig 1 7	Effect of shear rate on viscosity of ALKATHENE WVG23	26
Fig 1 8	Effect of shear rate on viscosity of POLYPROPYLENE KM61	27
Fig 1 9	Effect oft of shear rate on viscosity of RIGIDEX	28
Fig 1 10	Effect of shear rate on viscosity of POLYSTYRENE	29
Fig 1 11	Effect of temperature on viscosity of polymer	30
Fig 1 12	Effect of temperature of WVG23, KM61, RIGIDEX and POLYSTYRENE	31

Fig 1 13 Typical pressure tube and die 32

Fig 1 14 Nozzle-die unit (BISTRA) 33

Fig 1 15 Pressurised chamber 33

Fig 1 16 Pressure tube-die arrangement 34

Fig 1 17 Couette's viscometer, A is the inside guard rings F and F' 35

Chapter Two

Fig 2 1 Parallel bore pressure unit 39

Chapter Three

Fig 3 1 Schematic diagram of the drawing bench 56

Fig 3 2 Pressure Unit 57

Fig 3 3 Pressure Cylinder 58

Fig 3 4 Insert 1 59

Fig 3 5 Insert 2 60

Fig 3 6 Shaft 61

Fig 3 7 Pressure End Plate 62

Fig 3 8 Shaft End Plate 63

Chapter Four

Fig 4 1 Schematic Diagram of Pressure Unit Assembly 75

Chapter Five

Fig 5 1 Pressure Distribution of Glycerine for the different shearing speed at the Gap Ratio of 3 86

Fig 5 2 Pressure Distribution of Glycerine for different shearing speed at the Gap ratio of 5 87

Fig 5 3 Pressure Distribution of Glycerine for different shearing speed at the Gap ratio of 8 88

Fig 5 4 Pressure Distribution of Glycerine at the shearing speed of 0 5 m/sec for the different Gap Ratios 89

Fig 5 5 Pressure Distribution of Glycerine at these shearing speed of 1 0 m/sec for the different Gap Ratios 90

Fig 5 6 Pressure Distribution of Glycerine at the shearing speed of 1 5 m/sec for the different Gap Ratios 91

Fig 5 7 Pressure Distribution of Silicon5 for different shearing speed at the Gap ratio of 3 92

Fig 5 8 Pressure Distribution of Silicon5 for the different shearing speed at the Gap Ratio of 3 93

Fig 5 9 Pressure Distribution of Silicon5 for the different shearing speed at the Gap Ratio of 5 94

Fig 5 10 Pressure Distribution of Silicon5 for the different Speed at the Gap Ratio of 5 95

Fig 5 11 Pressure Distribution of Silicon5 for different shearing speed at the Gap Ratio of 8 96

Fig 5 12 Pressure Distribution of Silicon5 for the different shearing speed at the Gap Ratio of 8 97

Fig 5 13 Pressure Distribution of Silicon 5 at the speed of 0 25 m/sec for the different Gap Ratios 98

Fig 5 14 Pressure Distribution of Silicon 5 at the speed of 2 0 m/sec for the different Gap Ratio 99

Fig 5 15 Pressure Distribution of Silicon 5 at the speed of 12 5 m/sec for the different Gap Ratio of 3 100

Fig5 16 Pressure Distribution of Silicon 5 at the speed of 0 25 m/sec for Gap Ratio of 5 101

Fig 5 17 Pressure Distribution of Silicon 5 at the speed of 0 25 m/sec for the different Gap Ratio of 8 102

Fig 5 18 Pressure Distribution of Silicon12 5 at the speed of 0 5 m/sec for the different Gap Ratios 103

Fig 5 19 Pressure Distribution of Silicon 5 at the speed of
2 0 m/sec for the different Gap Ratios 104

Fig 5 20 Pressure Distribution of Silicon 5 at the speed of
1 0m/sec for the different Gap Ratio of 5 105

Fig 5 21 Maximum Pressure vs Speed for Glycerine for
The different Gap Ratios 106

Fig 5 22 Maximum Pressure vs Speed for Silicone5 for
the different Gap Ratios 107

Fig 5 23 Maximum Pressure vs Speed for Silicone12 5 for
the different Gap Ratios 108

Fig 5 24 Comparison of Maximum Pressure vs Speed for Glycerine
Silicon5 and Silicon 12 5 for the Gap Ratio of 5 109

Fig 5 25 Comparing the Theoretical Pressure Distribution of
Glycerine at 1 5 m/sec for the Different values of 'a' and 'b'
with the Experimental Results 110

Fig 5 26 Comparison of the Theoretical Pressure Distribution of
Glycerine at 1 5 m/sec for the different Values of 'a'
with the Experimental Results 111

Fig 5 27 Comparison of the Theoretical Pressure Distribution of
Silicone5 at the Speed of 1 0 m/sec for the different Values
of 'a' and 'b' with the Experimental Results 112

Fig 5 28 Comparison of the Theoretical Pressure Distribution of
Silicone5 at the Speed of 1 0 m/sec for the different Values of 'a'

with the Experimental Results 113

Fig 5 29 Comparison of the Theoretical Pressure Distribution of Silicon12 5 at the Speed of 1 0 m/sec for the different Values Of 'a' and 'b' with the Experimental Results 114

Fig 5 30 Comparison of the Theoretical Pressure Distribution of Silicon 12 5 at the Speed of 1 0 m/sec for the different Values of 'a' with the Experimental Results 115

Fig 5 31 Effect of Pressure on Viscosity for Glycerine 116

Fig 5 32 Effect of Pressure on Viscosity for Silicon5 117

Fig 5 33 Effect of Pressure on Viscosity for Silicon 12 5 118

Fig 5 34 Effect of Pressure on Viscosity for Silicon 5 and Silicon 12 5 at the Shear Rate 2000 sec^{1} 119

Fig 5 35 Shear Rate vs Shear Stress of Glycerine, Silicon5 and Silicon12 5 using the Brookfield Viscometer 120

Fig 5 36 Effect of Shear Rate on Viscosity of Glycerine,Silicon5 and Silicon 12 5 Using the BROOKFIELD Viscometer 121

Fig 5 37 Effect of Shear Rate on Viscosity of Glycerine at Atmospheric Pressure 122

Fig 5 38 Effect of Shear Rate on Viscosity of Silicon5 at Atmospheric Pressure 123

Fig 5 39 Effect of Shear Rate on Viscosity of Silicon 125 at Atmospheric Pressure 124

List of Plates

Chapter ***Page***

Chapter Three

Plate 3 1 Overallview of the rig 64

Plate 3 2 RDP machine, and Frequency Inverter 64

Plate 3 3 Electric motor and magnetic pickup 65

Plate 3 4 Pressure chamber 65

Plate 3 5 Pressure transducer and thermocouple 66

Plate 3 6 Electric Controller 66

Plate 3 7 Insert 1 67

Plate 3 8 End Plate 67

Plate 4 1 BROOKFIELD Viscometer 74

List of Tables

Chapter Number *Page*

Chapter 1

Table 1 1 Shear Rates Typical of Some Familiar Materials and Processes 5

Chapter One

INTRODUCTION AND LITERATURE REVIEW

1. Introduction

1 1 Hydrodynamic phenomena

Hydrodynamic means dynamics of fluids under certain flow conditions When a viscous fluid is present between the gap of the two solid surfaces and one of the surfaces moves relative to the other hydrodynamic pressure develops A common situation is when the fluid is flowing through a converging gap (like a journal bearing) The magnitudes of this hydrodynamic pressure are dependent on the shape of the surfaces, the viscosity of the fluid as well as the relative speed of movement The mechanics of fluid pressure generation can be explained by the fact that the moving surface drags the fluid into the gap formed between it and the fixed surface and the relative motion between the moving surface and the fluid gives rise to the pressure If the fluid is oil type then the generated pressure is not so high But if it is of polymer solution type then the generated pressure is many times higher However, for plastic processing equipment and food and mineral processing industries the pressure generation due to hydrodynamic phenomenon could be a significant design factor for the processing equipment This principle should be advantageous for designing a new rheometer for determining the rheological properties of viscous fluids such as glycerine and silicone, etc at higher than

atmospheric pressures The flow Characteristics of non-Newtonian fluids are influenced by many factors, which are described in relation to the present work for rheological studies of these fluids

1.2 Rheology of non-Newtonian fluids

"Rheology" is a general term for the study of deformation and flow of materials, it originates from the Greek word "rhein", which means, "to flow" Rheology is concerned with the flow and deformation of materials experiencing an applied force The term 'Rheology' was invented by Professor Bingham of Lafayette college, Easton, PA, USA on the advice of a colleague, a Professor of Classics It means the study of the deformation and flow of materials as mentioned earlier This definition was accepted when the American Society of Rheology was founded in 1929 That first meeting heard papers on the properties and behaviour of such widely differing materials as asphalt, lubricants, paints, plastics and rubber, which gives some idea of the scope of the subject and also the numerous scientific disciplines which are likely to be involved Nowadays, the scope is even wider Significant advances have been made in biorheology, in polymer rheology and in suspension rheology There has also been a significant appreciation of the importance of rheology in chemical processing industries Opportunities no doubt exist for more extensive applications of rheology in the biotechnological industries Rheology is becoming more and more important in plastic industry, both in areas of development and processing [1] Other applications of rheology are as follows (i) Pumping slurries-materials transport (ii) Thickening and de-watering of mineral slurries

(iii) Filtration (iv) Forming materials e g brick and ceramic products (v) Paint manufacture e g non-drip paints (vi) Reactions involving mineral slurries e g gold extraction (vii) Food chemistry and manufacture-texture of ice cream, pasta, desserts, processed meats, cosmetics chemistry (viii) Drilling mud for petroleum industry (ix) Polymer chemistry-solution and melts (x) Plastohydrodynamic wire drawing and wire coating i e rheological properties required for good coating performance

In recent studies of thermoplastic injection moulding, sophisticated rheological techniques have been employed to characterise the viscous behaviour Since the findings of rheology are of fundamental importance for the development, manufacture and processing of innumerable products Without rheology, nothing in materials and process engineering can function today Rheometry is the technology, which involves the rheological measurement of fluids The flow characteristics of non-Newtonian fluids are influenced by many factors, which are described in relation to the present work for developing a new type of rheometer for rheological studies of glycerine, silicone, liquid honey, polymer melt etc

1 3 Variables which affect viscosity

1 3 1 The effect of pressure on viscosity

Several theories suggest that the free volume [2-6] determines the viscosity of a fluid The free volume of a fluid is defined in various ways, but a common definition is the difference between the actual volume and a volume in which such close packaging of the molecules occurs that no motion can take place The greater

the free volume the easier it is for flow to take place The viscosity of liquids increases when the pressure is increased because the distance between the molecules, and hence their mobility decreases At very high pressures no free volume is left in the liquid which becomes solid [7] Free volume increases with temperature because of thermal expansion However, the most direct influence on free volume should be of the pressure An increase in hydrostatic pressure decreases the free volume and increases the viscosity of a fluid Viscosity, by definition, is the internal resistance to shearing stress due to intermolecular forces of attraction It is thought that if those forces of attraction are encouraged, the apparent viscosity of the polymer, which is one of the most important properties of these materials, may be increased

Westover [8] described a double piston rheometer for measuring viscosity as a function of pressure at 172 MN/m^2 He found that the viscosity of polystyrene increases by over a hundred times and the viscosity of polyethylene increases by a factor of five at a constant rate of shear as the pressure was increased Maxwell and Jung [9] , and Choi [10] demonstrated that the effect of hydrostatic pressure on the apparent viscosity of branched polyethylene and polystyrene at constant shear and temperature are appreciable and should not be neglected Cogswell [11] suggested that the effect of an increase in pressure may be linked to that due to a drop in temperature He observed that for low-density polyethylene, an increase in pressure of 100 MN/m^2 had the same effect on viscosity as that due to a drop in temperature of 53° C within the melt range It had been noted that at very high pressure (above 140 MN/m^2) the melt tended to recrystallise and in consequence the melt acted melt acted like a solid plug [12] For this reason, pressure viscosity measurements are often conducted at relatively high temperature Since the work carried out by Westover appears to be the most comprehensive, his results are used to determine the

pressure coefficient of viscosity Figure 1 1 shows the effect of pressure on shear stress-shear rate curves and figures 1 2 shows how shear rate effects the influence of pressure on viscosity

1 3 2 Effect of Shear rate

Table 1 1 shows the approximate magnitude of shear rates encountered in a number of industrial and everyday situations in which viscosity is important and therefore needs to be measured The approximate shear rate involved in any operation can be estimated by dividing the average velocity of the following liquid by a characterstic dimension of the geometry in which it is flowing (e g the radius of a tube or the thickness of a sheared layer)

Table 1 1 Shear rates typical of some familiar materials and processes

Situation	Typical range of shear rates(s^{-1})	Application
Extruders	10^0-10^2	Polymers
Chewing and swallowing	10^1 -10^2	Foods
Dip coating	10^1 -10^2	Paints, confectionary
Mixing and stirring	10^1 -10^3	Manufacturing liquids
Pipe flow	10^0-10^3	Pumping, Blood flow
Spraying and brushing	10^3-10^4	Spray-drying, painting Fuel atomisation
Lubrication	10^3-10^7	Gasoline engines

Since the non-Newtonian viscosity behaviour will be dealt with in this project, it is important to first define what the Newtonian behaviour is, in the context of the shear viscosity A Newtonian fluid has the characterstic that the shear viscosity does not vary with shear rate [1] For non-Newtonian behaviour, the apparent viscosity decreases as the rate of shear increases Figures 1 3, 1 4, 1 5 and 1 6 show the effect of shear rate on shear stress where the influence of temperature may be noticed These curves were produced by extruding polymer melts (Alkathene WVG23, polypropylene KM61, Rigidex (HDP) and Polystyrene) through an extrusion rheometer at different temperatures A non-linear relationship is seen to exist between shear stress and shear rate The viscosity of the polymer may be calculated at any known shear rate by measuring the slope of the curve A Newtonian fluid under shear stress condition exhibits linear relationship with shear rate where the slope of the line represents the viscosity of the fluids Figures 1 7, 1 8, 1 9 and 1 10 show another way of representing the effect of shear rate on viscosity, where the viscosity may be read off directly from known shear rate values (For a Newtonian fluid this curve would be a horizontal straight line)

1 3 3 Effect of Temperature on viscosity

An increase in temperature generally decreases the viscosity of the fluids This effect vastly differs for different types of polymer Figure 1 11 shows typical changes in viscosity against temperature at zero shear rates The slope of each line measures the activation energies has more deterioration effect on viscosity compared to those of lower activation energies This energy is a function of polarity in

polymers and the most non-polar polymers such as polyethylene with very small inter-molecular forces have low activation energy

Flow occurs when polymer molecules slide past each other and the ease of flow depends on the mobility of the molecular chains and the forces of holding the molecules together That an increase in temperature reduces viscosity is widely known and in general is a property easily understood Viscosity and temperature for a Newtonian fluid may be related by an Arrhenius equation of the form

$$\mu = Ae^{E/RT}$$

This equation together with a knowledge of A, a constant, and E, the activation energy, enables to calculate the coefficient of viscosity μ for an absolute temperature T, R is the universal gas constant A second (empirical) equation is often used for melts This is $\mu = a^{-bt}$ where both a and b are constants To obtain a fundamental explanation of the difference in temperature dependence of viscosity between different polymers a number of attempts have been made The application of "free volume theory" is most successful This theory suggests that at some temperature T_o there is no "free volume" between the molecules This free volume, f, is postulated to increase linearly with temperature so that at T_g the fractional free volume has a value f_g

The expansion coefficient α_f is defined by the equation,

$$F = fg + \alpha_f (T - T_g)$$

It has been proposed that f_g has the universal value of 0 0025 and α_f is a universal value of 4 8x10 $^{-4}$ Williams, etal [13] have argued from this that the viscosity η of a polymer at temperature T may be related to its viscosity η_a an arbitrary reference temperature t_a by the equation,

$$\log\frac{\eta}{\eta_a} = -\frac{C_1^a(T-T_a)}{C_2^a + T - T_a}$$

If the arbitrary temperature is taken as T_g then the above equation becomes

$$\log\frac{\eta}{\eta_a} = -\frac{C_1^g(T-T_g)}{C_2^g + T - T_g}$$

In this case C_1^g=1/2 303 f_g = 17 44 and C_2^g=1/2 303 $C_1^g \alpha_f$ = 51 6 have been proposed as universal constants The equations are known as the WLF equation [14] DIENES [15] believed that as the temperature increases the molecular arrangements within the polymer change more towards random configuration, therefore, it becomes easier for the polymer to flow at higher temperatures Figures 1 11 and 1 12 show the variation of viscosity versus temperature for these polymers at zero shear rates These graphs do not represent the complete behaviour since viscosity measurements are affected by pressure, shear rate, temperature etc and it is necessary to include these effects on viscosity of polymer melts

1 3 4 Effect of Flow Characteristics

In the plasto-hydrodynamic pressure unit the polymer melt is subjected to very high shear rates and pressures, much greater than those capable of being developed in any extrusion rheometer The presence of critical shear stress at low shear rate decreases the coating thickness, as concluded by Crampton[16] However it is also believed that, the poor performance of the unit at higher drawing speeds is related to a combination of factors such as shear rate, melt flow instability, partial crystallisation, compressibility etc and not just by the critical shear stress The high-pressure generation is believed to have the effect of increasing the melt viscosity in the unit Crampton maintained the temperature at a steady value when the tests were conducted thus minimising the effects inherent with changing temperature However to understand these effects fully further investigation is needed

1 3 5 Critical Shear Stress

The critical shear stress is the stress at which the uniformity of the non-Newtonian fluids such as polymer melt flow ceases to exist Several workers [17-19] investigated this phenomenon and they showed that certain flow defects are associated with the polymer Ripple, Bamboo, Spiral, ZigZag or Helix for different types of polymers The terms "Melt fracture", "Elastic turbulence" and "Flow disstortion" have been used to describe this effect

However, there is a general agreement on the following points

1 The critical Shear Stress (CSS) has values in the region of 0 01 to 1 0MN/m^2 for most polymers
2 The CSS is independent of the die length and diameter
3 The CSS does not vary widely with temperature
4 The flow defects always take place when non-Newtonian fluids are involved
5 A discontinuity in the viscosity shear stress curves occurred
6 The CSS was shown by the cinematography method to take place in the die

1 4 Literature Review

1 4 1 Historical background of hydrodynamic lubrication

As the demand for higher quality wire increased, better lubrication proved necessary to promote efficiency, surface finish, quality, heat dissipation and a reduction m production time The latter may be summarised as (i) Reduced drawing time (ii) Reduction of number of inter- pass heat treatment (iii) Elimination of redrawing time (iv) Reducing down time due to changing dies because of excessive wear Christopherson and Naylor [20] pioneered the development of hydrodynamic lubrication in wire drawing They employed a long tube, with very close tolerances, attached to the front end of a conventional die as shown in Figure 1 13 Oil was used for lubrication purpose and as the wire was pulled through the dies, it pressurised the lubricant by viscous action and fed into the die inlet This pressurised lubricant then completely separated the wire from the die, preventing metal to metal contact

Experimental results provided by them showed evidence of deformation of the wire in the tube before the die entrance Although it was shown that hydrodynamic lubrication was achieved under the designed conditions, the pressure nozzle had to be placed vertically and was of such a length that the wire industry found it too inconvenient to put it into practice

Wisterich [21] carried out experimental work on the forced lubrication based on a pressure tube system Soap powder was used as the lubricant in a short nozzle, which was attached to the entry side of the die Experimental results showed that the speed, temperature and the tube gap had a direct effect on the property of the film thickness produced He also noted that oil produced a thicker film than soap A schematic diagram of the unit used by Wisterich is shown in Figure 1 14

Tattersal [22] published a detailed analysis of plasto-hydrodynamic lubrication action in wire drawing taking some rheological and metallurgical properties of the process into account Experimental results and theory showed that these were in reasonable agreement More recently Chu [23] using the work of Tattersal presented a chart for the inlet tube he designed Subsquently Bedi [24] introduced an analysis for wire drawing assuming complete hydrodynamic lubrication Studies of the lubricant film thickness which would be developed under practical drawing conditions have been presented in references [25-26] Middlemiss [27] improved the previously used drawing unit by using an externally pressurised lubrication system

Kalmogov et al [28] also conducted experimental work on tube sinking under conditions of hydrodynamic action In contrast to similar devices for wire drawing there was no seal between the nozzle and the die, because the lubrication process in tube sinking was much lower Soap powder was used as the lubricant in that work

Bloor et al [29] produced a theoretical analysis for elasto-plasto hydrodynamic lubrication action for strip drawing through wedge shaped dies They took account of elastic component in the strip at entry and exit to the die and the pressure and viscosity characteristics of the lubricant It has shown that by comparing the magnitude of the predicted lubricant film thickness that hydrodynamic lubrication could be accomplished during the process

Double die arrangements were developed by Orlov et al [30] Their version of the pressure nozzle/die is shown in Figure 1 15 The lubricant is transported into the chamber formed by the exit cone of the pressure die and the entry part of the drawing die, where the pressurised lubricant provides the hydrodynamic lubrication during drawing Although claim was made for reduced power consumption and reduced die wear there was however a lack of substantial evidence to support this claim

1 4 2 Background Literature of Polymer Melt as a Lubricant in Drawing Process

Polymers were first used as lubricants in deep drawing and hydrostatic extrusion They were chosen because of the radically differing characteristics from either soap or oil There are many important differences between the rheology of molten polymer and conventional lubricants such as oil The most obvious of these is the very high viscosity of polymer melts at higher temperatures, which would preclude the use of oil as a lubricant Non-Newtonian lubricants have been previously investigated for journal bearing [30] and these have been found to be advantageous for bearings subjected to oscillatory load which induce fatigue loading The use of a polymer melt as the coating material in the drawing process was

suggested by Symmons and Thompson [31] They investigated the adherence of a polymer coat onto the drawn wire There was some hydrodynamic lubrication achieved but not as much as expected Both Stevens [32] and Crampton [33] conducted experiments which showed that polymer coating of wire was possible, depending on the temperature, viscosity of the polymer and drawing speed of the wire The experiments they carried out reduced the cross-sectional area of the wire They also noted that the polymer coat thickness on the wire decreased as the drawing speed increased The apparatus used was a modification of Cristopherson tube A schematic diagram of this unit is shown in figure 1 16

Other experimental work carried out by Crampton et al [34] has shown that effective reduction of the wire diameter should be possible using a polymer melt in conjunction with a stepped bore tubular unit only Panwher et al [35-37] reported work carried out on the dieless tube sinking process and presented an analytic solution based upon Newtonian characteristics Subsequently Panwher [38] analysed the system taking account of the Non-Newtonian characteristics of the polymer Symmons et al [39-40] presented analysis of a die-less wire drawing process using a viscosity-pressure and viscosity - temperature relationship of experimental form For the deformation of strip using a stepped parallel bore unit, Memon et al [40-44] also published theoretical and experimental works

Parvinmehr et al [45-49] carried out similar experiments to Crampton's but used two different types of pressure tubes in which the smallest diameter of the tube was greater than the initial diameter of the wire being drawn The units had no reduction die since Crampton and other researchers previously noted that deformation started to occur before the entrance to the reduction die The two pressure tubes he used in his experiment were of stepped and tapered bored nature

His experimental results showed that polymer-coating thickness varied with the wire drawing speed, the polymer type and the polymer temperature Hashmi and Symmons [50] developed a numerical solution for a conical tubular orifice through which a continuum is drawn Very good agreement between the theoretical and experimental results was observed at low drawing speed, where as for higher drawing speeds the agreement between the predicted and the actual percentage reduction in area was very poor

Investigation was carried out by Al-Natour and Hashmi [51-52] using a combined parallel and tapered bore pressure unit in conjunction with a polymer melt They developed a theoretical analysis assuming Newtonian pressure medium Also, hydrodynamic lubrication was achieved Nwir and Hashmi [53-56] then published the pressure model considering the polymer as a non-Newtonian fluid Akhter and Hashmi [57] developed new mathematical models for different types of pressure unit using the polymer as non-Newtonian fluid

1 4 3 Background literature of rheometers and rheological research

Many methods have been devised to study the flow properties of liquids Traditionally Rheological measurements are performed with Capillary rheometers (viscometers) and Rotational rheometers (viscometers) The earliest attempts to measure the flow properties of fluids dealt mainly with the principles of Capillary viscometry Probably the first scientific experiment in which a capillary or tube was used to measure viscosity was made by Hagen in 1839, followed shortly thereafter by Poiseuille's work Poiseuille studied capillary flow problems in order to understand better the circulation of blood through capillary vessels in the human

body He discovered the relation slip (known as the Hagen Poiseuille law) between flow rate and pressure drop This discovery was the foundation of capillary viscometry With developments in hydrodynamics and advances in the technology of non-Newtonian fluids, capillary viscometry became a reliable method of measuring the flow properties of a fluid [58] The capillary viscometer provides an improvement in shear capability Novak and Winer [59] used a capillary viscometer to measure the viscosity of polymer/ mineral oil mixtures at pressures to 0 3 GPa and shear stresses to 10^5Pa They reported Newtonian behaviour in two ranges of shear stress at low shear stress a "first Newtonian" associated with the viscosity of the blend and above about 10^4 Pa shear stress, a transition to a "second Newtonian" for which viscosity was again rate independent but with a value reduced to nearly that of the mineral oil solvent With the capillary technique the hydrostatic pressure varies across the length of the capillary requiring foreknowledge of the effect of pressure on material parameters

Couette devised the first practical rotational viscometer in 1890 [60] Couette's Concentric cylinder viscometer consisted of a rotating cup and an inner cylinder which was supported by a torsion wire and rested in a point bearing in the bottom of the cup (fig 1 17) 23 years later Hatcheck described a modified version of the Couetteviscometer, which improved on the design of the guard rings and minimised effects with very low viscosity fluids Many aspects of the new theories (non-Newtonian or complex fluids) pioneered by Reiner, Bingham, et al , required innovations is design Barber et al [61] operated a rotational viscometer at atmospheric pressure with gaps approaching one micron Shear rates as high as 10^6sec^{-1}were obtained However the shear stress was limited to 10^4 Pa Galvin [62] developed a high pressure, high shear rate capillary viscometer It was used in a

lubrication research laboratory that covers a wide range of rate of shear at ambient pressures substantially above atmospheric pressure and at various temperatures

A new slit rheometer with a continuously adjustable gap was developed to characterise the shear Viscosity material functions of structured fluids (suspensios, dispersios, gels) as a function of deformation rate and temperature [63] The rheology and hydrodynamic analysis of grease flows in a circular pipe was investigated by Young [64] Rheological properties and pumping characteristics of two greases were investigated in the temperature range of 5^0 C to 35^0 C The high pressure rheology of a soap-thickened grease and the base oil has been characterised using a falling-body viscometer, high pressure couette viscometer, and a high pressure penetrometer by Scott [65] He demonstrated the modified Bingham model to describe the experimental observation A modified Bingham type rheometer, designed for operation at temperature of up to 500^0F and pressures of up to 200 p s i is described by Nasan [66]

The relationship of wall shear rate for closed couette flow has been determined for power law fluids with a helical barrel rheometer [67] The principle of this rheometer is based upon measuring the pressure differential across one flight of special extruder wherein the helix is cut in the barrel rather than in the screw A correlation for the pressure and temperature dependence of viscosity is demonstrated by Jagadish [68] Mamdouh et al [69] studied the rheological properties of silicone fluids (polydimethylsiloxanes) Their studies include the depiction of the rheological fingerprints of two PDMS solutions with the zero-shear viscosities 1000 and 30000 mPa's For the sake of brevity they call these solutions PDMS1 and PDMS30, respectively Also included in the study are the transient shear stress responses, the measurements of yeild stresses, the thixotropy, and the creep-recovery tests Their

experiment shows the influence of temperature on the rheological fingerprints of PDMS1 and PDMS30 PDMS1 solutions exhibit Newtonian behaviour and their viscosities decrease by almost 45% when the temperature is raised from 10 to 50^0 C However, PDMS30 shows two distinct ranges of Newtonian and non-Newtonian flow behaviour Over the initial range of Newtonian flow, the viscosity of PDMS30 decreases with temperature from 10 to 40^0 C and slightly increases at 50^0 C

Compamk et al [70] studied the effect of chain length and ion size on the viscosity and ion conductivity of poly (dimethylsiloxane) systems They applied free volume, Arrhenius type viscosity, and ion conductivity models Graebling et al [71] studied the viscoelastic properties of poly (dimethylsiloxane)–poly(oxyethylene) blends They characterised the polymer blends by high values of the storage modullus at low frequencies and by long relaxation times The related the rhelogical behaviour to a few physically significant parameters such as the zero-shear viscosity of phases, the dispersed particle size, and the interfacial tension between phases Allcock et al [72] described the importance of PDMS applications in medicine, which is due to its resistance to blood fluids

1 5 Present Project and its aim

This thesis outlines the author's effort in the area of non-Newtonian fluid rheology A novel rheometric device, using a stepped bore unit is developed based on hydrodynamic principles This new technique would be useful in determining the viscosity of non-Newtonian fluids at different shear rates and high pressures The experimental work was carried out and the theoretical model has been developed in conjunction with the experimental work Included in this work are,

measurement of the variation of pressures with speed and changing the fluid, the insert and determination of viscosity and coefficients of the viscosity equation in conjunction with the experimental results

The scope of the present design and research is to

a) Design and development of an experimental device permitting the determination of pressure-dependent viscosity of non-Newtonian fluids

b) Measure the developed pressure in the Rheometric unit for different types of fluids at different with the shear rates, and for different gap geometrics

c) To develop a mathematical model for the prediction of various parameters involved in the process such as pressure, viscosity, shear rate, viscosity, coefficients of the viscosity equation in conjunction with the experimental results

d) To determine the viscosity of the different types of fluids at different pressures developed at different shear rates

e) To study the effects of pressures on the viscosity of the fluids which is developed in the unit

f) To measure the viscosity of different fluid with a Brookfield viscometer with different shear rate and to determine the effect of shear rate on viscosity at the lower shear rate range

g) To develop a new type of equation at the shear rate range 0-4000 Sec^{-1} and only at atmospheric pressure

h) To discuss the viability of the process and its limitations in relation to practical applications

1 6 Overview of the Project

The details and background of the investigation are presented m this thesis as following

In chapter one, a background literature of the rheology of non-Newtonian fluid and the effect of pressure, shear rate and the temperature on viscosity of fluids as well as the literature review of the hydrodynamic phenomena and its presence in wire drawing process have been presented The aim of the research is also included in the first chapter The theoretical analysis for the rheometer is given in chapter two A discussion on the equipment used during the course of tests is given in chapter three, also the design of the pressure unit is discussed in details in chapter three The materials and the equipment used during the course of the tests and the experimental procedure is given in chapter four The experimental results using the new rheometric device and the Brookfield Viscometer are given in chapter five The discussions are also given in this chapter Finally, chapter six states relevant conclusion and gives suggestions for both theoretical and experimental future work

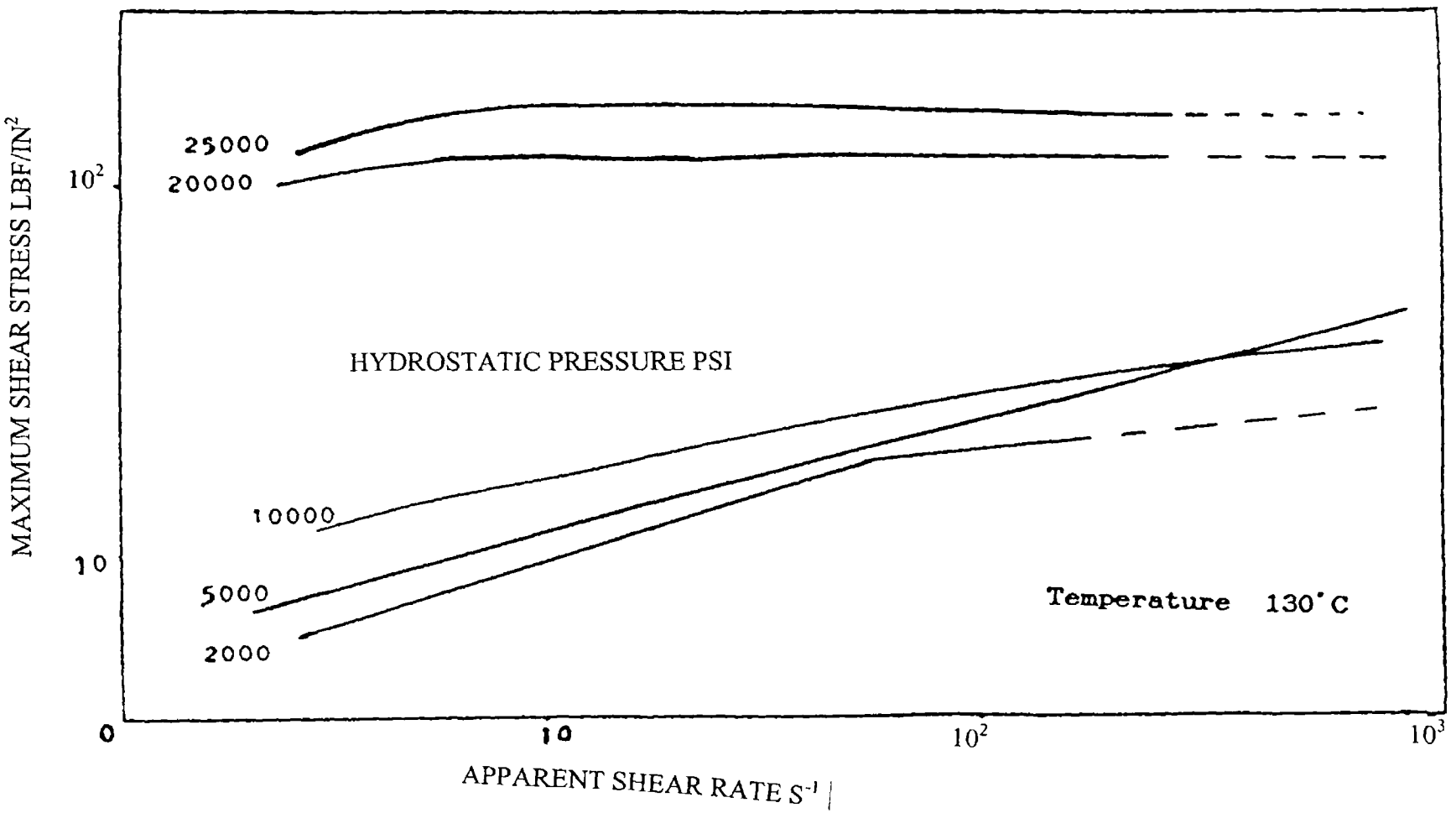

FIG 1 1 Flow Curves for 0 92 polyethylene at 130^0C [49]

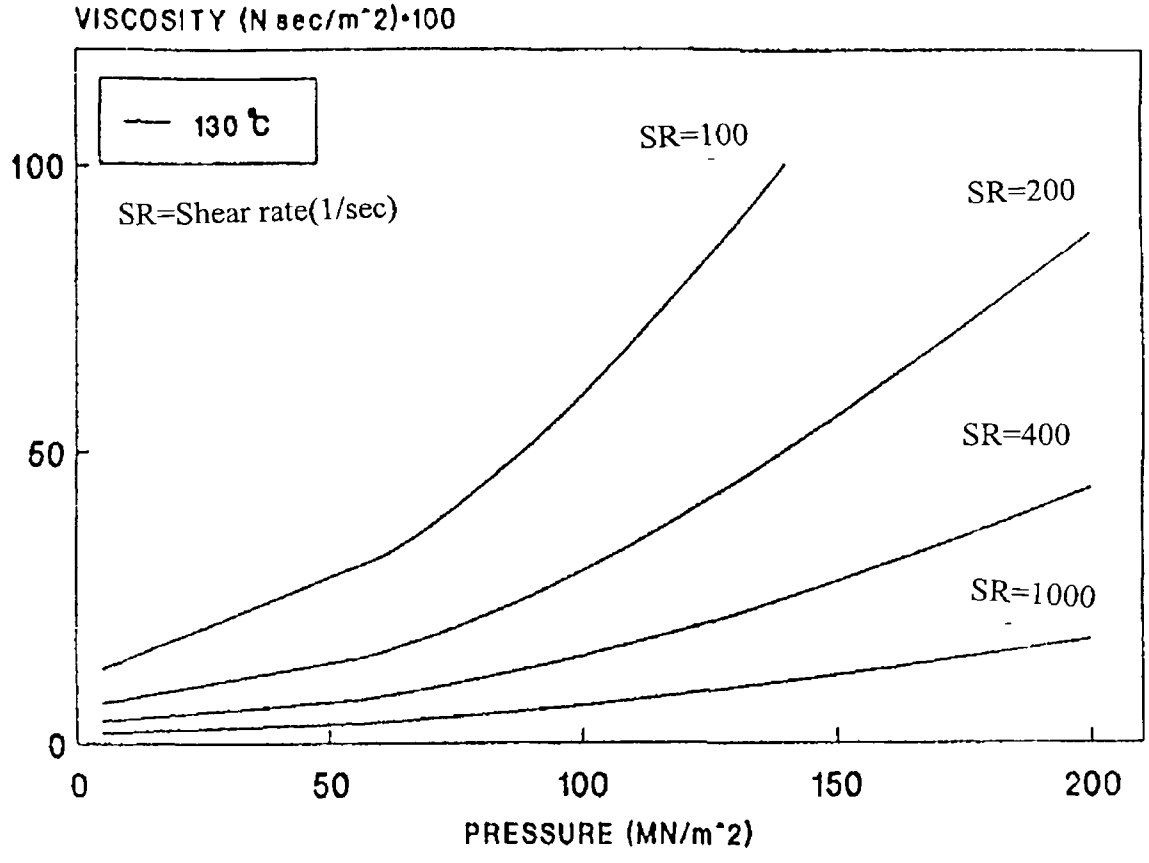

Figure 1 2 Viscosity vs Pressure for different shear rates (0 92 Polyethylene 130°)[49]

Fig 1 3

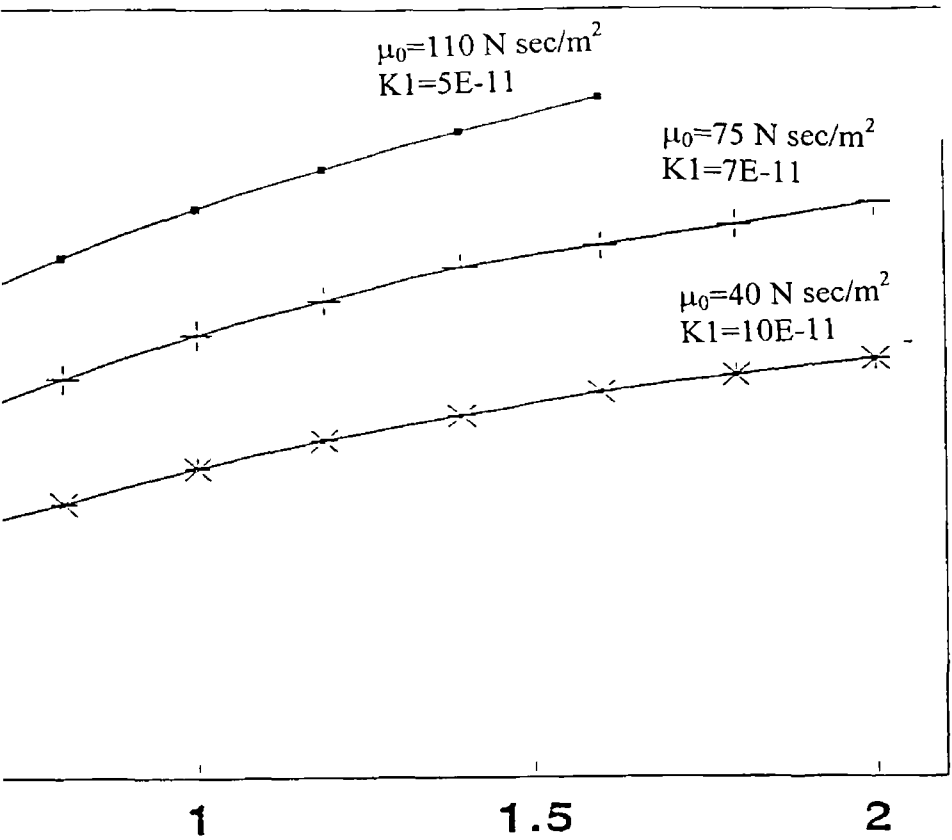

Flow Curve for ALKATHENE WVG23

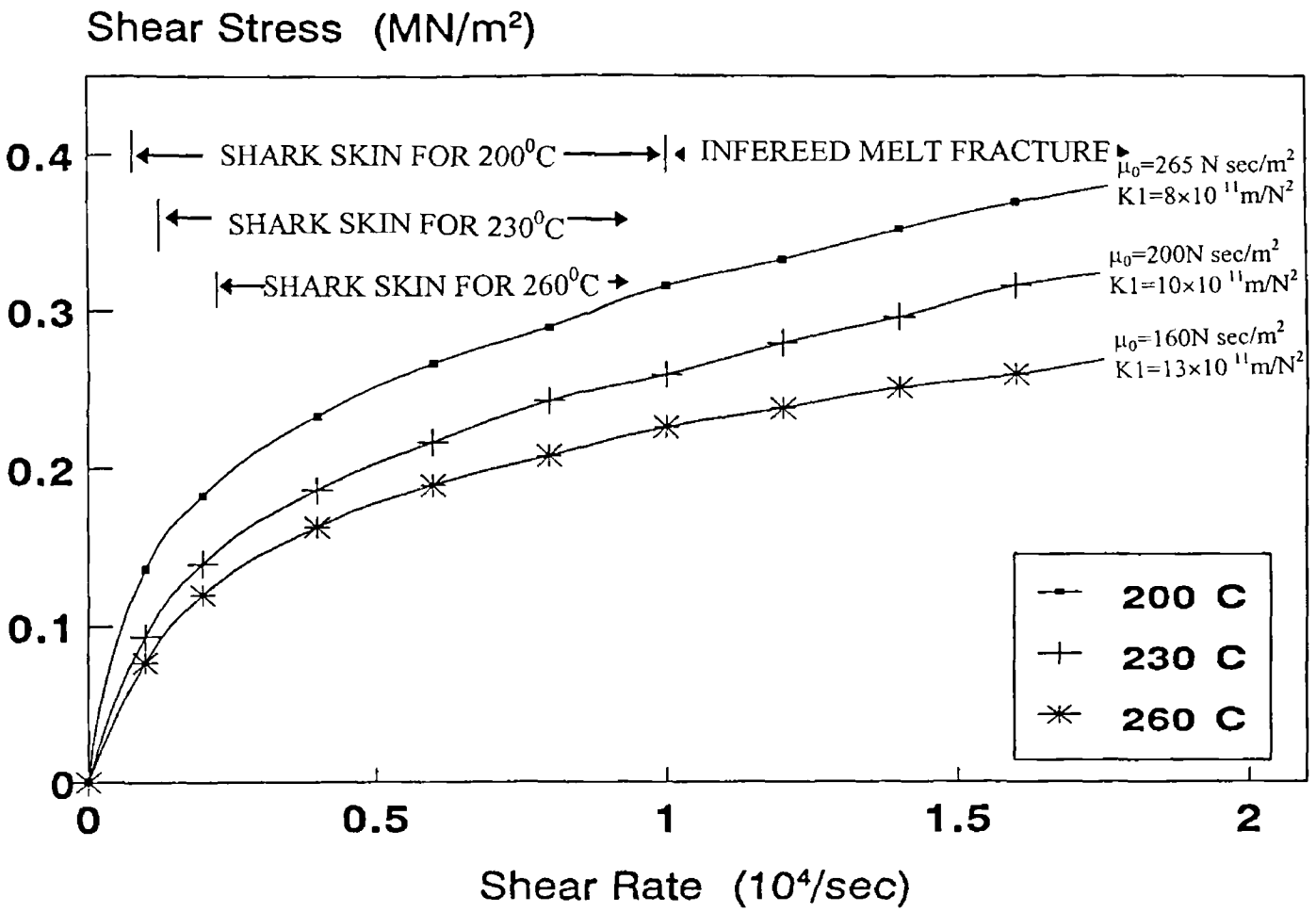

Fig 1 4 Flow curve for POLYPROPYLENE KM61

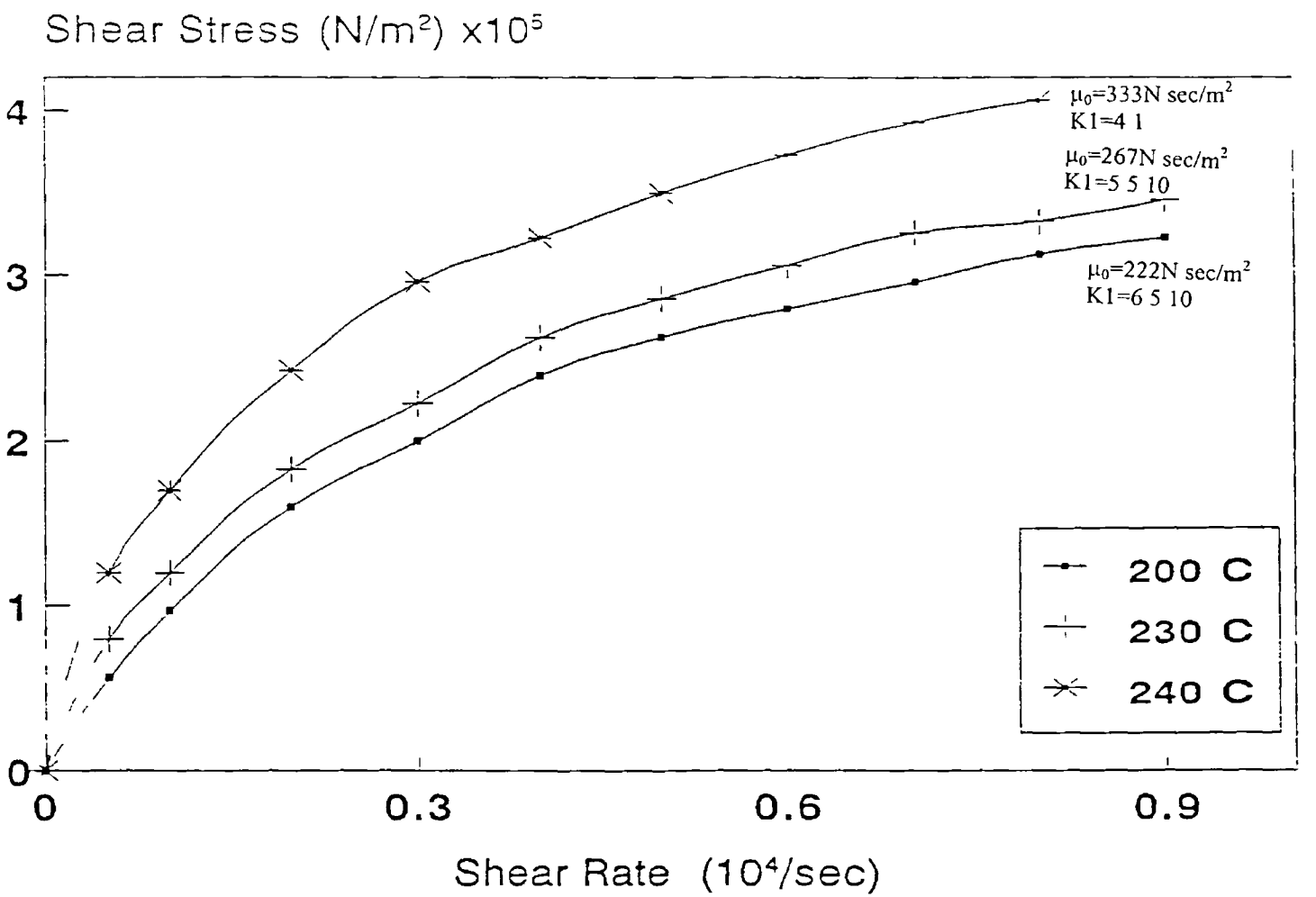

Fig 1 5 Flow curves for RIGIDEX

Fig 1

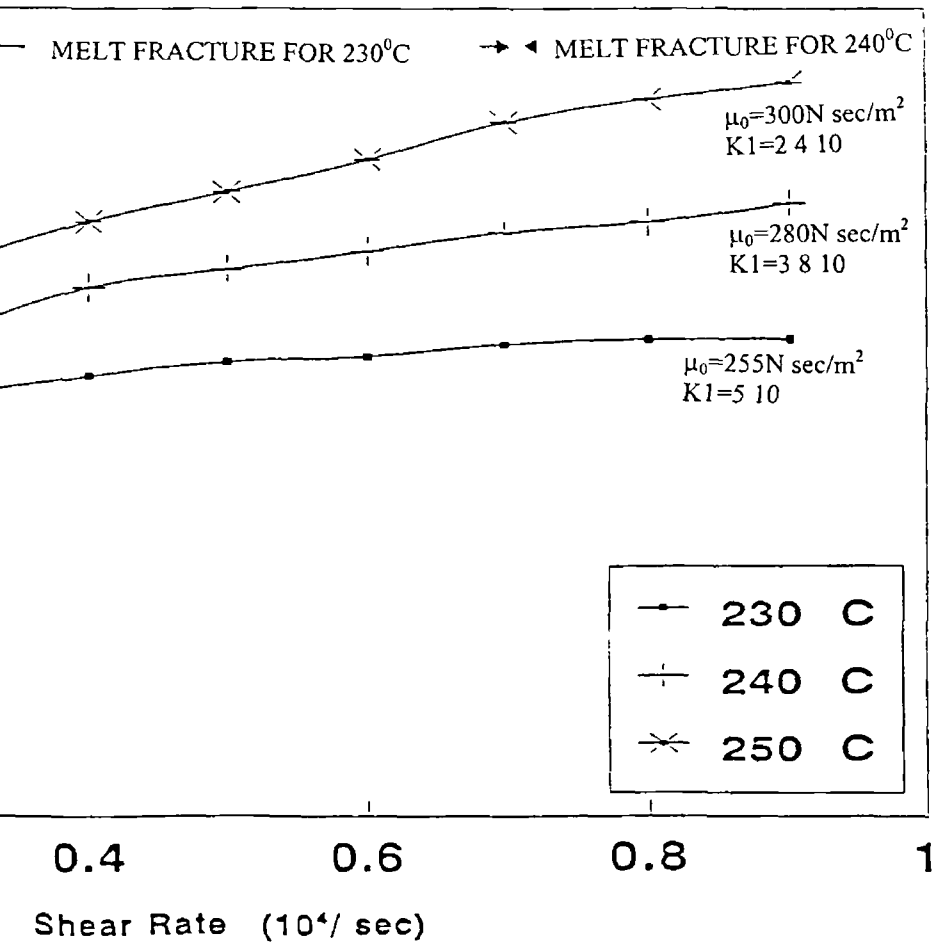

6 Flow curves for POLYSTYRENE

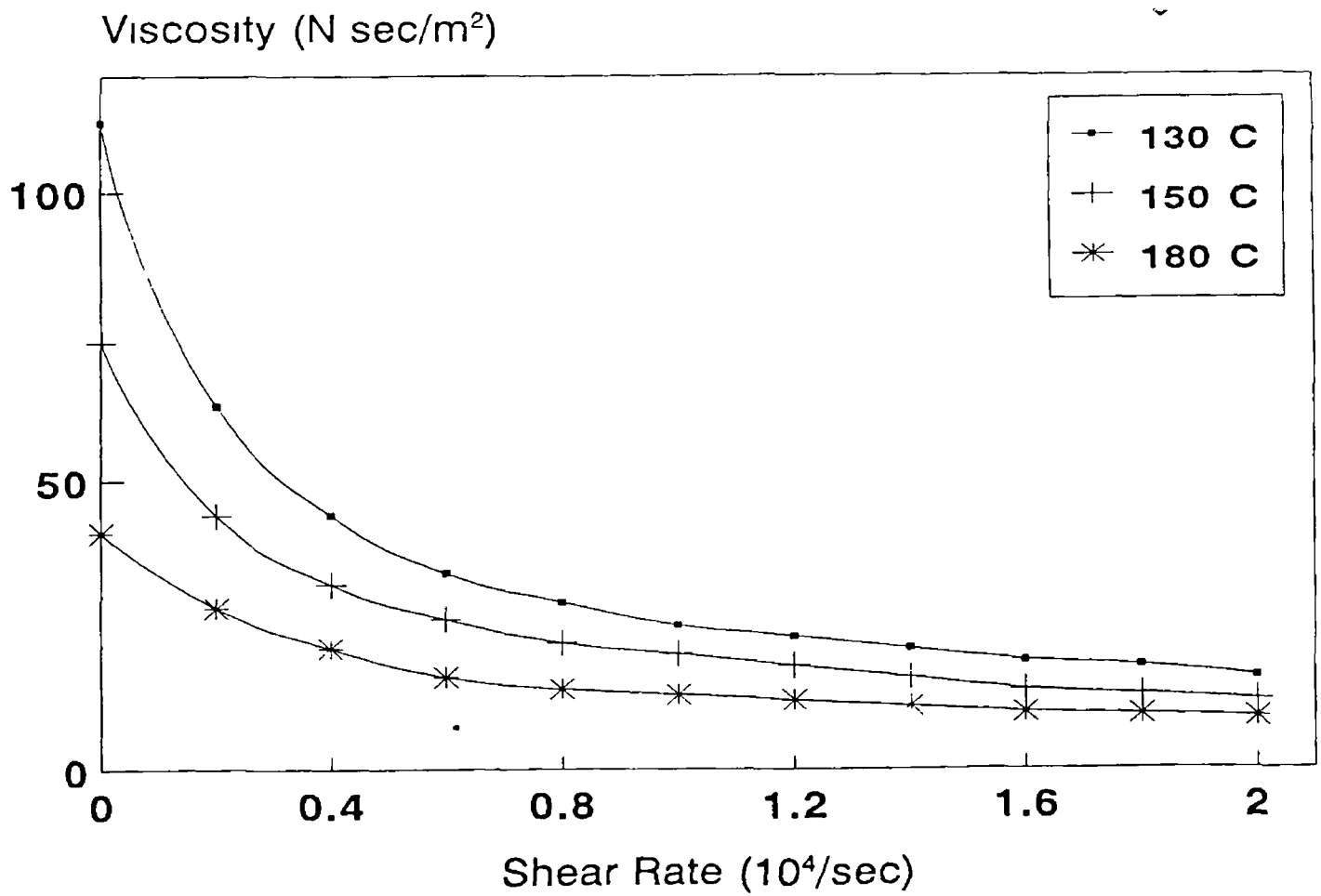

Fig 1 7 Effect of shear rate on viscosity of ALKATHENE WVG23

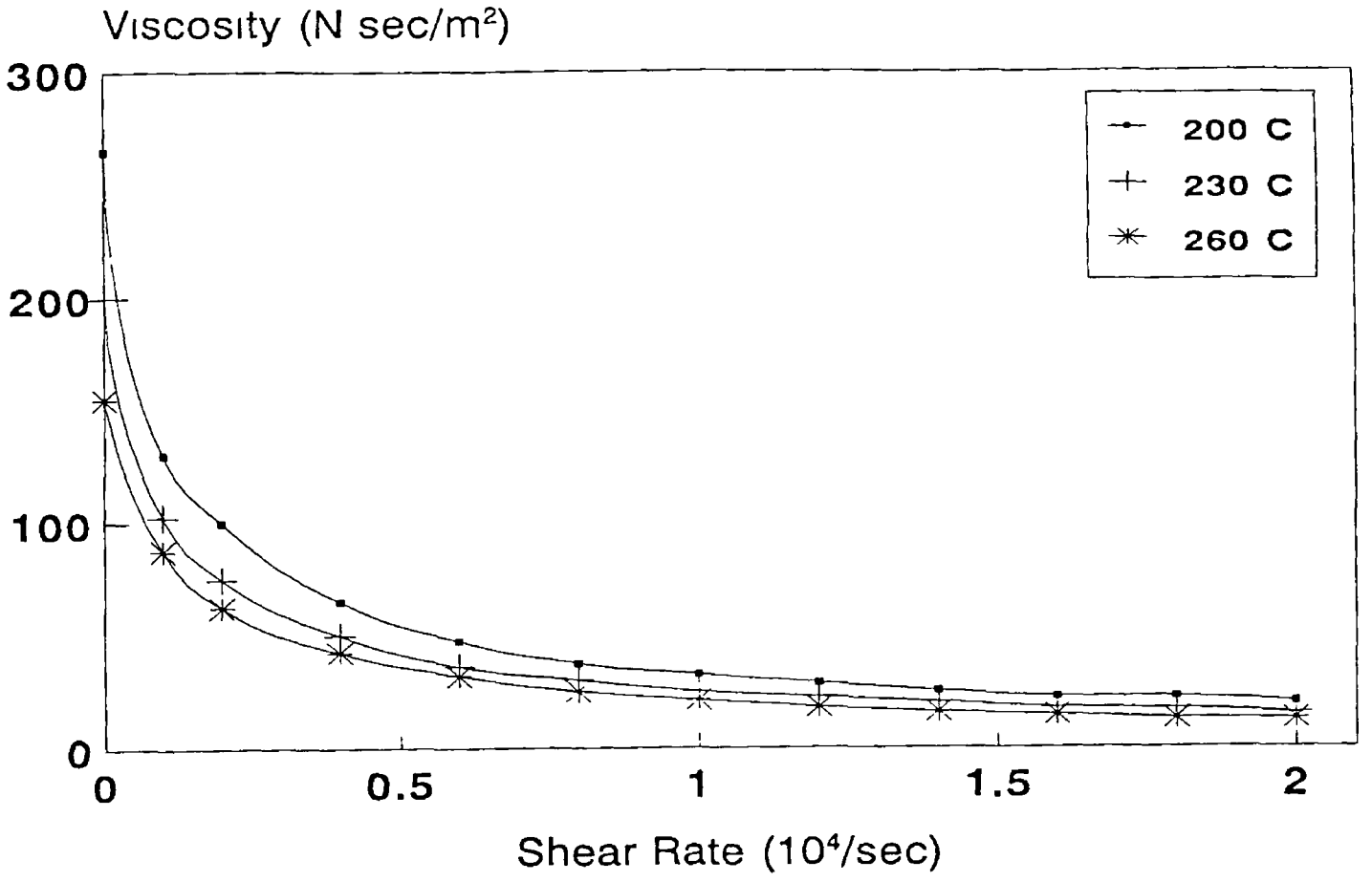

Fig 1 8 Effect of shear rate on viscosity of *POLYPROPYLENE KM61*

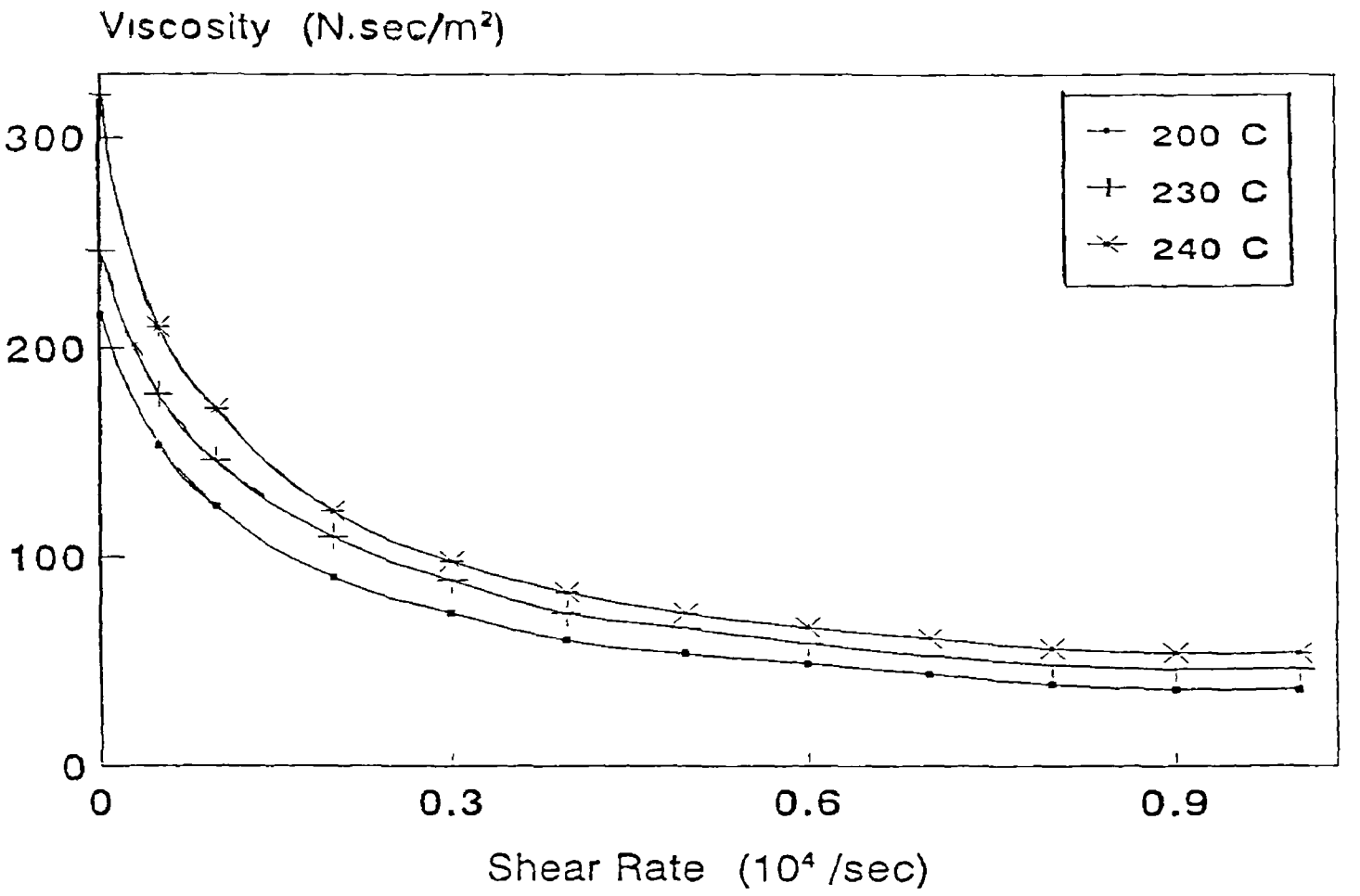

Fig 1 9 Effect of shear rate on viscosity of RIGIDEX

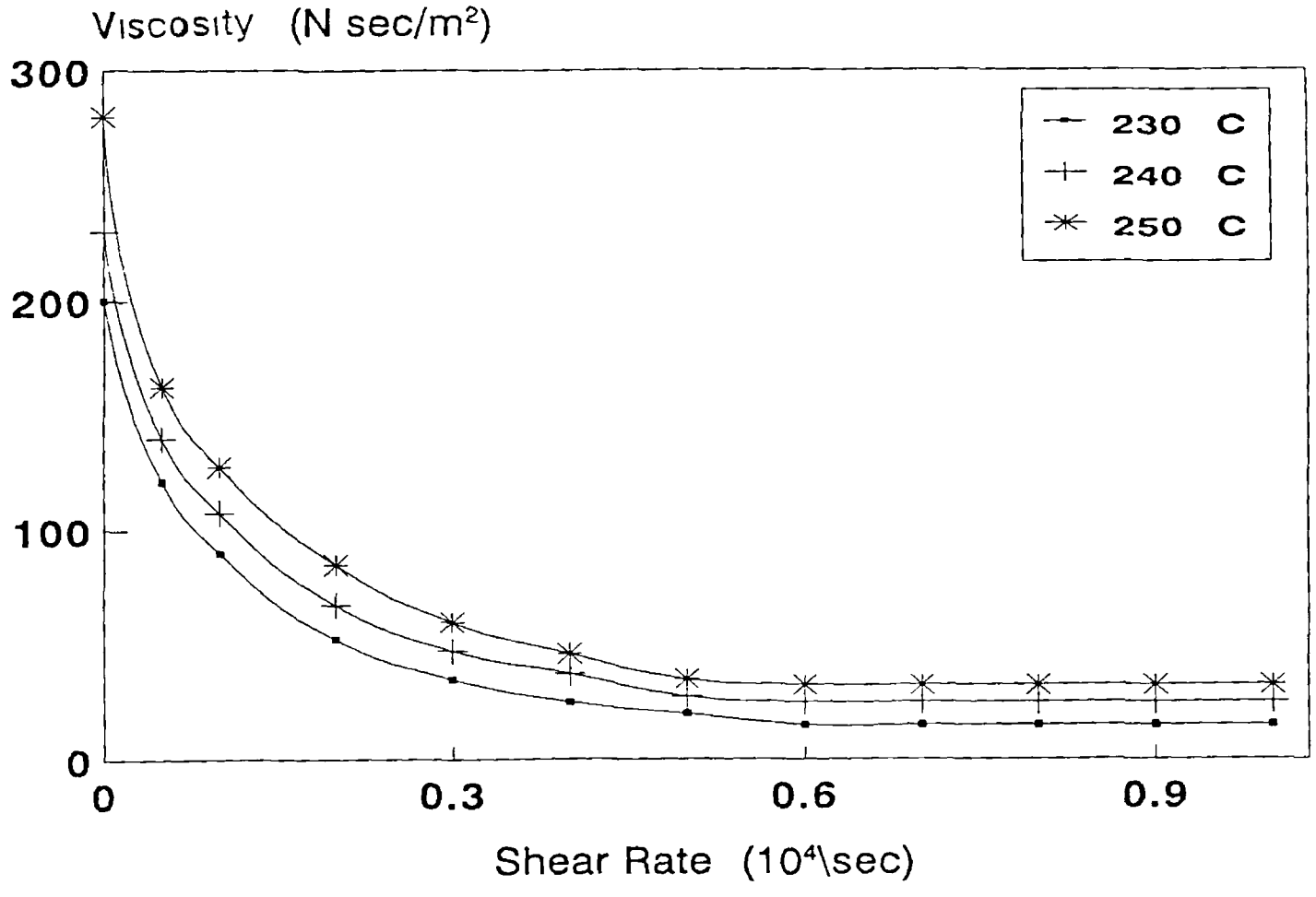

Fig 1 10 Effect of shear rate on viscosity of POLYSTYRENE

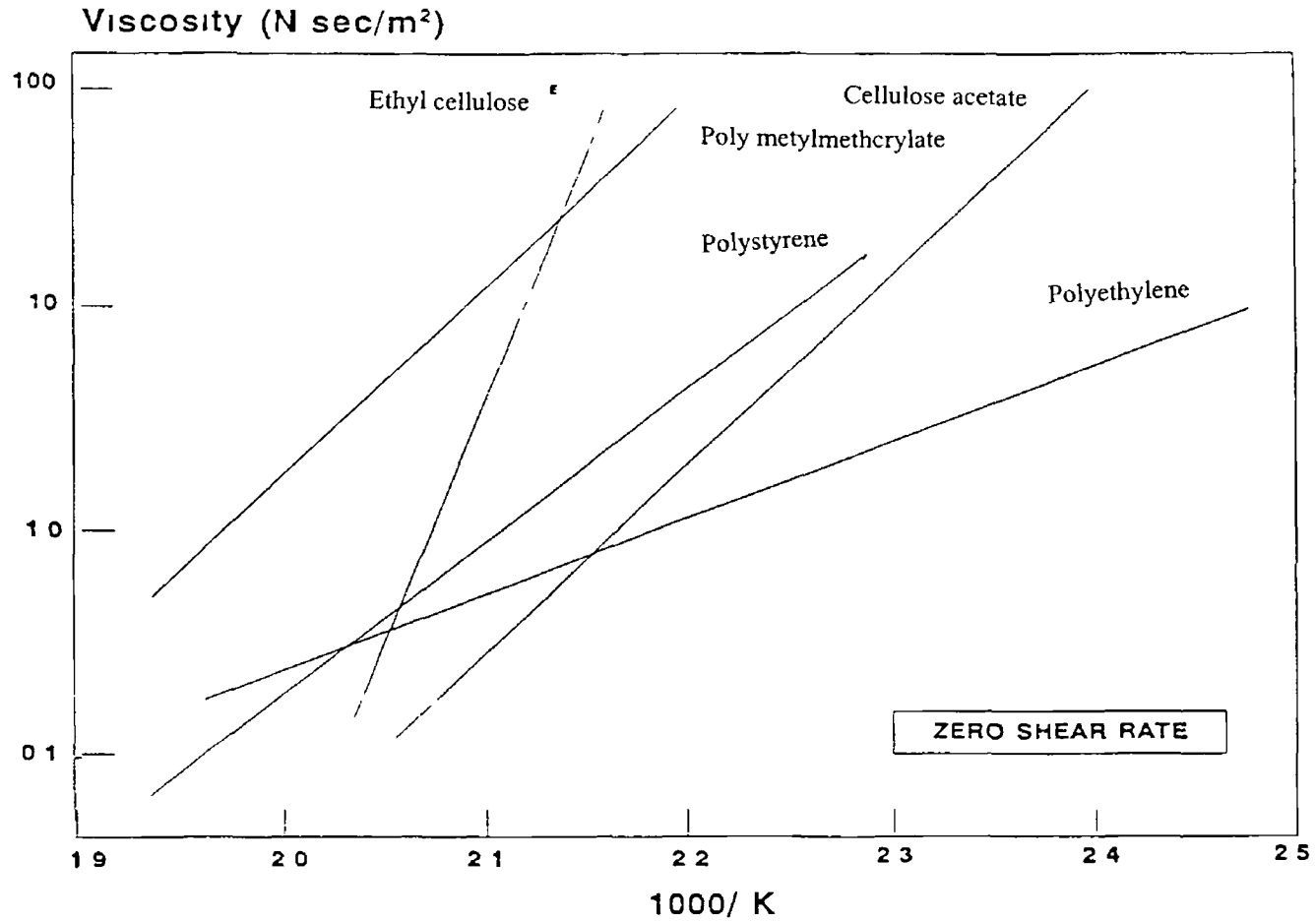

Fig .1 11 Effect of temperature on viscosity of polymer

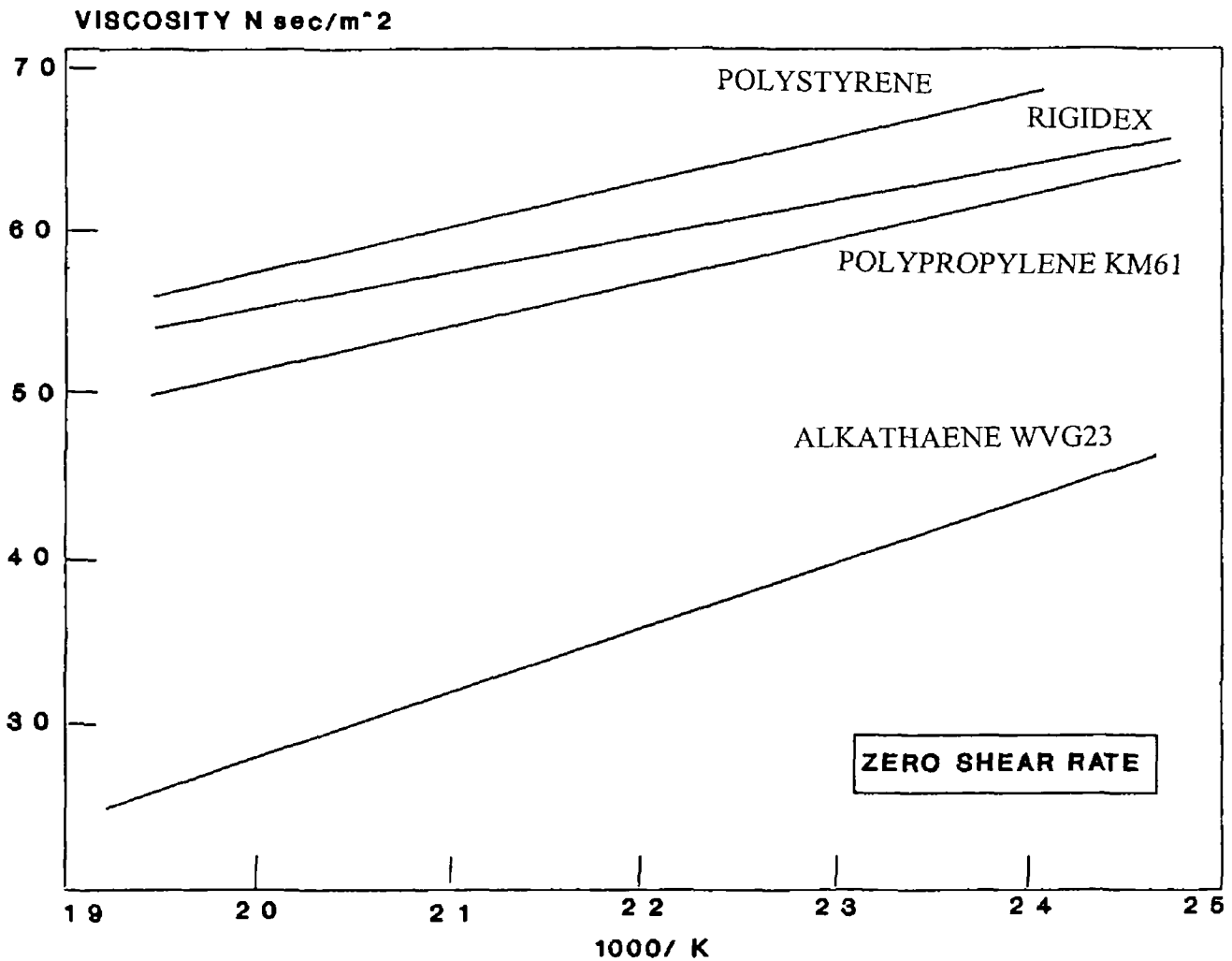

Fig 1 12 Effect of temperature on viscosity of WVG23, KM61, RIGIDEX and POLYSTYRENE

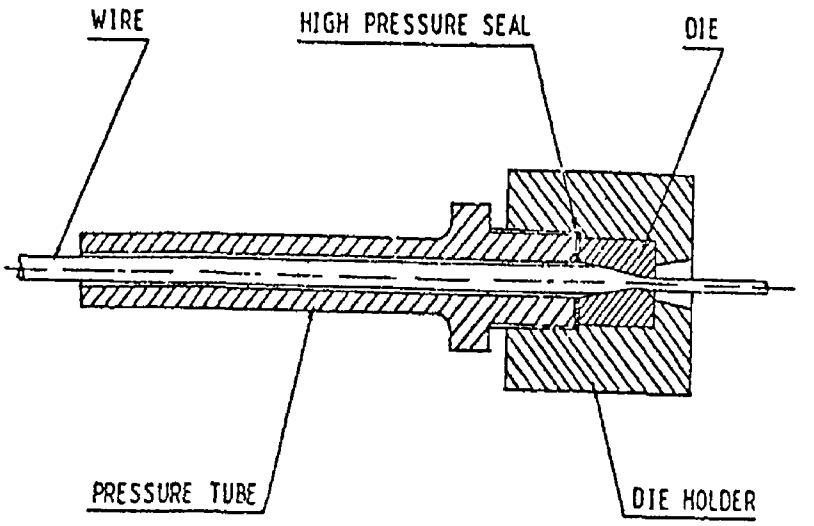

Fig 1 13 Typical pressure tube and die

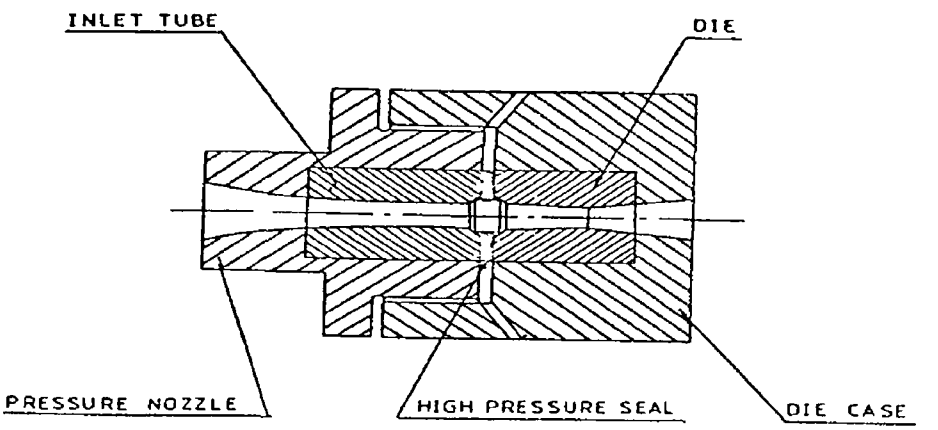

Fig 1 14 Nozzle-die unit (BISTRA)

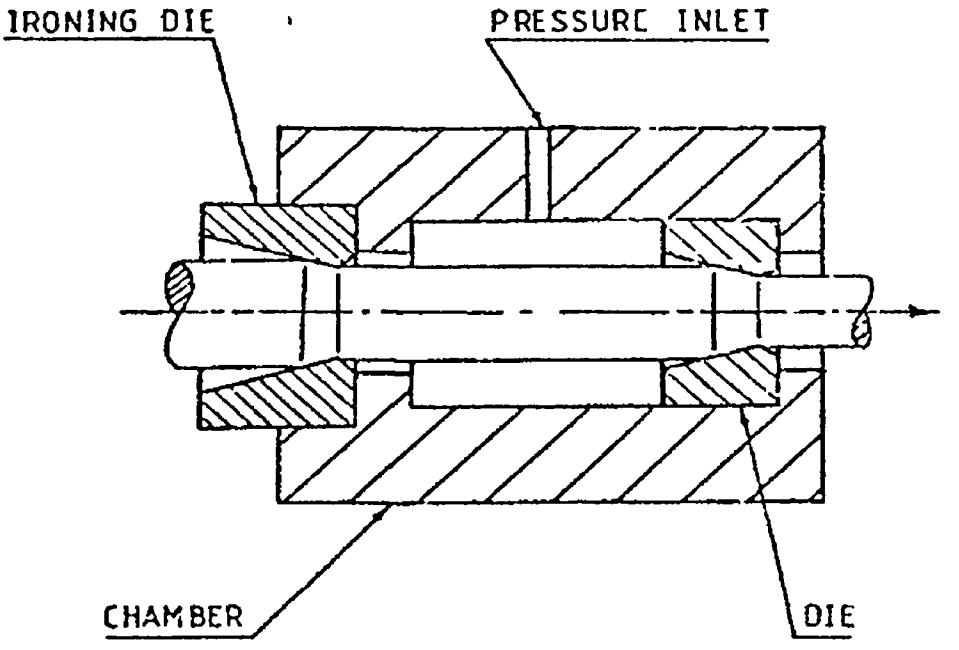

Fig 1 15 Pressurised chamber

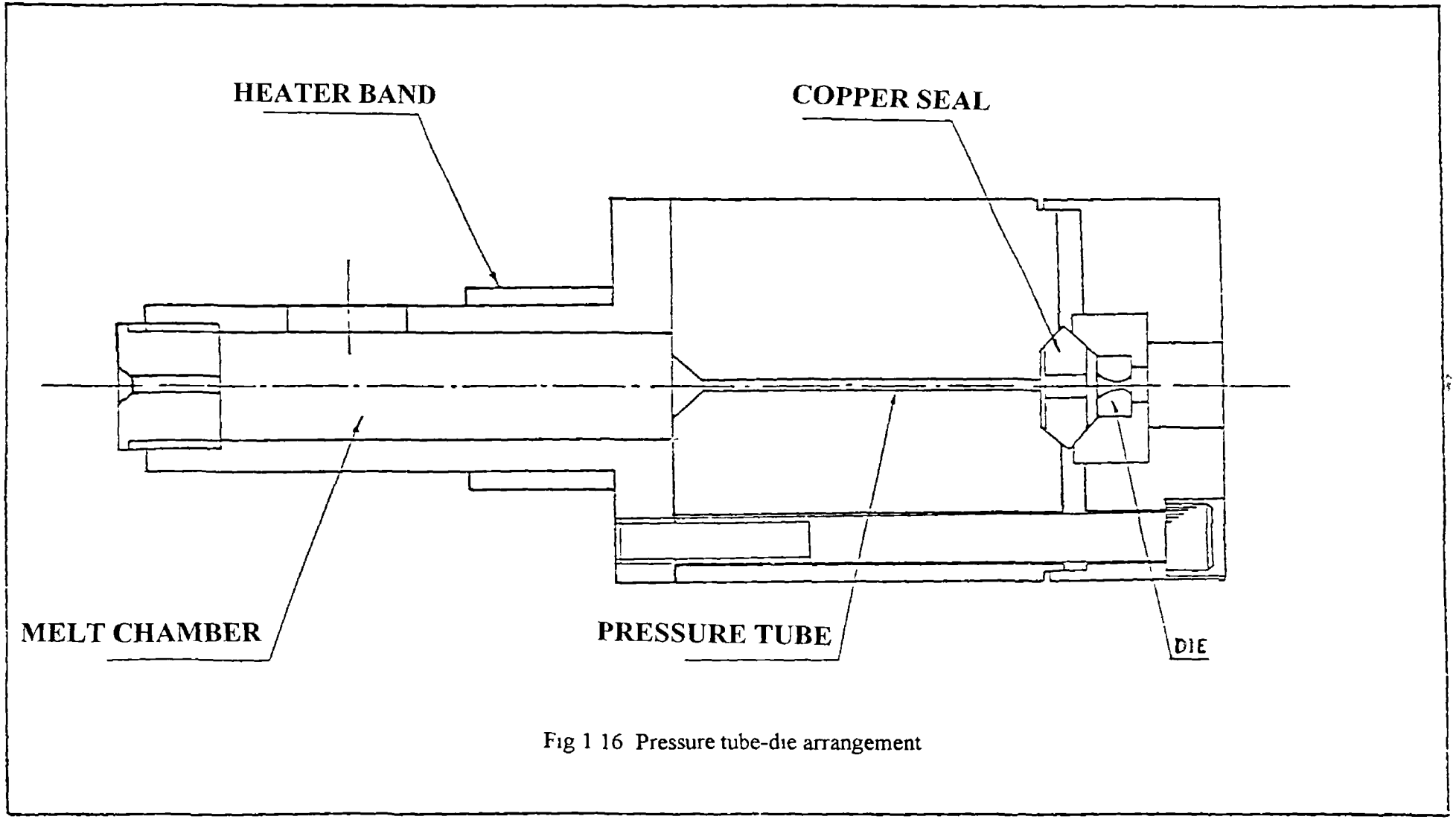

Fig 1 16 Pressure tube-die arrangement

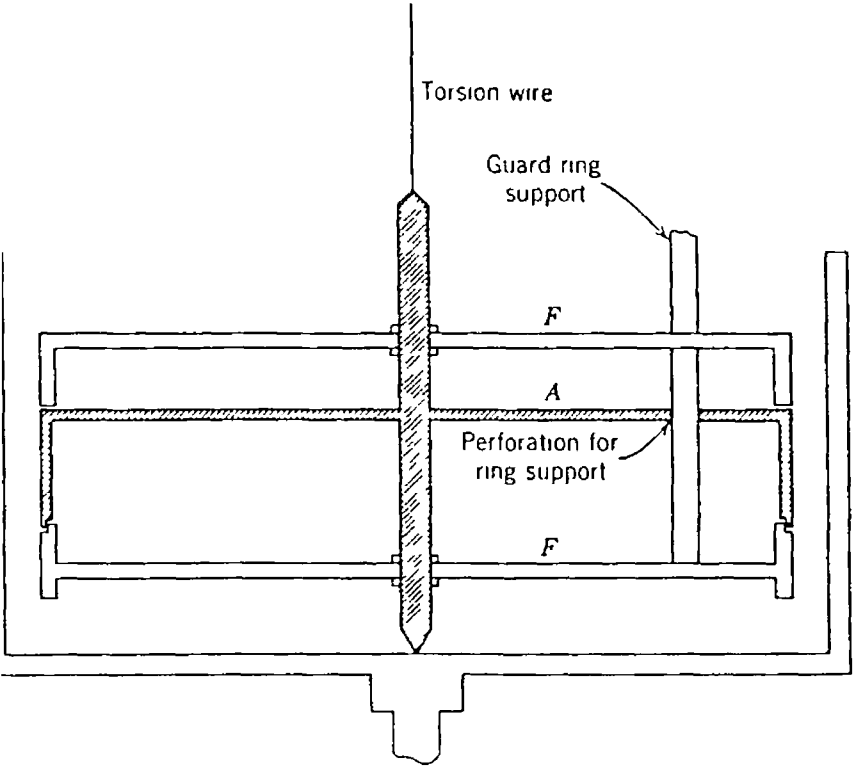

Fig 1 17 Couette's viscometer, A is the inside guard rings F and F'

Chapter Two

HYDRODYNAMIC ANALYSIS

2 1 Introduction

When a solid surface is rotated within another surface (orifice) filled with a viscous fluid, shearing takes place and in addition to the shear force a hydrodynamic pressure is generated The magnitude of the shearing and the pressure depends upon the speed with which the solid surface is rotated, the viscosity of the fluid and the geometrical configuration of the unit In order to verify the mechanics of the process of hydrodynamic pressure development within the unit it is important to develop a suitable mathematical model assuming non-Newtonian characteristics This chapter outlines details of a model developed by the author for the proposed high-pressure rheometer

Rheologies of fluids were discussed and several mathematical models developed, for wire drawing were reviewed in chapter one Theoretical and experimental works have also been carried out to observe the effectiveness of different lubricants and to calculate the film thickness during deformation process in the presence of hydrodynamic lubrication Different types of Rheometers have been discussed in chapter one Theoretical solutions for a novel plasto-hydrodynamic die-less drawing process were presented in references [46-50] for circular cross–section wires and rectangular strips

In the present study the geometrical configuration is different from the previous researchers A non-Newtonian plasto-hydrodynamic analysis of the process is presented for

a stepped parallel gap in which glycerine and silicone is used as the pressure medium The effects of shear rate and pressure on the viscosity of glycerine and silicone, together with the shear stress are included in the analysis

2 2 Theoretical analysis

The following analysis is based on the geometrical configuration shown in figure 1

To formulate the analysis the following assumptions were made

1 Flow of non-Newtonian fluid is isothermal
2 Flow of non-Newtonian fluid is axial
3 Flow of polymer is laminar
4 Thickness of the fluid layer is small compared to the dimension of the stepped gap rheometric unit

Analysis of the parallel gap rheometric unit is presented in two parts

1 Determination of the pressure in the unit

2 Determination of the viscosity of polymer within the unit and the coefficients of the viscosity equation

2 2 1 Determination of the pressure and coefficients of viscosity equation of non-Newtonian fluids

Two different equations are generally used to express the shear stress and shear rate relation for a polymer solution The first is a power law equation given by

$$\tau = \mu\left(\frac{dU}{dy}\right)^{n} \qquad (1)$$

This equation is applicable for any type of fluid Here n is the power law index which equals to 1 for non-Newtonian fluid, greater than 1 for a dilettante fluid and less than 1 for psudoplastic fluid In this equation τ is the shear stress, μ is the viscosity coefficient for power law fluid and $\left(\frac{dU}{dy}\right)$ is the shear rate

The second is an empirical equation relating shear stress and shear rate of a viscous fluid suggested by Rabinowitch [12] in the form,

$$\tau + K\tau^{3} = \mu\left(\frac{dU}{dy}\right) \qquad (2)$$

This equation was later used by Hung and Muster (74) to determine the non-Newtonian flow in a step bearing and also by Swamy et al (75) to calculate the load capacity of a finite width journal bearing Other workers have also used this equation to analyse the behaviour of non-Newtonian fluids [33,49] In equation (2) K is the non-Newtonian factor, μ is the viscosity of the fluid, τ and $\left(\frac{dU}{dy}\right)$ are the shear stress

and shear rate respectively In the analysis, which follows, is based on the second empirical equation

Flow of non-Newtonian fluid in the parallel stepped gap unit is divided into two sections The first section being the entry part of the unit before the step and the second section being the tube after the step

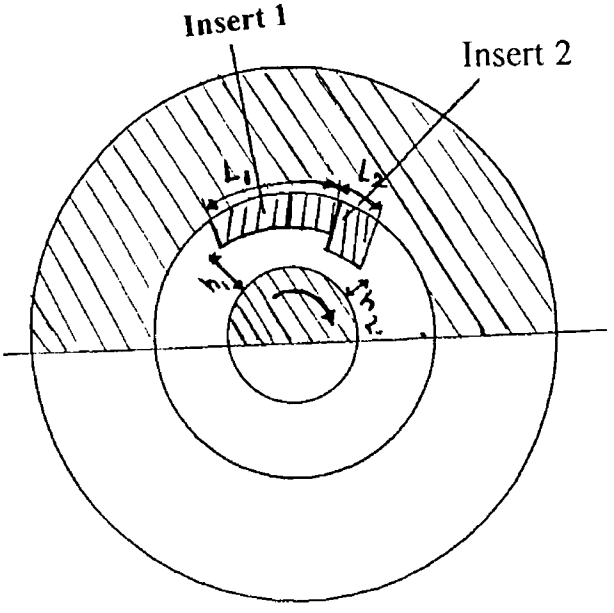

Figure 2 1 Parallel Stepped gap rheometric pressure unit

In the first part of the unit in Fig (2 1) the relationship between the pressure and shear stress gradient is given by

$$\left(\frac{dp}{dx}\right)_1 = \left(\frac{d\tau}{dy}\right)_1 \qquad (2)$$

Integration with respect to y gives,

$$\tau_1 = P_1 'y + \tau c_1 \qquad (3)$$

where τ_{c_1} is the shear stress at y = 0 and $P_1' = (dp/dx)_1$ is constant across the gap

Substituting equation (3) into equation (1) becomes,

$P_1 'y + \tau c_1 + K(P_1 'y + \tau c_1)^3 = \mu(\frac{du}{dy})_1$

or

$$\mu\left(\frac{dU}{dy}\right)_1 = p_1'y + \tau c_1 + K(p_1'^3 y^3 + \tau c_1^3 + 3p_1'^2 y^2 \tau c_1 + 3\tau c_1^2 p_1'y) \qquad (4)$$

After integration equation (4) becomes

$$U_1 = \frac{p_1'y^2}{2\mu} + \frac{\tau c_1 y}{\mu} + \frac{K}{\mu}(\frac{p_1'^3 y^4}{4} + \tau c_1^3 y + p_1'^2 y^3 \tau c_1 + \frac{3}{2}\tau c_1^2 p_1'y^2) + C_1 \qquad (5)$$

where C_1 is the constant of integration,

The boundary conditions are,

(a) at $y = 0$, $U_1 = V$ and (b) at $y = h_1$, $U_1 = 0$

Since at $y = 0$, $U_1 = V$ hence $C_1 = V$ hence equation (5) becomes

$$U_1 = \frac{p_1'y^2}{2\mu} + \frac{\tau c_1 y}{\mu} + \frac{K}{\mu}\left(\frac{p_1'^3 y^4}{4} + \tau c_1^3 y + p_1'^2 y^3 \tau c_1 + \frac{3}{2}\tau c_1^2 p_1'y^2\right) + V \qquad (6)$$

$$\tau c_1^3 + \frac{3}{2}(p_1' h_1)\tau c_1^2 + \left(\frac{1}{K} + p_1'^2 h_1^2\right)\tau c_1 + \left(\frac{\mu v}{K h_1} + \frac{p_1' h_1}{2K} + \frac{p_1'^3 h_1^3}{4}\right) = 0 \qquad (7)$$

Now, let

$$J_1 = \frac{3}{2} P_1 h_1, \quad M_1 = \frac{1}{K} P_1^2 h_1^2,$$

And

$$N_1 = \frac{\mu v}{k h_1} + \frac{P_1 h_1}{2k} + \frac{1}{4} P_1^3 h_1^3,$$

So that,

$$\tau c_1^3 + J_1 \tau c_1^2 + M_1 \tau c_1 + N_1 = 0 \qquad (8)$$

Also, let

$$\tau c_1 = \phi_1 - \frac{J_1}{3} \qquad (9)$$

Substituting for τc_1 from equation (8) into (9) we get,

$$(\phi_1 - \frac{J_1}{3})^3 + J_1(\phi_1 - \frac{J_1}{3})^2 + M_1(\phi_1 - \frac{J_1}{3})^2 + M_1(\phi_1 - \frac{J_1}{3})^2 + N_1 = 0$$

Which, after substitution for J_1, $M_1 and N_1$ from above and simplification becomes,

$$\phi_1^3 + \phi_1 (\frac{1}{k} + \frac{1}{4} P_1^2 h_1^2) + \frac{\mu v}{k h_1} = 0$$

which may be written as

$$\phi_1^3 + A_1\phi_1 + B_1 = 0 \qquad (10)$$

$$A_1 = \frac{1}{k} + \frac{1}{4}P_1^{\,2}h_1^{\,2}$$

and

$$B_1 = \frac{\mu v}{kh_1}$$

Equation (10) is a cubic equation, which can be solved by applying Cardan's formula as outlines in Appendix B

$$\phi_1 = [\ -q + (\ q^2 + P^3\ )^{\frac{1}{2}}\ ]^{\frac{1}{3}} + [\ -q - (\ q^2 + P^3\ )^{\frac{1}{2}}\ ]^{\frac{1}{3}}$$

Substituting the values of ϕ_1, A_1, B_1 and J_1 in above equation becomes,

$$\tau c_1 = (-\frac{\mu v}{2Kh_1} + (\frac{\mu^2 v^2}{4K^2 h_1^{\,2}} + \frac{1}{27}(\frac{1}{K} + \frac{1}{4}p_1'^2 h_1^{\,2})^3)^{\frac{1}{2}})^{\frac{1}{3}} +$$
$$(-\frac{\mu v}{2Kh_1} - (\frac{\mu^2 v^2}{4K^2 h_1^{\,2}} + \frac{1}{27}(\frac{1}{K} + \frac{1}{4}p_1'^2 h_1^{\,2})^3)^{\frac{1}{2}})^{\frac{1}{3}} - \frac{1}{2}p_1' h_1 \qquad (11)$$

The flow of polymer gives $Q_1 = \int_0^{h_1} U_1\, dy$ (12)

Substituting for U_1 from equation (6) into the above equation and integrating gives,

$$Q_1 = \frac{p_1' h_1^3}{6\mu} + \frac{\tau c_1 h_1^2}{2\mu} + \frac{K}{\mu}\left(\frac{p_1'^3 h_1^5}{20} + \frac{\tau c_1^3 h_1^2}{2} + \frac{p_1'^3 h_1^4 \tau c_1}{4} + \frac{\tau c_1^2 p_1' h_1^3}{2} \right) + V h_1 \quad (13)$$

Also the steady state flow gives, $\frac{d}{dx}(Q) = 0$ Differentiating equation (13) and setting it equal to zero we note that the right hand side of equation (13) is constant As such τc_1 and hence from equation (11)

$$p_1' = \left(\frac{dp}{dx} \right)_1 = const = \frac{p_m}{l_1}$$

where p_m is the pressure at the step and l_1 is the length of the first section of the unit

Continuity of flow gives, $Q_1 = Q_2$ and therefore it is necessary to establish the flow equations for the second part of the unit before P_m can be predicted The steady state flow in the second part of the unit gives,

$$\left(\frac{dp}{dx} \right)_2 = -\left(\frac{d\tau}{dy} \right)_2$$

The boundary conditions are as for part one, so that shear stress in the second unit becomes

$$\tau c_1 = (-\frac{\mu v}{2Kh_1} + (\frac{\mu^2 v^2}{4K^2 h_1^2} + \frac{1}{27}(\frac{1}{K} + \frac{1}{4} p_1'^2 h_1^2)^3)^{\frac{1}{2}})^{\frac{1}{3}} +$$

$$(-\frac{\mu v}{2Kh_1} - (\frac{\mu^2 v^2}{4K^2 h_1^2} + \frac{1}{27}(\frac{1}{K} + \frac{1}{4} p_1'^2 h_1^2)^3)^{\frac{1}{2}})^{\frac{1}{3}} - \frac{1}{2} p_1' h_1 \quad (14)$$

And the flow becomes,

$$Q_2 = -\frac{p_2' h_2^3}{6\mu} + \frac{\tau c_2 h_2^2}{2\mu} + \frac{K}{\mu}\left(-\frac{p_2'^3 h_2^5}{20} + \frac{\tau c_2^3 h_2^2}{2} + \frac{p_2'^2 h_2^4 \tau c_2}{4} - \frac{\tau c_2^2 p_2' h_2^3}{2}\right) + V h_2 \quad (15)$$

Again from steady state flow, $\frac{d}{dx}(Q_2) = 0$, Thus differentiating equation (15) and noting

that τ c2 = constant we have $p_2' = \left(\frac{dp}{dx}\right)_2 = const = \frac{p_m}{l_2}$ where p_m is the pressure at the step

and l_2 is the length of the second section of the unit It is shown that the pressure profile in the first and the second section of the unit is linear It is known that pressure increases the viscosity of polymers and this effect should be included in the analysis for a satisfactory solution With reference to Figure 1 2 a generalised equation relating viscosity and pressure may be shown to take the form [49]

$$\mu = \mu + \frac{a + bp^2}{\gamma}$$

where, a and b are constants and μ is the initial viscosity of non-Newtonian at ambient pressure, γ is the apparent shear rate and is given by γ = v/h

Hence, substituting γ into above equation gives,

$\mu_1 = \mu_o + \frac{h_1}{V}(a + bp^2)$ for the first section and $\mu_2 = \mu + \frac{h_2}{V}(a + bp^2)$ for the second section

The apparent shear rate in the first section is v/h_1 and the apparent shear rate in the second section is v/h_2 Since v/h_2 is much higher than v/h_1 Also the length of the first segment is 4 times grater than the length of the second segment at the lower shear rate the effect of pressure on viscosity is more influential than at the higher shear rate So, considering $\gamma = v/h_1$,

$$\mu = \mu_o + \frac{h_1}{V}(a + bp^2) \qquad (16)$$

Equation (16) enables to calculate the viscosity of the polymer at known pressure and shear rate This equation together with equations (12), (13), (14) and (15) may be solved simultaneously Numerical values of $p = p_m$ and hence p_1' and p_2' may be substituted into the above equations by assuming the value of 'b' in the same manner as in reference [49] and then, progressively changing the value of 'a' until the theoretical and experimental results show close agreement and the equation $Q_1 = Q_2$ is satisfied 'a' is obtained by using an iteration technique Therefore the pressure in the unit, viscosity of the polymer and shear stresses (τc_1 and τc_2) can be determined The pressure values for different velocities when compared with those obtained experimentally from the rheometer enable determination of the constants, a and b The value of constants, pressure and viscosity can of course be determined for any other form of the viscosity – shear rate pressure relationship, eg,

$$\eta = K_2 \gamma^{n-1} \qquad [17]$$

This is the well known " power- law" model and n is called the power-law index K_2 is called the consistency (with the strange unit of $P_a s^n$) [1]

Newtonian model

If the polymer is considered as a Newtonian fluid, the relation between the shear stress, viscosity and shear rate is given by $\tau = \mu(\frac{du}{dy})$ and the pressure at the step is [49]

$$p_m = \frac{6 \mu V (h_1 - h_2)}{\frac{h_1^3}{L_1} + \frac{h_2^3}{L_2}} \qquad (18)$$

Chapter Three

DESIGNING AND COMMISSIONING OF THE RHEOMETRIC DEVICE AND TEST PROCEDURE

3 1 General Description

Experiments were carried out using a general purpose test bench, which has been newly constructed The general view of the test bench is shown in plate 3 1 and Fig 3 1(Schematic diagram) The test bench is approximately 1 5 m long and 1m wide The Rheometric Device is driven by means of an electric motor, squirrel cage 3kw, 380 volts, 3 phase power supply The build-up of speed is determined by the accelerator time set on the frequency inverter, which varies the motor speed settings The actual motor speed (rev/min) is obtained using a remote hand held digital tachometer (Shimpo type DT-205) which measures the speed of a mark rotating on the out-put shaft of the motor The above arrangement facilitated shearing speeds between 0 25 to 2m/sec The accelerator time and remote hand held digital tachometer are shown in plate 3 2 Two pressure transducers were mounted in two different locations in the pressure unit, which enabled the pressure distributions along the unit to be measured The output from the transducers was taken from the RDP data recording unit One thermocouple was mounted to monitor the temperature within the unit The test bench supported all electrical and mechanical equipment and ensured that the drive system was rigid It contains a flat surface area on which experiments can be done safely

3 2 Instrumentation

In order to determine the feasibility of the system and the correlation between the theoretical and experimental results, a number of piece of equipment and variousdevices were used to monitor, control, display and record various parameters during the experimental tests These included pressure transducers, digital magnetic pickup, thermocouple, electric motor, digital tachometer, RDP data unit Details of each are given below

3 2 1 Pressure Transducers

Two pressure transducers (model S/1542-09G) were used to monitor the fluid pressure in the rheometric pressure unit The pressure transducers feature small physical size with an excellent frequency response and are eminently suitable for the measurement of dynamic pressures and pressure transients The S/1542-09G pressure unit is threaded M8X 1, the front face of the unit providing a flat surface for sealing The bonded strain gauge system results in a robust transducer of high accuracy that is suitable for both static and dynamic pressure measurements The maximum working pressure limit of 1000 PSIG, calibrated at 1000PSIG and with a maximum excitation voltage of 5 volts, calibration factor 2 3614MV/V, shunt resistor 59KΩ Plate 3 5 shows the pressure transducers

3 2 2 Digital Magnetic Pickup

The model RS304-172 pickup provides a digital pulse output whenever there is an abrupt change from non-magnetic to magnetic material moving past the piece The rise –fall times and amplitude of the output pulse are independent of the characteristics and speed of the magnetic discontinuity The maximum rise time is 1000 nanoseconds, the maximum fall time is 50 nanoseconds The magnetic pickup was connected between the motor and the shaft The shaft of the machine was driven by means of the motor via the digital magnetic pickup Plate 3 3 shows the magnetic pick up in place

3 2 3 Thermo-couple

To monitor the temperature continuously, a K type thermocouple "fibre glass insulated with 2 mm insulation diameter" was used to carry out the experiments The working temperature range of the thermocouple is 0 to +45 ^{0} C This is shown in plate 3

3 2 4 The Variable Speed Motor

A variable speed motor , standard squirrel cage 3 kW, 380 volt, 3 phase power supply was used This was estimated to give the motor an operating speed range of between 150-2800 RPM, but in reality gave a speed range of 100-2600 RPM The motor's direction can be altered easily The electric motor can be over speeded The sizing of the motor was carried out allowing 50% factor of safety The motor is shown in plate 3 3

3 2 5 Digital Tachometer

A digital tachometer was used to either monitor or to control the speed of the shaft It had a frequency regulator to control the speed The frequency was directly read from the tachometer It was manually controlled to increase or to decrease the speed of the shaft The frequency inverter was normally operated from the remote control unit From the remote control unit, one could run the motor forward or reverse, start or stop the motor, adjust the speed of the motor and read the frequency at which the motor was being run at

3 2 6 RDP Unit

The E308 is a comprehensive transducer indicator instrument providing signal conditioning, excitation and ±19999 digit indication for strain gauge type transducers such as load cells, etc and for transducers with built-in electronics producing high output (e g 5 volts) signals The two pressure transducers were connected to the RDP unit Transducer 1 was connected to RDP1and Transducer 2 was connected to RDP2 RDP1 was callibrated at 631 and RDP2 was callibrated at 275 according to their shunt resistance The RDP unit is shown m plate 3 2

3 3 Design of the Rheometric Device

The principal objective of the experimental programme was to develop a novel Rheometric Device and to investigate the pressure dependent rheological

properties of non-Newtonian fluids The Rheometric Device developed is actually a stepped gap pressure hydrodynamic unit made from mild steel parts The total length of the pressure unit is 15cm which consists of the pressure cylinder, two sets of inserts, the central shaft, the pressure end plate, and the shaft end plate The original layout of the pressure unit can be seen in plate3 2 and plate 3 4 The detailed design of the pressure unit is shown in Figs 3 2 and 3 3 It was designed so that one could gain easy access to the pressure unit without having to dismantle the whole unit

3 3 1 Insert 1

The length of each of the three insert 1 is 40mm and the widths are of insert is 24 2, 24 5 and 24 7mm The Insert1 is attached to the outer casing by two M6 socket head cap screws (SHCS) The screws were drilled in 15mm deep and copper sealing was used to prevent leakage through the threads of the screws There is a hole in the middle of insert1 to mount the pressure transducer When the shaft rotates, pressure develops within the units and the pressure reading was obtained from the RDP unit The details of the insert 1 is given in Fig 3 4 And a photograph of the insert 1 is shown in plate 3 7

3 3 2 Insert 2

The length of the insert 2 is 10mm and width is 24 9mm The Insert 2 is attached to the outer casing of the pressure unit by SHCS in two places One pressure

transducer was mounted in the middle of the insert 2 The screws were drilled in 15mm deep and again copper sealing was used to prevent leakage through the threads of the screws The pressure reading was obtained from the RDP unit The Insert 2 was attached adjacent to insert 1 within the pressure cylinder The detailed drawing is shown in Fig 3 5 The photograph of the insert 2 is shown in plate 3 7

3 3 3 shaft

The Pressure chamber consists of two inserts, shaft and pressure end plate The shaft is rotated inside the pressure chamber The shaft is a solid cylinder whose diameter is 50mm and the length is 90mm and is made of stainless steel The shaft was supported by two Fag6012 type bearings The shaft was attached to the shaft end plate and there is a V groove for fixing a 'O' ring The dimension of the o ring is 3 0widex2 0deep The shaft is attached to the motor via the digital magnetic pick-up A frequency inverter to regulate the frequency adjuster can regulate the shaft speed The output shaft speed was monitored using the tachometer The detailed design of the shaft is given in Fig 3 6 Plate 3 3 shows a photograph of the shaft

3 3 4 Pressure End Plate

The pressure end plate was made of mild steel The diameter of the pressure end plate is 150mm The thickness is 6mm The end plate is attached to the pressure chamber by four M8 bolts The bolts were drilled through 6 5mm dia on a 125mm

P C D in four places The drawing is shown in Fig 3 7 Plate 3 8 shows the pressure End plate

3 3 4 Shaft end plate

The diameter of the shaft end plate is150mm The thickness is 15mm The end plate is attached to the pressure cylinder by four M8 bolts The bolts were drilled through 8 5mm diameter on a 125 P C D in 4 places The drawing is shown in Fig 3 8 and plate 3 8 shows the shaft end plate

3 4 Design of the Electrical Installation

The electrical system for the bench were designed so as to allow multi-user facilities with associated interlocks so that equipment cannot be turned on without its control sensor to monitor the process

The electrical installation basically is divided into two parts -

1 The electrics for the motor

2 The electrics for the RDP unit

The bench was to be connected by a 3 phase plug to the main supply and all electrical on the bench were isolated from the outside by means of a 3 phase isolated switch and a fuse box From the fuse box, electricity was fed to the motor controller and the RDP unit From the fuse box, the 3 phases were brought to the KEB

combivert 56-frequency inverter The 3KW motor was then connected from this inverter by means of a shielded cable Photo 3 6 shows the shielded electrical insulation

3 5 Test procedure with the Novel Rheoemetric Device

Experimental work was carried out using the purpose built test bench instrumented to measure the drawing speed, the temperature and the hydrodynamic pressure distribution within the stepped gap pressure unit The schematic diagram of the test bench is shown in Figure 3 1 The motor was attached to the shaft of the pressure unit via a coupling (magnetic pick up) for running the machine

The test bench is instrumented to facilitate continuous monitoring and recording of the pressure with the pressure transducers, which were mounted on the pressure unit at two different points to measure the pressure Thermocouples were used to monitor the temperature The shearing speed of the shaft was measured using a digital tachometer

In carrying out the experiments, the following procedure was followed

First the hydrodynamic pressure chamber was cleaned out mechanically and assembled together To prevent leakage during the test period, all the parts of the unit were sealed properly Then the pressure chamber was filled with enough fluid for a complete test programme The pressure transducers were connected to the RDP unit The RDP1 and RDP2 were calibrated at a desired value After switching on, it was ensured that the readings from the RDP were not stable The readings from the RDP unit were made at the calibrated value and after one hour the readings were at the

desired calibrated value Then the RDP units were switched on from the calibration level and the readings were made to reach zero level About an hour was needed for the of RDP reading to reach zero level The speed of the motor was increased slowly to a certain speed by the accelerator set on the frequency inverter The pressure within the unit was recorded from the RDP unit keeping the temperature constant at 25 ± 1^0 C for the selected speed The temperature was monitored from the thermocouple The speed of the motor was monitored from the digital tachometer For each speed and every fluid at least 6 data were recorded At the end of each test, the speed of the motor was increased and the pressure reading and the temperature were recorded Tests were carried out for at least 4 speeds for the same fluid and the same insert combinations After completing the tests, the insert 1 was changed and a similar number of data were recorded for the same fluid Then both the fluid and the insert 1 were changed and tests were carried out following the same procedure At the end of each test, the motor and the display units were switched back to their original positions, the test number was recorded on the data sheet and all the parameters were recorded for subsequent collection and analysis

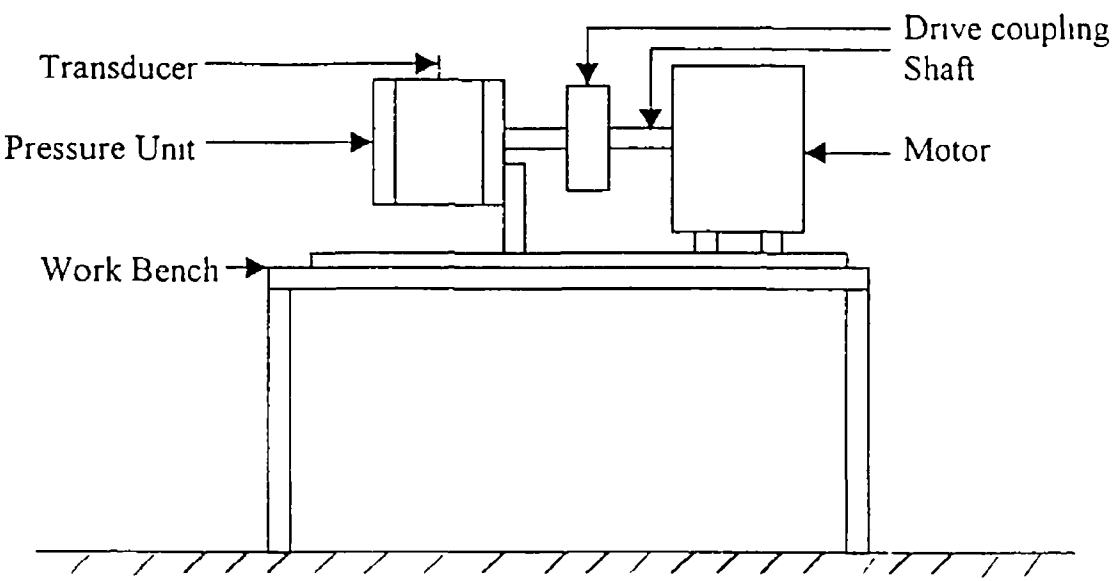

Fig 3 1· Schematic diagram of the drawing bench

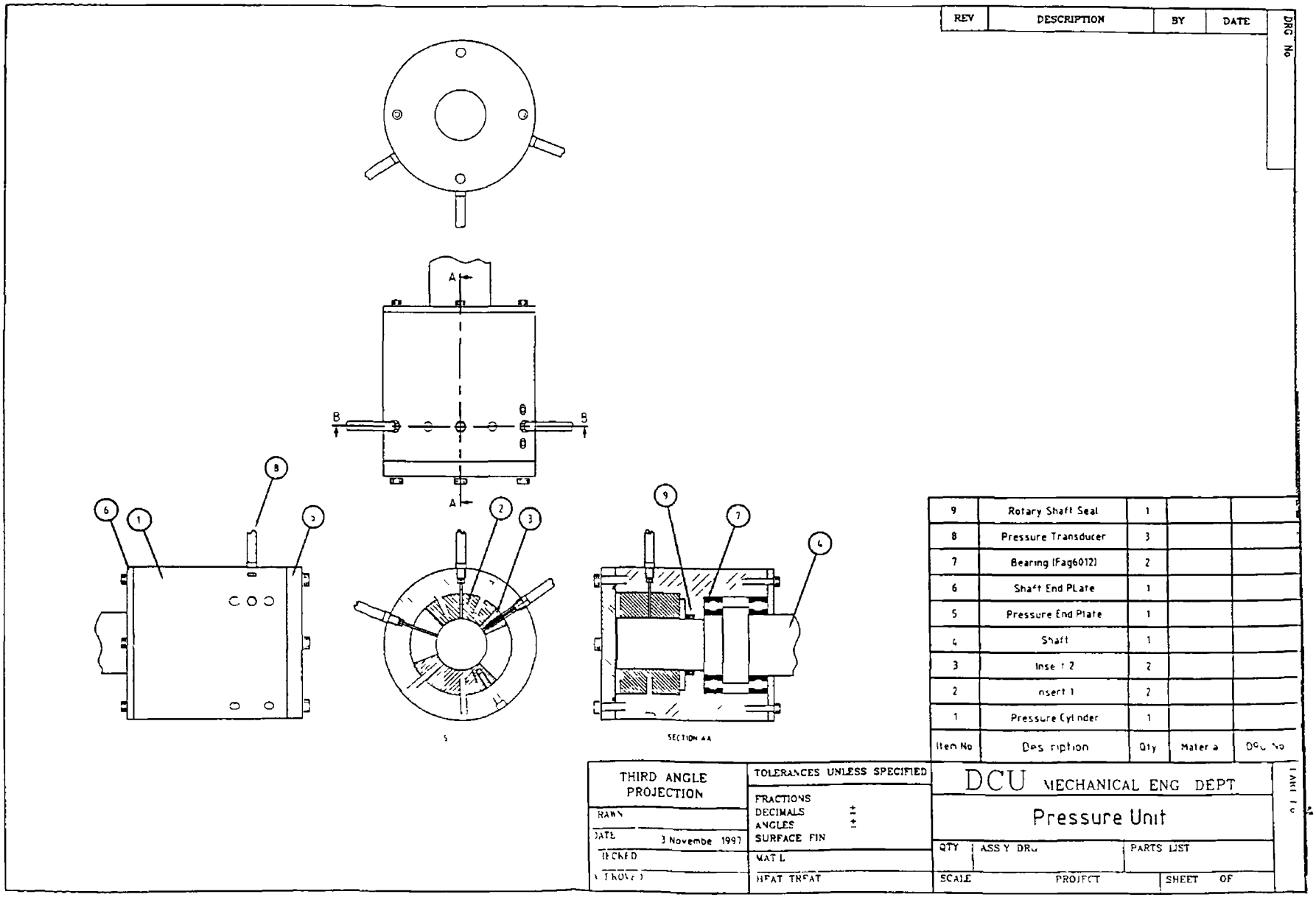

Fig. 3.2: Pressure Unit.

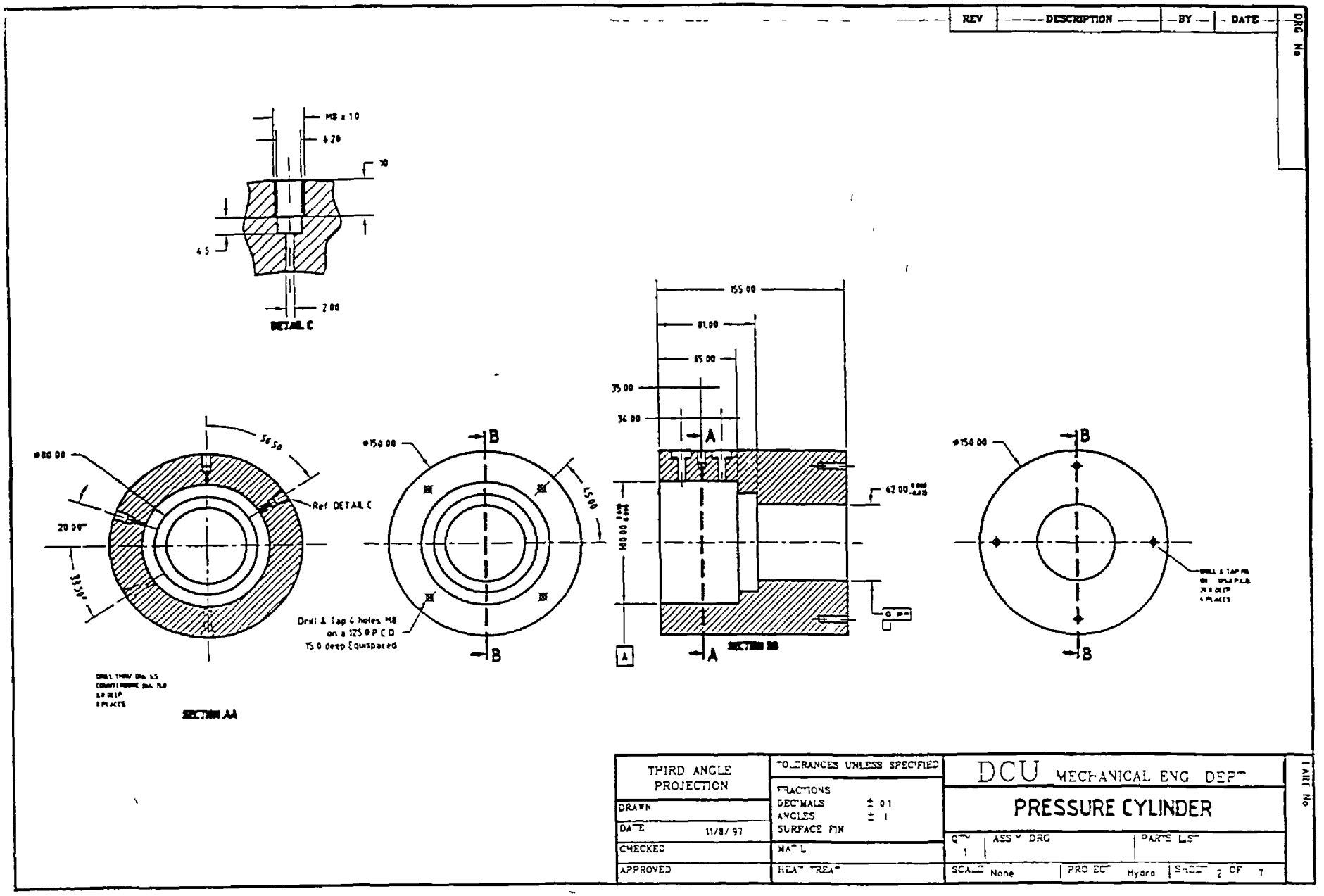

Fig 3 3· Pressure Cylinder

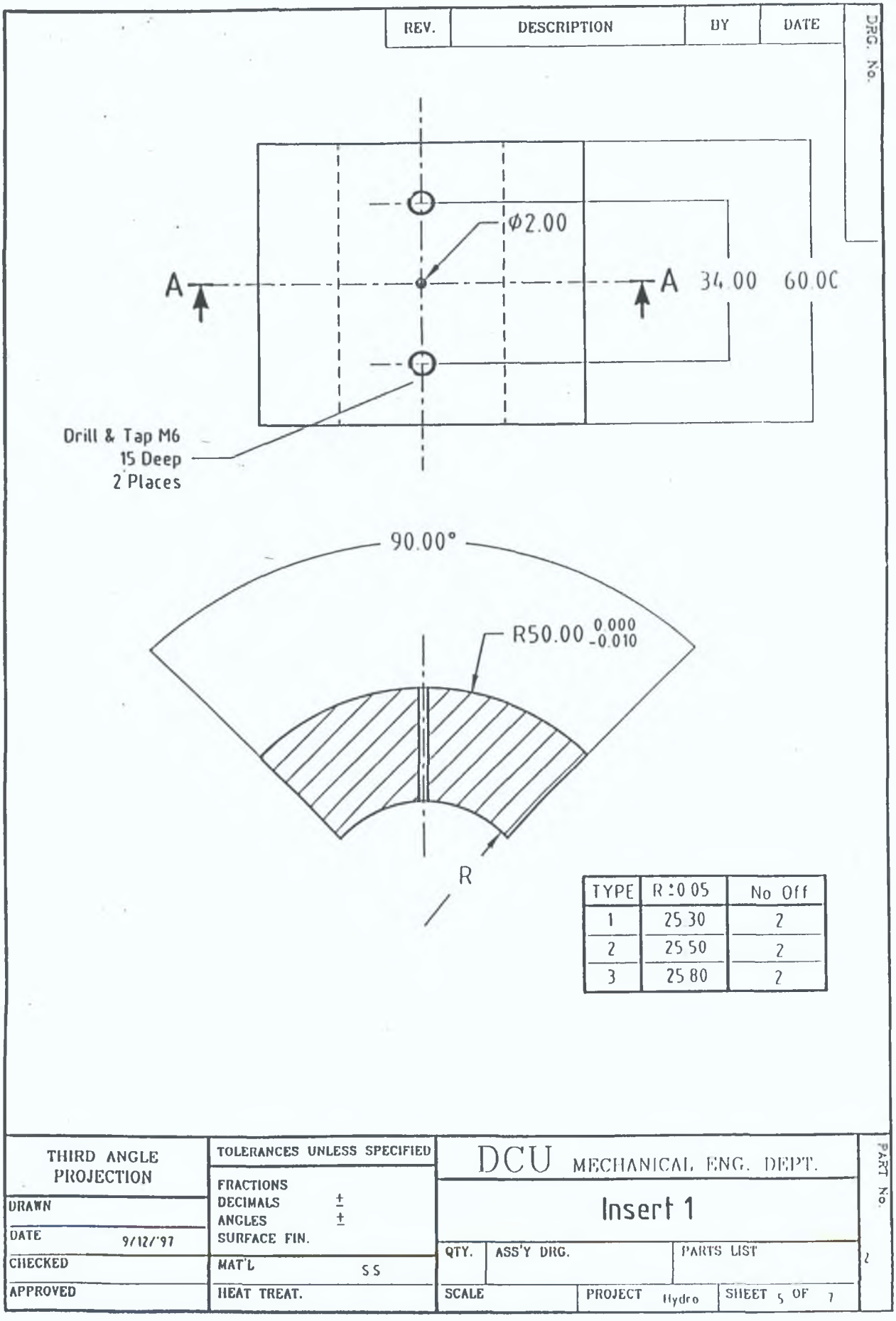

Fig.3.4: Insert 1.

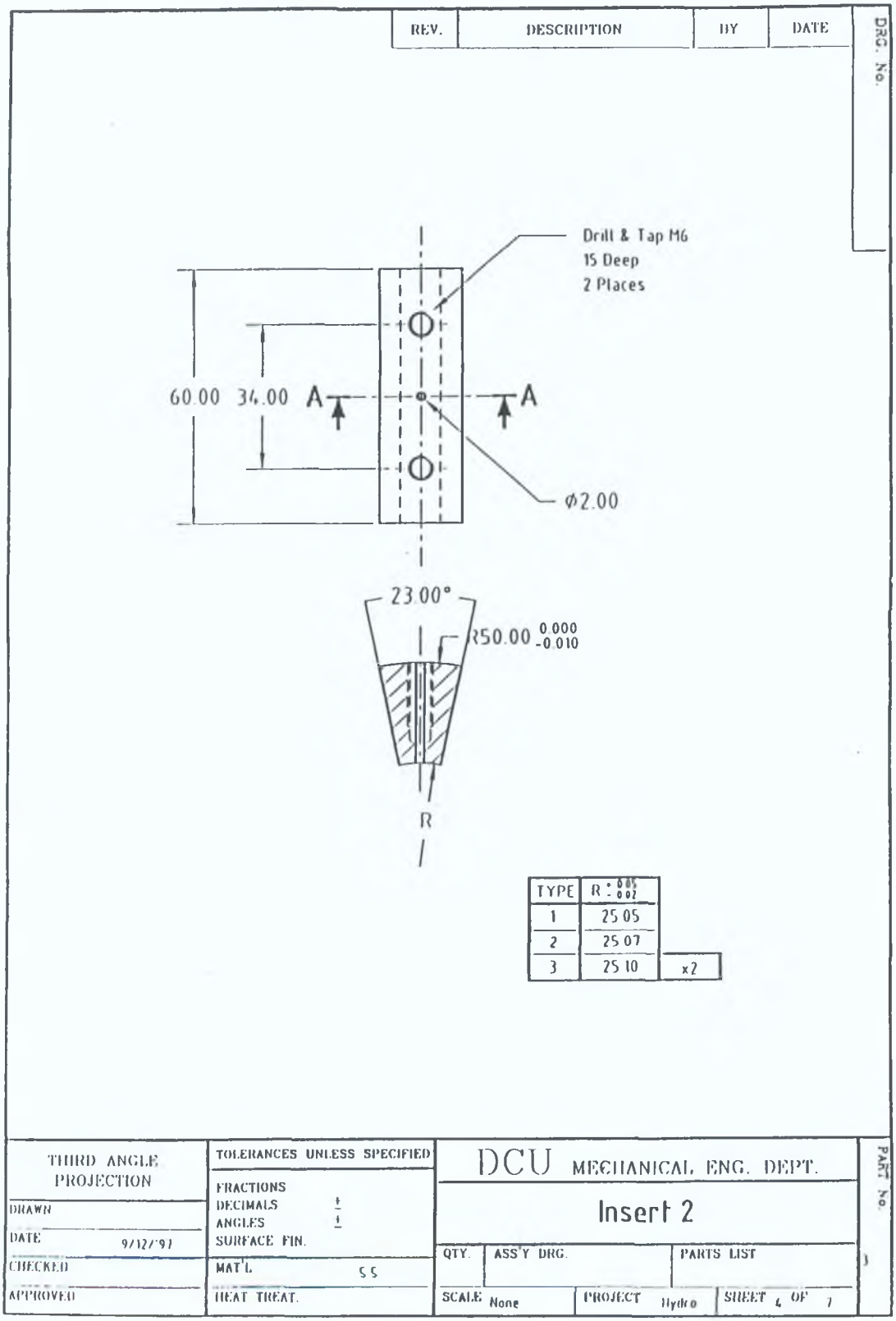

Fig.3.5: Insert 2.

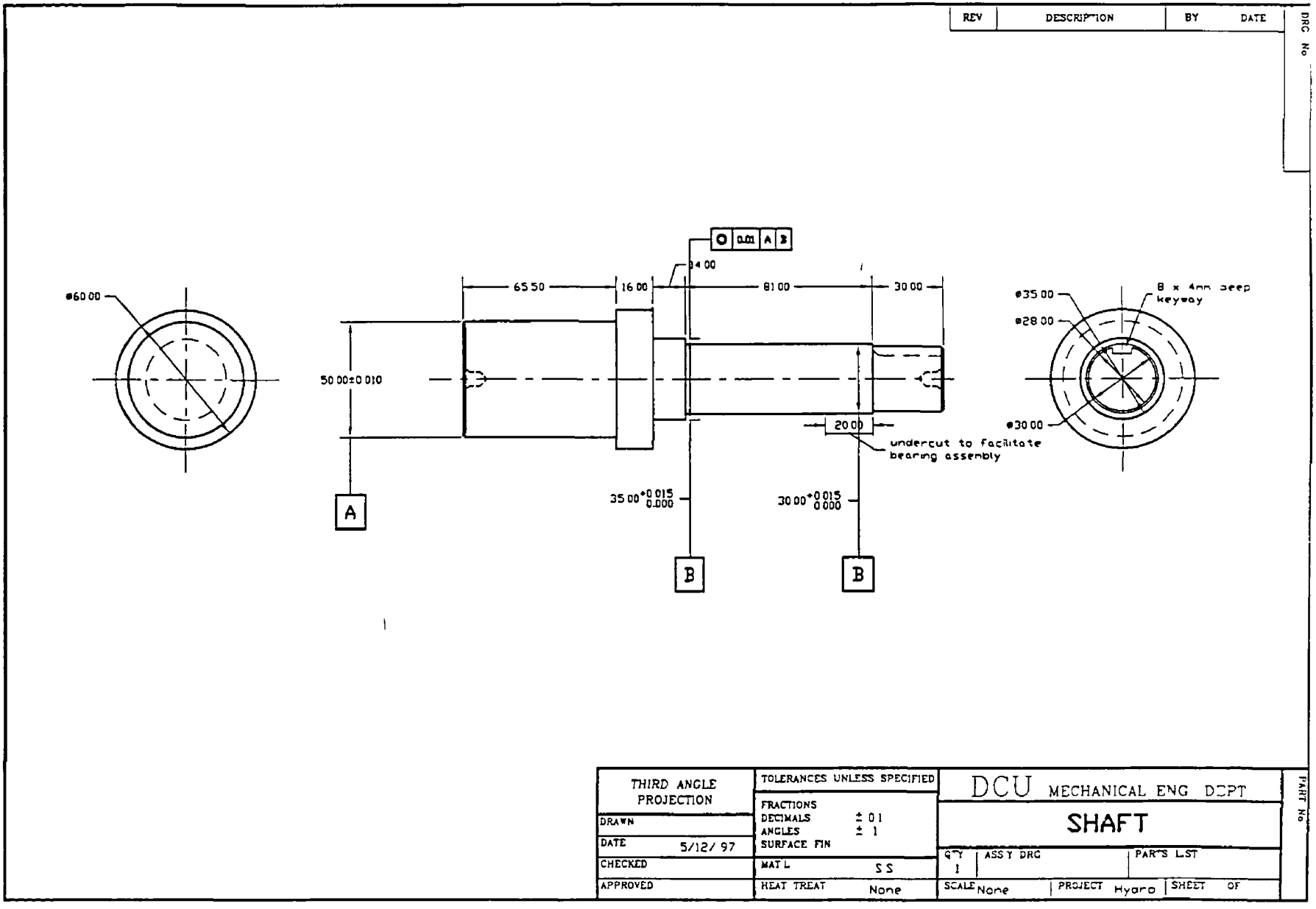
REV
DESCRIPTION
BY
DATE
DRG No
Ø60 00
50 00±0 010
65 50
16 00
4 00
81 00
30 00
20 00
undercut to facilitate bearing assembly
35 00 +0 015 0 000
30 00 +0 015 0 000
A
B
B
Ø35 00
Ø28 00
Ø30 00
8 x 4mm deep keyway
THIRD ANGLE PROJECTION
DRAWN
DATE 5/12/97
CHECKED
APPROVED
TOLERANCES UNLESS SPECIFIED
FRACTIONS
DECIMALS ± 0 1
ANGLES ± 1
SURFACE FIN
MAT L SS
HEAT TREAT None
DCU MECHANICAL ENG DEPT
SHAFT
QTY 1
ASSY DRG
PARTS LST
SCALE None
PROJECT Hydro
SHEET OF
PART No

Fig 3 6· Shaft

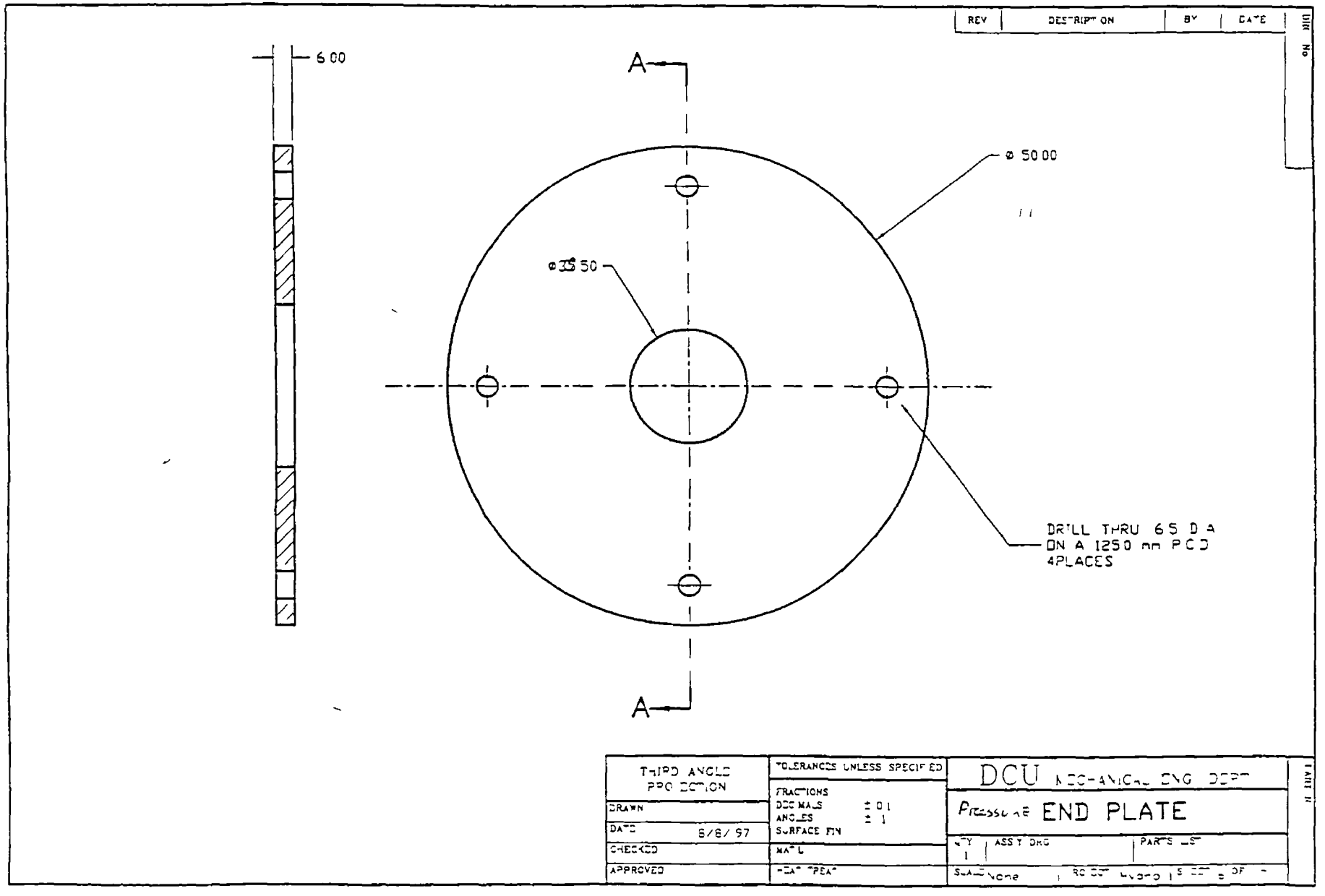

Fig. 3.7· Pressure End Plate.

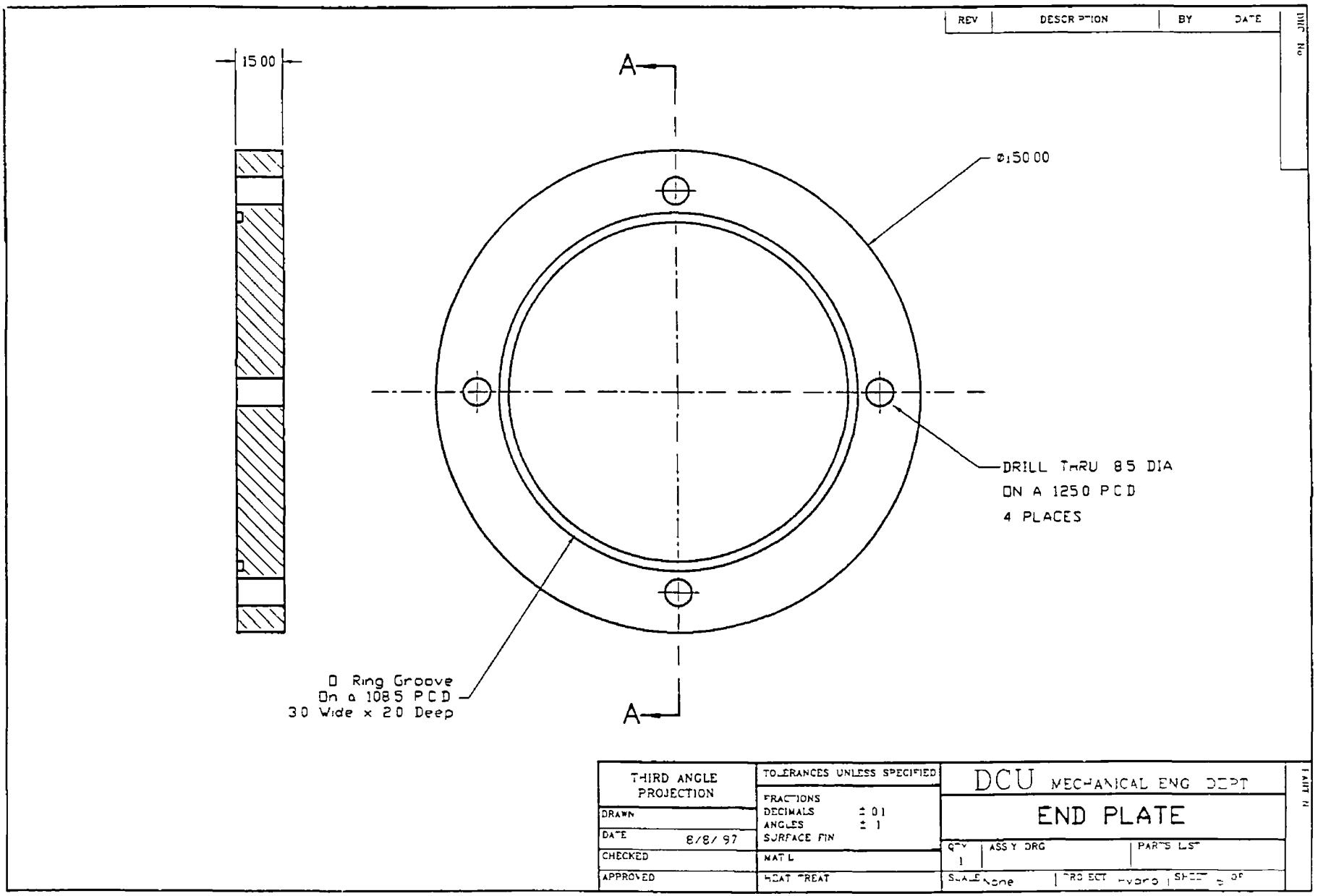

Fig 3 8 Shaft End Plate

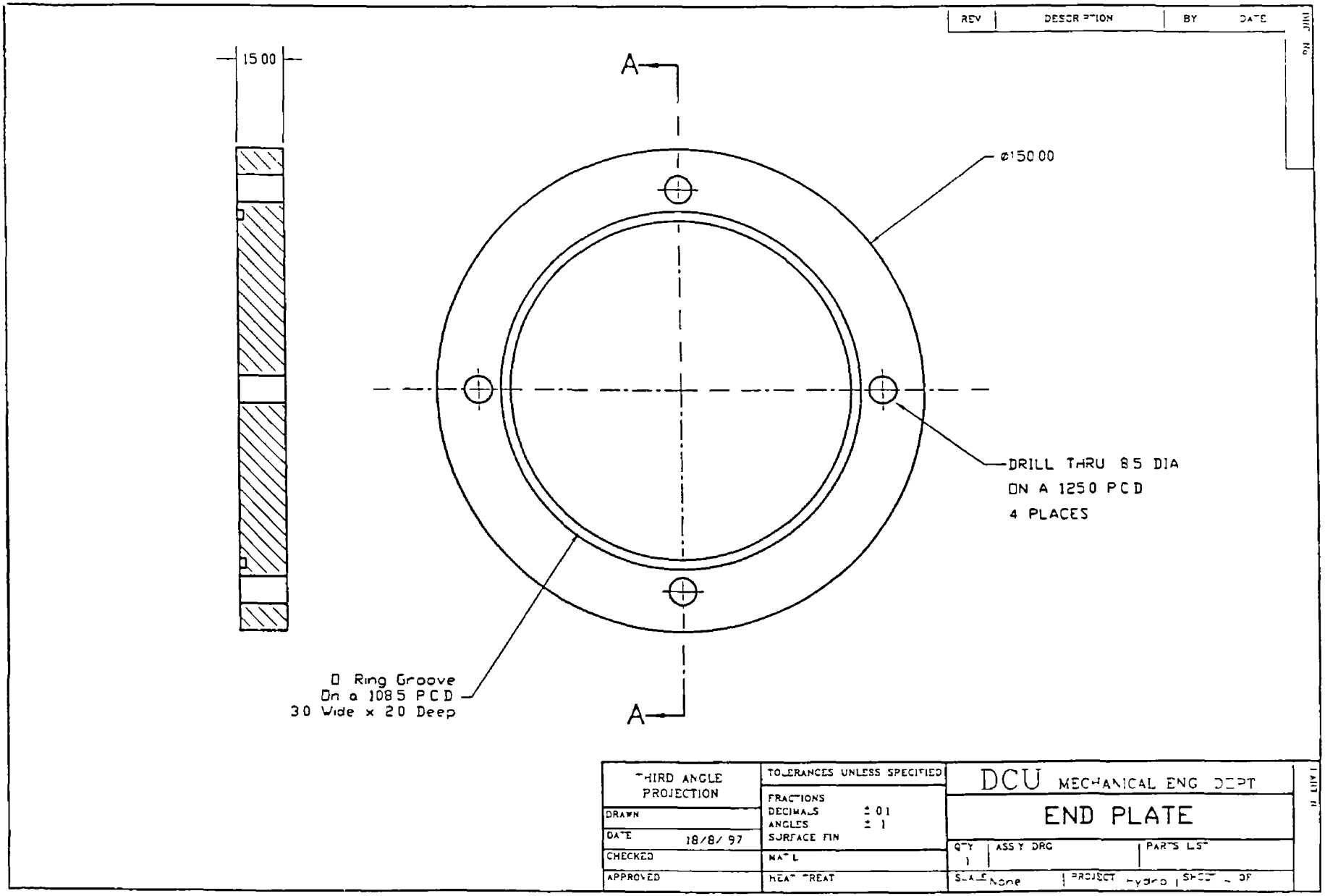

Fig 3 8· Shaft End Plate

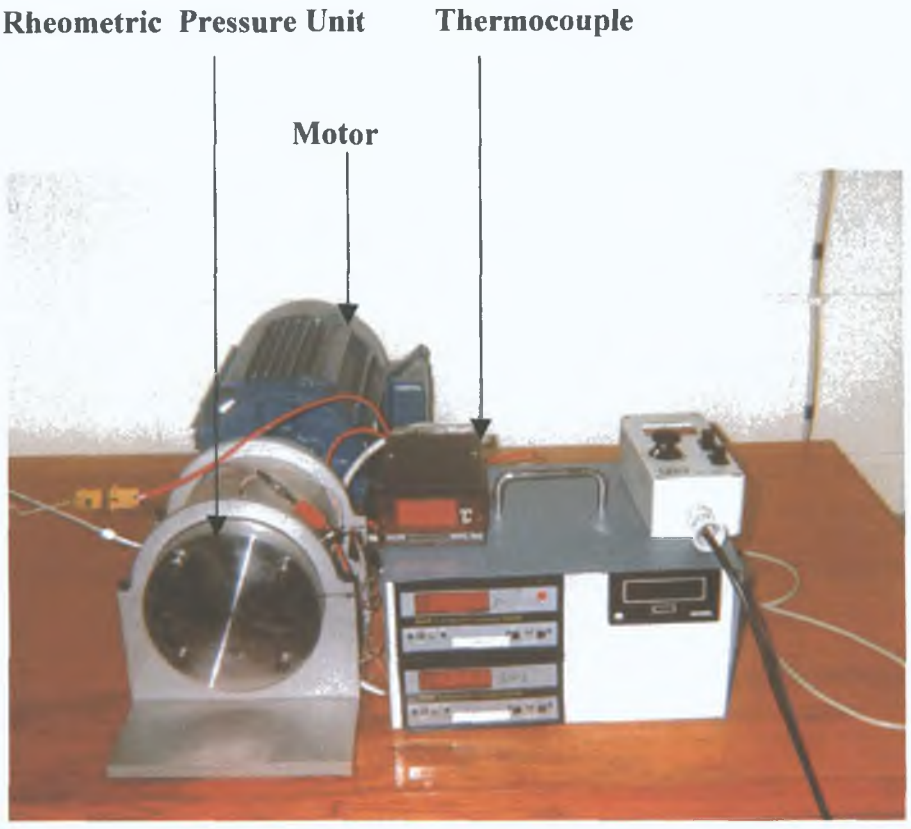

Plate 3.1 : Overall view of the rig.

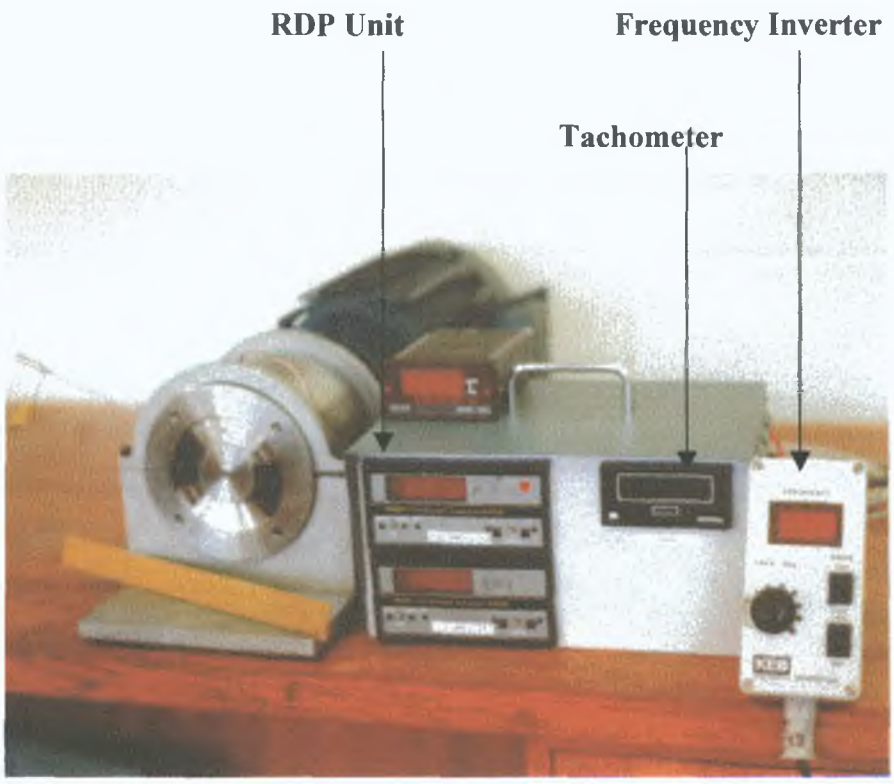

Plate 3.2: RDP Unit, and frequency Inverter.

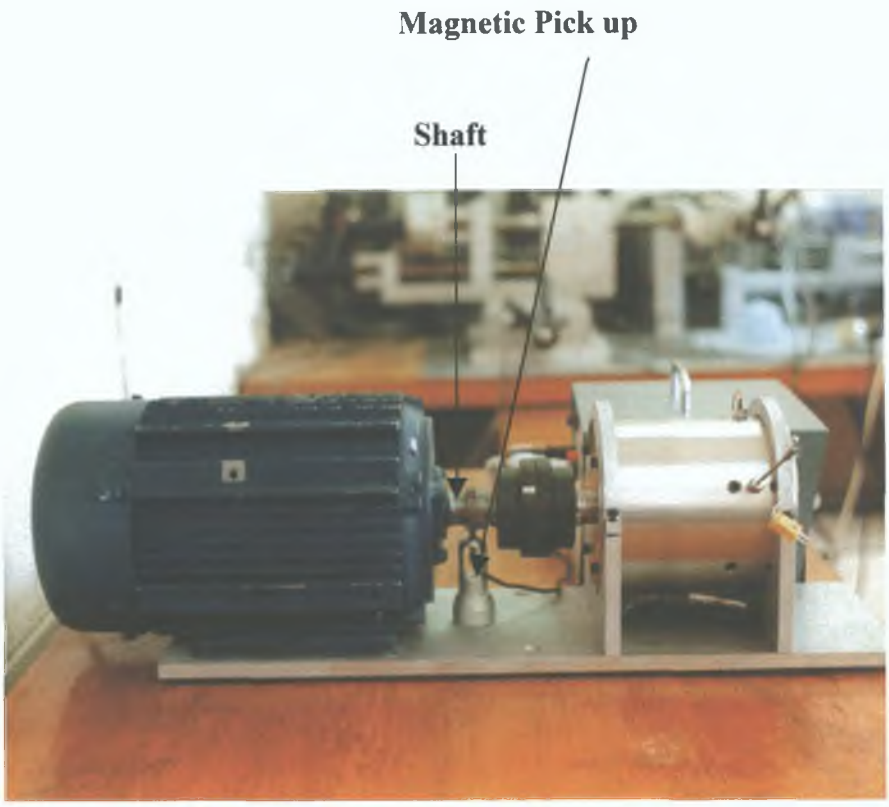

Plate 3.3 : Electric motor and magnetic pickup.

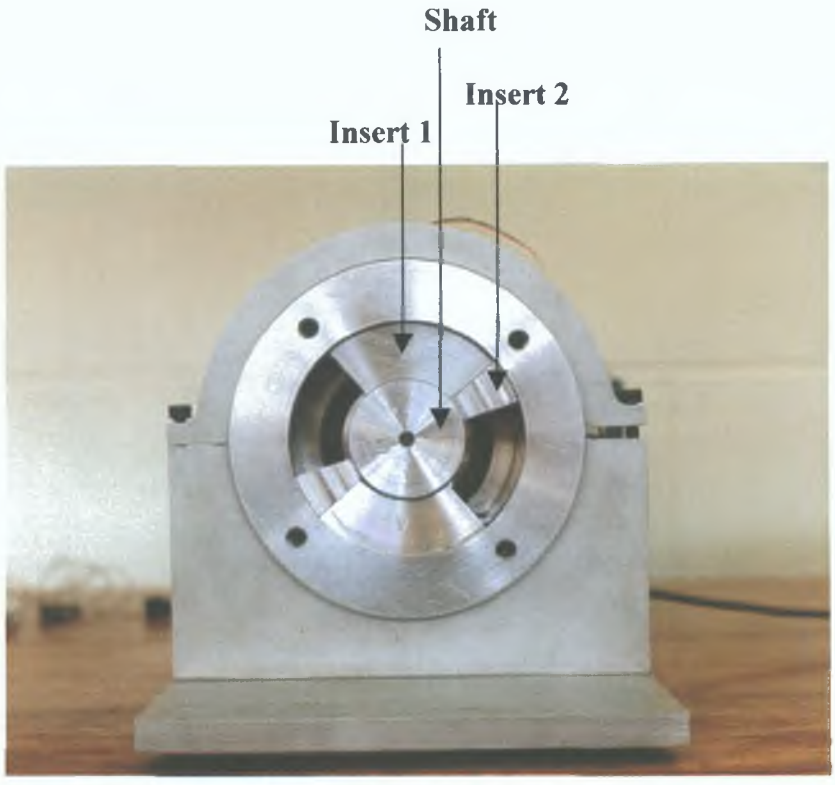

Plate 3.4: Pressure Chamber.

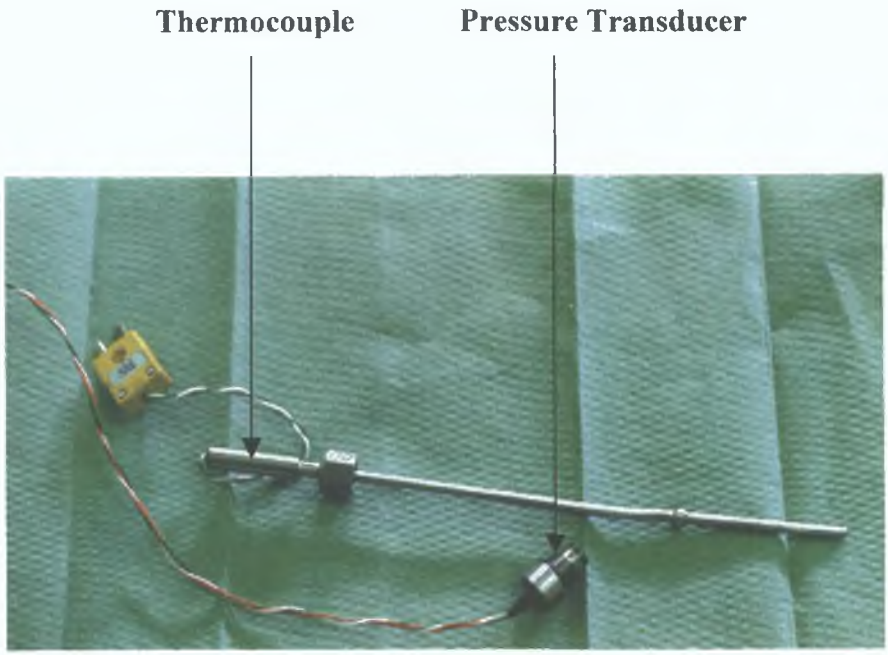

Plate 3.5 : Pressure transducer and thermocouple.

Plate 3.6: Electric Controller.

Plate 3.7: Insert 1.

Plate 3.8: End Plate.

Chapter Four

EXPERIMENTAL WORK AND MATERIAL

4 1 The high Pressure Rheometric Device and the Test Procedure

The details of the new rheometric device and the experimental procedure were described in chapter three However a brief description of these is repeated here The experimental set-up consists of the test bench, the electrical installation, the drive system, the motor, the pressure unit, thermocouple, pressure transducer, Schematic diagram of the process is shown in Fig 3 1

The pressure chamber was filled with the selected fluid for a complete test programme Two-pressure transducers and one thermocouple were connected to the pressure unit

The pressure transducers were connected to RDP unit and calibrated at a desired value After switching on, the reading of the RDP unit was to set the desired values It takes about one hour to establish the RDP setting Then switching on the frequency inverter in reverse direction for running the motor it was set at a desired speed, keeping the temperature at 25 ± 1°C The pressure readings from the two transducers were taken For each set of inserts at least 6 readings were taken at the same speed for the same fluid For different fluids and different speeds a number of experiments were carried out

4 2 Working Principle of the Device

The new rheometric device (Fig 4 1) consists of two cylinders, one is the hollow fixed cylinder and the other is a rotating solid shaft The gap between the two surfaces was filled with viscous non-Newtonian fluid The shaft is attached to the motor via a coupling Two pressure transducers were attached to the pressure unit to monitor the pressure developed in the unit The shaft can be rotated at different speeds to generate different shear rate and due to drag force, hydrodynamic pressure develops At different shear rates, different pressure readings were obtained A thermocouple has been inserted into the pressure unit at the position A shown in Fig 4 1 to monitor the fluid temperature continuously

4 3 The Pressure Fluid

Polymer melts have been used in die-less drawing process by previous workers because of their inherent high viscosity, which permitted reduction of length of the required pressure unit, offered the flexibility and the provision of a coating of the product for several industrial applications Several types of polymer melts have previously been tested to meet various industrial requirements in which a melt chamber was heated to a temperature suitable for the particular polymer, which has been used at the entry end of the pressure unit

The present experimental investigation concentrates on the performance of the high-pressure rheometric unit using glycerine and two silicones with vastly different viscosities, 5 and 12 5 N Sec/m^2 Glycerine, a very important polyhydroxy alcohol, has been traditionally produced as a by-product in soap and fatty acid

industry It was produced for the first time on a large scale using the sulphite-steered yeast process during World War I when demanded for glycerol as explosives for wartime use exceeded the supply from the soap industry [73]

The term glycerol applies only to the pure chemical compound 1,2,3-propanetriol CH_2OH $CHOH$ CH_2OH The term glycerine applies to the purified commercial products normally containing >95% of glycerol Several grades of glycerine are available commercially, which differ somewhat in their glycerol content and in other characteristics such as colour, odour and trace impurities Glycerine is a clear, water-white, viscous, hygroscopic liquid with a sweet taste at ordinary room temperature above its melting point Glycerine is completely soluble in water and alcohol, lightly soluble in diethyl ether, ethyl acetate and dioxane and insoluble in hydrocarbons Glycerine has a high boiling point of 290 $^{\circ}C$ at atmospheric pressure [74]

The study of the chemistry of silicon and its compounds began with the discovery of the element in 1824 Silicon polymers are made from organosilicon intermediates prepared in various ways from elemental silicon, which is produced by reducing quartz in an electric furnace The silicon fluids are low polymers produced by the hydrolysis reaction [75]

The silicon fluids (polydimethyl silonone) are widely used in many industrial applications due to their numerous advantages In particular, they are transparent liquids that have remarkable mechanical, chemical and thermal stability Among other features, they have low surface tension coefficients, around 20dyn/cm, and high zero shear viscosity values of upto 30,000 mpa s

Silicons are polymers melted at ambient temperature Consequently they can be used in cold state They have been commonly used in the production of fibre-optic

cables They are common place in many industrial-coating mixtures in paper coating processes In general, silicon fluid has been used in coating, seals, gaskets, adhesives, and medicine [76] These compounds are used for paper and textile treatment In the present study, the rheological properties of two silicon fluids with viscosities of 5 and 12 5 N Sec/m^2 have been discussed For the shake of brevity these fluids will be called silicon 5 and silicon 12 5 respectively

4 4 Brookfield Digital Viscometer (Model DV-1+ Version 2 0)

A number of tests were carried out using a BDV to determine the viscosity of the fluids used in this study Three tests provided viscosity values at shear rates of upto 2-29 sec^{1} and at atmospheric pressure only

The Brookfield DV-1+ Viscometer measures fluid viscosity at lower shear rates The principle of operation of the DV-1+ is to drive a spindle (which is immersed in the test fluid) through a calibrated spring The viscous drag of the fluid against the spindle is measured by the spring deflection Spring deflection is measured with a rotary transducer The measuring range of a DV-1+ is determined by the rotational speed of the spmdle, the size and the shape of the spindle, the container and the full scale torque of the calibrated spring The viscometer can measure the viscosity in the range 15 m Pas to 2,000,000 m Pas and with the spindle no 16 for the shear rate range of is 0 to 29 0 per second For this shear rate range the viscosity will be between 120 to 400,0000 m Pas [77] Plate 4 1 shows the Brookfield viscometer

4 5 Test Procedure with the Brookfield Viscometer

The power cord to the socket on the back panel of the instrument is connected and plugged into the appropriate AC line

4 5 1 Autozero

Before taking any reading, the viscometer must be Autozeroed Once power switch is turned to the on position, the DV-1+ is in autozero sequence After removing the spindle and the pressing key, the viscometer becomes autozeroed

4 5 2 Spindle Selection

Spindle selecting screen displays a screen indicating as shown below

Cp 0 0	sp 01
0 0 RPM	%0 0

where cp = viscosity, sp = select spindle, RPM = speed, % = % of torque The spindle was chosen LV4 and it was attached to the lower shaft The shaft was lifted slightly, held it firmly with one hand while screwing the spindle on with the other hand The spindle was inserted and centered in the test material until the fluid level is at the immersion groove in the spindle's shaft The code was 64 for the spindle LV4 Pressing the "SELECT SPINDLE" key and using the up and down arrow, the code of the spindle was made 64

4 5 3 Speed Selection

There are 18 speeds programmed into the standard DV-1+ The viscometer speed was chosen by pressing the "UP" and "DOWN" arrow keys The speed and the viscosity readings were selected or noted when the % torque was greater than 10% For different sets of speeds, the viscosity readings have been recorded The same procedure was carried out for different types of fluids

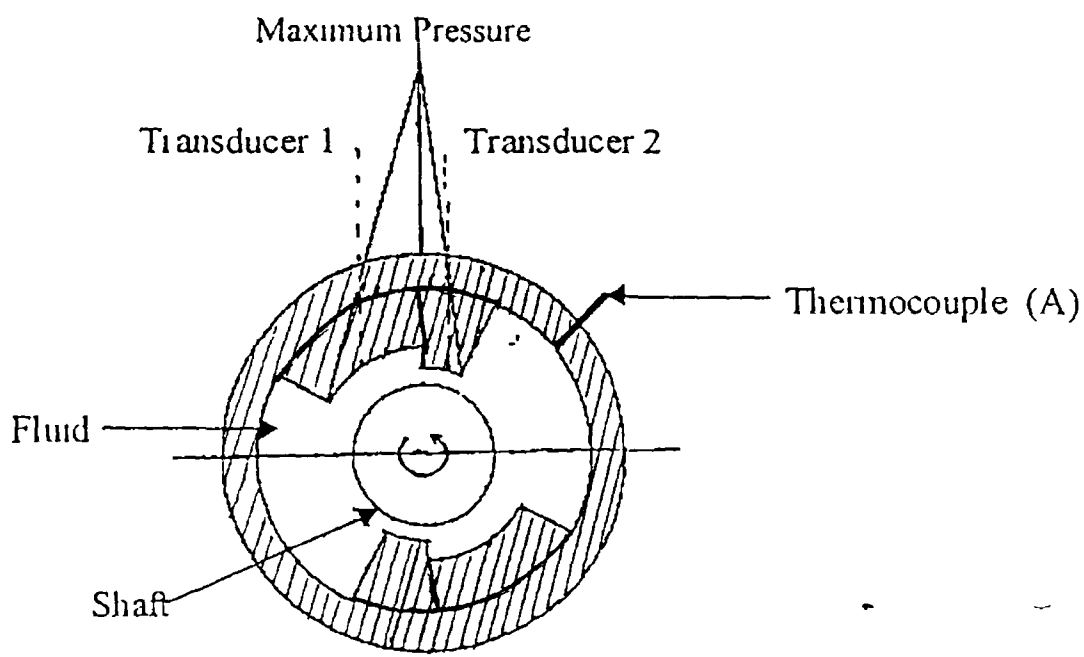

Figure 4 1 Schematic diagram showing the pressure unit

Plate. 4.1:BROOKFIELD Viscometer.

Chapter Five

RESULTS AND DISCUSSIONS

5 1 Introduction

Experimental results obtained by using the novel Rheometric Device (the stepped gap pressure unit) and the Brookfield Viscometer are presented in graphical form in this section A number of experiments were carried out to investigate the performance of the unit by using glycerine, silicon 5 and silicon 12 5 as the pressure medium In obtaining experimental results, the inlet gap h_1 was changed whilst the outlet gap h_2 was kept constant at 0 1 mm

To achieve change in gap ratios, the parameter h_1 was changed to 0 8 mm, 0 5mm and 0 3 mm The temperature was kept constant at18 $\pm$ 1°C for glycerine and 25 + 1°C for the silicon 5 and silicon 12 5 For each gap ratio, tests were performed at linear speeds of between about 0 25 m/sec and about 2 0m/sec for both types of fluids Using the Brookfield viscometer the viscosity values were measured at atmospheric pressure and at shear rates between 2 to 29 sec^{-1}

5 2 Results of Pressure

The generated pressures in the stepped parallel gap pressure unit of the Rheometric Device were measured by means of pressure transducers, which were mounted on the unit

The results of the pressures are divided into two sections

(i) The pressure profiles along the length (pressure distribution)

(ii) Maximum pressure Vs speed

5 2 1 Results of the Pressure Distribution

Pressure distribution within the stepped gap pressure unit, based on experimentally measured pressure at two different locations, one in the middle of the first insert of the unit and the other in the middle of the second insert of the unit, have been obtained and plotted for the gap ratio h_1/h_2 = 8, 5 and 3 These results exhibited similar trends with slight differences as the ratios and speeds were altered Pressures were found to increase from the entry point of the stepped parallel gap in the unit towards the location of the first pressure transducer and the step and decreases after the step A straight line is drawn through the zero pressure at the entry part of the unit and the pressure reading at the location of the transducer 1 and is extended up to the step A second line is drawn from the step to the pressure reading at the transducer 2 and is then extended to the exit end of the unit where the pressure is again zero The pressure distribution line from the location of transducer 1 to step and from the step to the location of transducer 2 is shown as a dotted line in the figures The pressure readings at the entry and the exit points of the unit are zero The pressure at the step could not be measured since it was found difficult to mount a pressure transducer there without damaging the step configuration

Fig 5 1 shows the pressure profiles for glycerine for different velocities at the gap ratio (h_1/h_2=3) It is evident from fig 5 1 that for the range of shearing speeds considered, the maximum pressure occurs at the step and that this maximum pressure

increases with the shearing speed For example, at the shearing speed of 0 5 m/sec, the maximum pressure is about 4 bar whereas at 1 5 m/sec shearing speed, a, maximum pressure of 13 bar is obtained Fig 5 2 shows the pressure distribution of glycerine for different velocities at the gap ratio of 5 The maximum pressure is about 3 bar when the velocity is 0 5m/sec and the maximum pressure is 9 bar at the velocity of 1 5m/sec which is higher than the maximum pressure at the speed of 0 5m/sec Fig 5 3 shows the pressure distribution for glycerine at the gap ratio of 8 for different velocities Fig 5 3 shows the similar trends as those in Figs 5 1 and 5 2, i e as the shearing speed increases, the maximum pressure increases Fig 5 4 shows the pressure profiles for glycerine at the speed of 0 5 m/sec at three different gap ratios For a higher gap ratio (gap ratio of 8) the maximum pressure 2 3 bar was obtained at the shearing speed of 0 5 m/sec which is low compared to the maximum pressure at the lower gap ratio From the figure 5 4 it is evident that the higher the gap ratio lower is the maximum pressure Figs 5 5 and 5 6 show the pressure profiles for glycerine at the speed of 1 0 m/sec and 1 5 m/sec at three different gap ratios These two figures (Figs 5 5 and 5 6) show the similar trend as in Fig 5 4

Figs 5 7 to 5 12 show the pressure distribution curves for silicon fluid whose viscosity is 5 Ns/m^2 Fig 5 7 shows the pressure distribution curve for silicon 5 at the gap ratio of 3, the shearing speed is 0 25m/sec and 0 5m/sec Fig 5 8 shows the pressure profile at the same gap ratio and the shearing speed of 1 0-2 0m/sec These figures show that the pressure increases with the increase of speed Figs 5 9 and 5 10 show the pressure profile for silicon 5 at the gap ratio of 5 From the Fig 5 9 results of maximum pressure is 16 1 bar at the speed of 0 25m/sec and the maximum pressure is 18 6 bar at the shearing speed of 0 5m/sec Speed appears to be the dominant factor for the pressure distribution Figs 5 11 and 5 12 also show the

pressure profile for silicon 5 for different shearing speeds at the gap ratio of 8.These two figures show the similar trend as in Fig 5.1. Fig.5.13 shows the pressure distribution of silicon 5 at the speed of 0.25 m/sec at different gap ratios. It is found that if the gap ratio is 5 then the maximum pressure is16.1 bar, at the gap ratio of 3 the maximum pressure is 15.1 bar and at the gap ratio of 8 the maximum pressure is 12 bar. At the same speed the maximum pressure is higher at the gap ratio of 5. Fig 5.14 shows the pressure profile of silicon 5 at the speed of 2m/sec for different gap ratios. The pressure values are 35.83 bar, 33.07 bar and 26.18 bar for the gap ratio of 5, 3, and 8. The gap ratio 5 is the optimum gap ratio. As the inlet gap decreases, the fluid flow rate also decreases in the unit, which in turn is thought to be responsible for lower pressure. An increase in the inlet gap may cause back flow of the polymer, which would also reduce pressure.

Figs 5.15, 5.16 and 5.17 show the pressure distribution for silicon 12.5 at the speeds of between 0.5 m/sec and 2.0 m/sec at different gap ratios. For the gap ratio of 3, the pressure distribution curves for different shearing speeds such as 0.5m/sec, 1.0m/sec, 2.0m/sec are presented in Fig 5.15 for silicon 12.5. For the gap ratio of 5, the pressure distribution curves for different shearing speeds are presented in Fig 5.16. Fig 5.17 shows the pressure profile for the three different velocities at the gap ratio of 8. The pressure profile for silicon 12.5 at the speed of 0.5m/sec for different gap ratios are presented in Fig 5.18.The maximum pressure is 34.5 bar, 38.5 bar and 30.3 bar for the gap ratio of 3, 5, and 8 respectively. The pressure profiles for this fluid at the velocity of 2.0m/sec have been presented in Fig 5.19 for different gap ratios. Fig 5.20 shows the pressure profiles for glycerine, silicon 5, silicon 12.5 at the speed of 1m/sec and at the gap ratio of 5. The maximum pressure for silicon 12.5 is higher than the other two fluids. This is due to the higher viscosity of silicon

12 5 Almost similar trends of pressure distribution could be noticed from these figures even for these gap ratios, the difference is that the overall gap ratio affects the magnitude of the pressure generated

5 2 2 Results of Maximum Pressure Vs Speed

Experimental results were obtained in terms of the maximum pressure within the pressure unit of the Rheometer Experiments were carried out by varying h_1 in a systematic manner keeping h_2 constant For different shearing speed of up to 2m/sec, the maximum pressures were monitored for three different viscous fluids These results are presented in the following figures Fig 5 21 shows the effect of speed on the maximum pressure generated within the unit when glycerine is used as the pressure fluid at different gap ratios This figure shows that at gap ratio of 3, 5 and 8 the pressure Vs velocity curves are almost linear Fig 5 22 shows the effect of speed on pressure for the silicone 5 fluid The pressure vs speed curves are almost linear for all three gap ratios, and the maximum pressures occur at the gap ratio of 5 It is evident that the speed increases, the maximum pressure increases Fig 5 23 shows the effect of speed on pressure for silicone 12 5 At all the gap ratios the maximum pressure readings are increasing almost linearly with the increase of speed and maximum pressures are obtained for the gap ratio of 5 For the non-Newtonian fluid the developed pressure increases because viscosity changes with the shear rate and affects the pressure It is evident that as the speed increases, the maximum pressure also increases Fig 5 24 shows the comparison of the effect of speed on the maximum pressure for glycerine, silicon 5 and silicon 12 5 This figure shows that the maximum pressure is highest for silicon 12 5 The generated pressure depends upon

the viscosity of the fluid, the geometry of the unit and the relative speed of movement

5 3 Determination of the Rheology(Values of the Coefficient a and b)

The values of the coefficients of 'a' and 'b' for three different viscous fluids have been calculated in conjunction with the experimental and the theoretical results In reference [49] it was suggested that the value of 'b' in equation (16) for a viscous fluid may be taken as equal to $4x10^{11}$ m^2/N for calculating the pressure distribution for theoretical results The initial viscosity, μ_0=1N sec/m^2 and the non-Newtonian factor K=5 $6\times10^{11}m^4/N^2$ were taken from reference [49] Fig 5 25 shows the comparison of experimental pressure distribution of glycerine with the theoretical result at the velocity of 1 5 m/sec for different values of 'a' and 'b' It is clear that for b = $4x10^{11}$ m^2/N, the value of 'a' is 300N/m^2, which satisfies the continuity equation Q1 = Q2 and also gives the theoretical results very close to the experimental results Therefore, this value of b has been chosen for further iteration of results For 'b' = $4x10^{11}$ m^2/N, the value of 'a' has been changed until the values of theoretical and experimental maximum pressure were very close Fig 5 26 shows the theoretical pressure distribution for different values of 'a' (for b = $4x10^{11}$ m^2/N) and the experimental pressure distribution at the speed of 1 5 m/sec When the value of a = 500 N/ m^2, the experimental and theoretical results are almost same for the shearing speed of 1 5m/sec for the gap ratio of 3 The experimental and theoratical pressure values are very close for all the speeds between 0 5-1 5m/sec, when the values of a=300 N/m^2 As such b = $4x10^{11}$ m^2/N and a = 300 N/m^2 have been accepted as the value for glycerine Fig 5 27 shows the comparison of experimental pressure

distribution with the theoretical results at the velocity of 1 0 m/sec of silicon 5 for different values of 'a' and 'b' For the value of a = 7000 N/m^2 and b = 5x10 ^{11} m^2 /N, the experimental and the theoretical results are very close Fig 5 28 shows the theoretical pressure distribution for the different values 'a' (For b = 5x10 ^{11} m^2/N) and the experimental pressure distribution at the speed of 1 0 m/sec When the value of a=7340N/m^2 the theoretical results are almost same for the gap ratio of 5 at the shearing speed of 1 0m/sec The experimental and the theoretical pressure results are very close for all the speeds between 0 25-2 0m/sec,when the value of a=7100N/m^2 and b=5×10 ^{11}m^2/N So that a = 7100 N/m^2 and b = 5x10 ^{11} m^2/N have been accepted as the value of silicon 5

Fig 5 29 shows the comparison of experimental pressure distribution with the theoretical results at the velocity of 1 0 m/sec of silicon 12 5 for different values of ' a' and 'b' Fig 5 30, the theoretical pressure distribution for different values of 'a' (For b = 5 6 x10 ^{11} m^2) and the experimental pressure distribution at the speed of 1 0 m/sec When the value of a=17100N/m^2 the experimental and the theoretical values are almost same For a = 17,000 N/m^2 and b = 5 6 x 10 ^{11} m^2/N, the experimental and the theoretical results are very close for the speeds between 0 5-2 0 m/sec So that a = 17000 N/ m^2 and b = 5 6 x 10 ^{11} m^2/N have been accepted as the value of Silicon 12 5 For the different values of 'a' and 'b', the comparison of experimental and theoretical pressure values for the three different types of fluids at the different speeds and the error analysis are given in Appendix C

5 4 Effect of Pressure on Viscosity

Viscosity, by definition, is the internal resistance to the shearing stress due to intermolecular forces of attraction It was thought that when the molecular attractions are encouraged, the apparent viscosity of the fluids, which is one of the most important properties of these materials, might be increased

The effect of pressure on viscosity at different shear rates for glycerine is presented in Fig 5 31 The developed pressure for glycerine in the rheometer was in the range 2 to 13 bar The viscosity of glycerine has been calculated using the coefficient values of the viscosity equation within the range of 0 to 100 bar and from the figure it is evident that with the increase of pressure, the viscosity values are increasing for a given shear rate The effect of pressure on viscosity for silicon 5 for different shear rates are presented in Fig 5 32 The experimental pressure values were between 10 to 35 bar Using the coefficient values the viscosity values were calculated and plotted This figure shows similar trend like those in Fig 5 31 Fig 5 33 shows the effect of pressure on viscosity for silicon12 5 at different shear rates The developed experimental pressures were between 30-60 bar Within these pressure values the viscosities were calculated and are presented in graphical form and from the figure it is shown that with the increase of pressure the viscosity increases at the same shear rate Fig 5 34 shows the comparison of viscosity values of glycerine, silicone 5 and silicone 12 5 at the shear rate of 2000 sec^{-1}

5 5 Effect of Shear Rate on Viscosity

Newtonian fluids under shear stress condition exhibit linear relationship with shear rate where the slope of the line represents the viscosity of the fluids For the non-Newtonian behaviour, the apparent viscosity decreases as the rate of shear increases From the experimental results, using a Brookfield viscometer viscosity values can be determined for low shear rates Fig 5 35 shows shear stress vs shear rate curves obtained using the Brookfield viscometer for glycerine, silicon 5 and silicon 12 5 From the figure it is evident that the curves are almost linear for all three fluids Using the viscometer the viscosity has been measured for the three different types of fluid at the lower shear rates The effect of shear rate on viscosity is presented in Fig 5 36 From the figure the viscosity increases with the decrease of shear rate

Experimental work carried out using the Brookfield viscometer was at the shear rate range of up to 30 per second whereas tests carried out using the new Rheometer was in the shear rate range of 500-4000 per second The values of the coefficients in equation (16) have been determined according to the pressure values obtained experimentally at shear rate range of between 500-4000sec ^{1}

Fig 5 37 shows the effect of shear rate on viscosity of glycerine at atmospheric pressure Using the viscosity equation $\mu = \mu_0 + \left(\frac{a + bp^2}{\gamma}\right)$ and the viscosity values are much higher than the values obtained at lower shear rate range obtained by using the Brookfield viscometer Figs 5 38 and 5 39 show the effect of shear rate on viscosity of silicon5 and silicon 12 5 also at the atmospheric pressure Once again the viscosity results from the Brookfield viscometer are much lower than

those predicted according to equation (16) is for shear rate range between 500 and 4000 per second as the novel Rheometer can not be operated at lower than about 500 per second Furthermore, the new Rheometer is more appropriate for viscosity measurements at higher than atmospheric pressure As such the comparison of low pressure and low shear rate viscosity values may not be appropriate The experimental data from the novel Rheometer were used to determine the viscosity-shear rate equation given in reference [1] as,

$$\eta=K_2\gamma^{n\ 1} \qquad (17)$$

The results according to this equation are also shown in figs 5 37,5 38 and 5 39 and are similar to those given by equation (16) The constants of the equation for three fluids are given

As K_2= 7 36 n= 75 for glycerine

K_2=1634 n= 234 for silicon 5

K_2=7855 n= 12 for silicon 12 5

A curve fitting exercise using the experimental points from the novel Rheometer and the Brookfield viscometer produces the following form of equations ($\mu=A\gamma+B$)

μ = -7E-05γ+1 3237 For glycerine

μ = -0 0012γ+7 8883 For silicon 5

μ = - 0016γ+12 265 For silicon 12 5

These equations may be taken as valid over the entire shear rate range of up to 4000 per second but only at atmospheric pressure

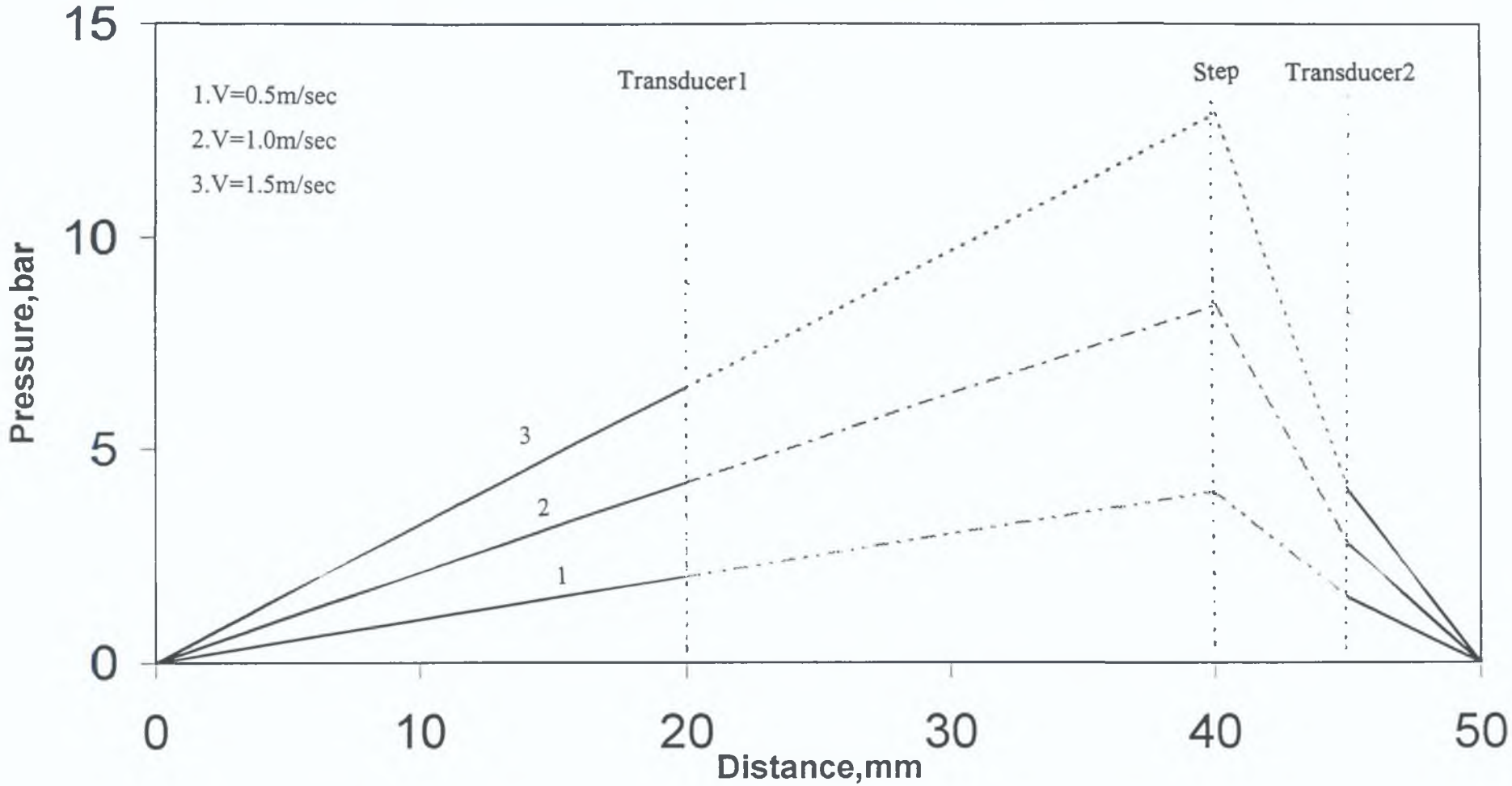

Fig 5.1: Pressure distribution of glycerine for different velocities at the gap ratio of 3.

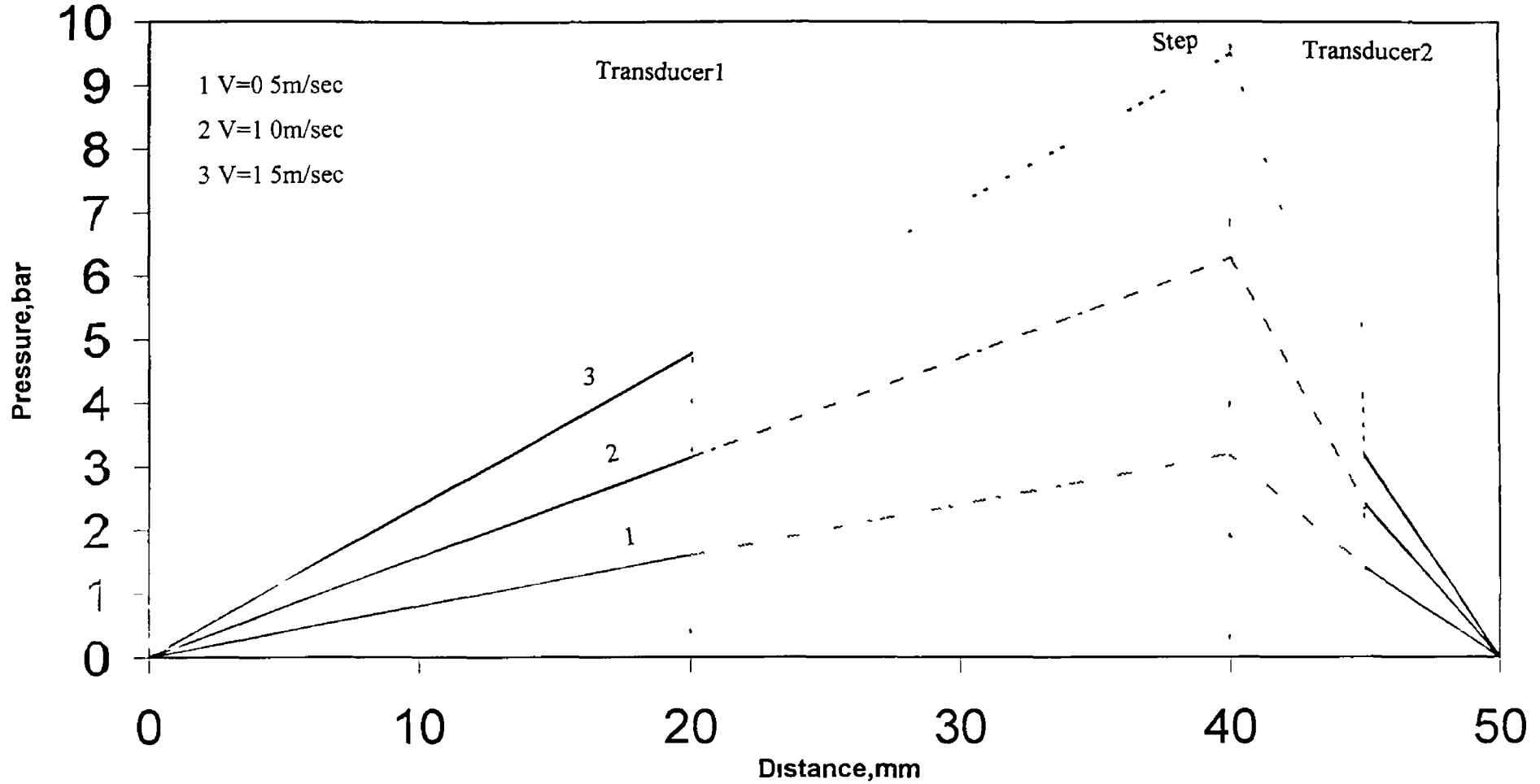

Fig 5.2: Pressure distribution of glycerine for different velocities at the gap ratio of 5.

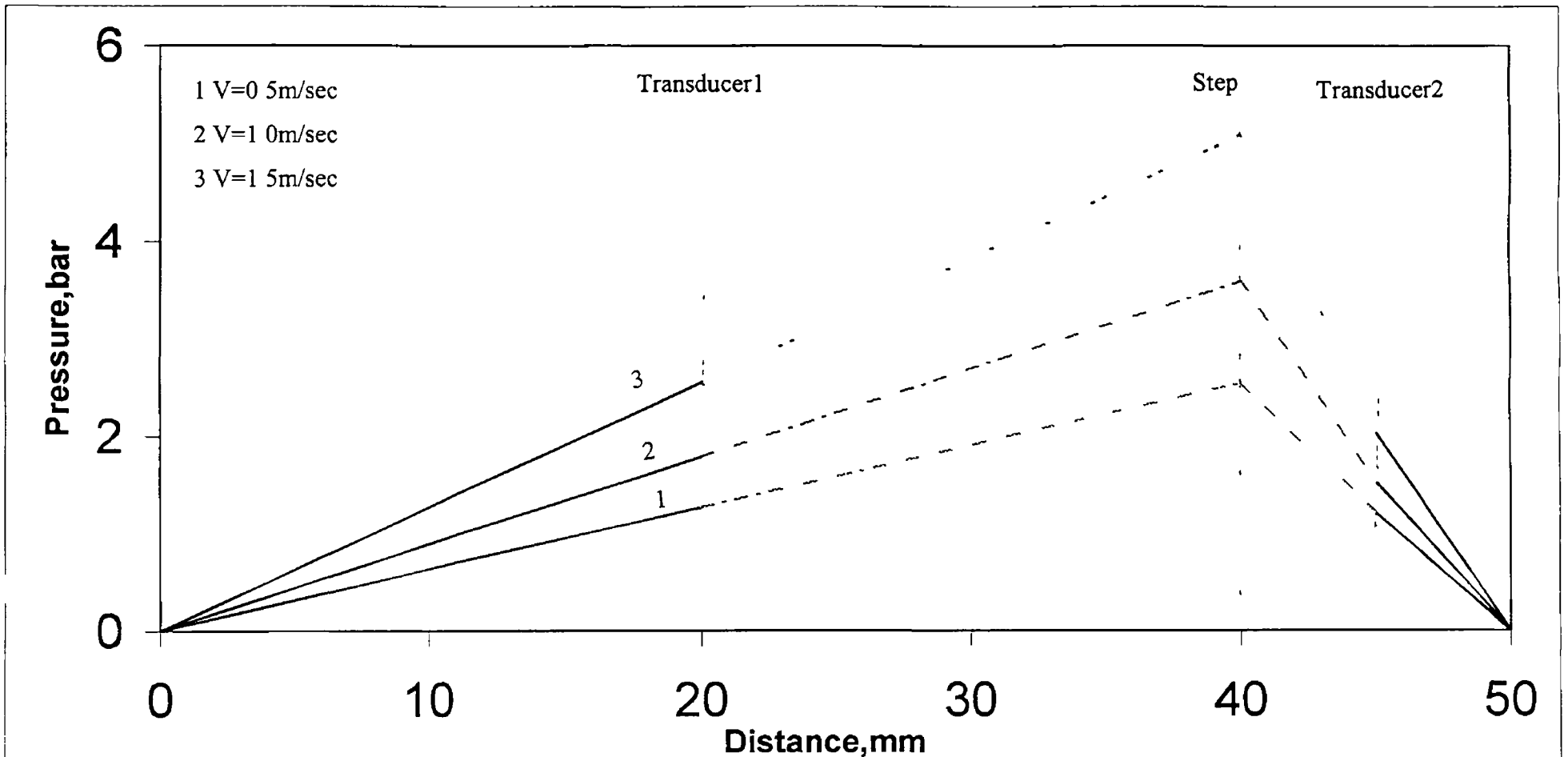

Fig 5.3: Pressure distribution of glycerine for different speeds at the gap ratio of 8.

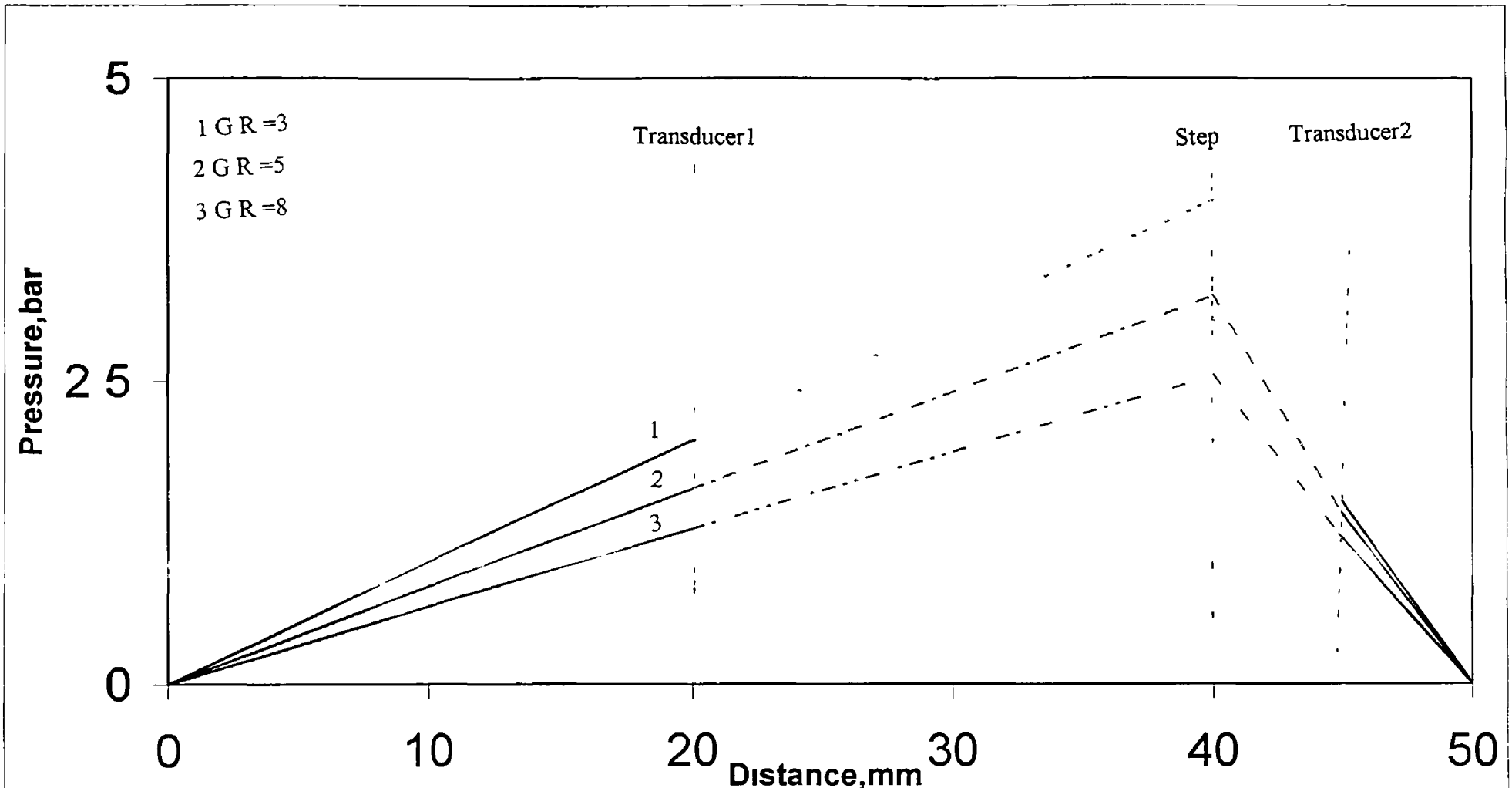

Fig 5.4: Pressure distribution of glycerine at the velocity of 0.5m/sec for different gap ratios.

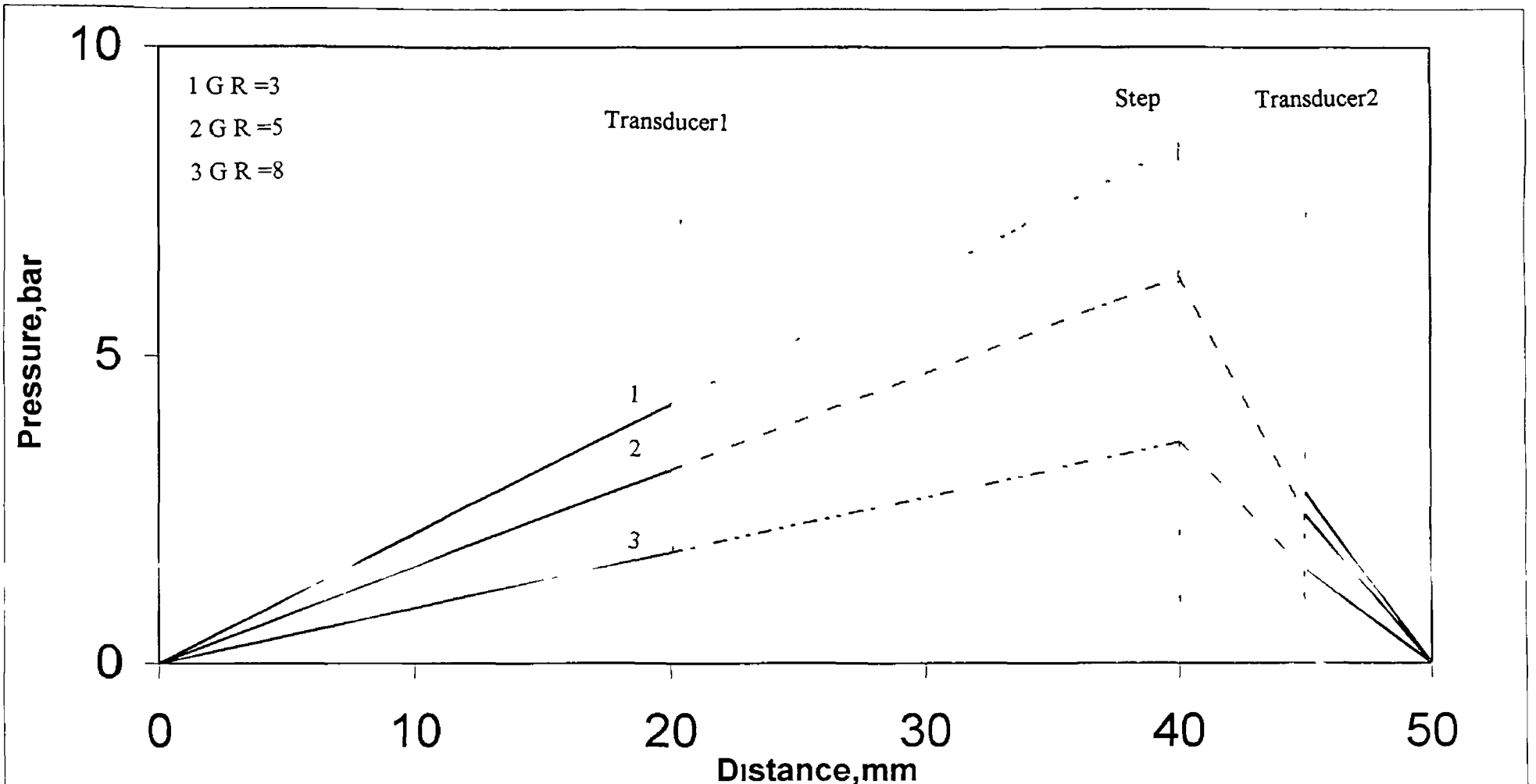

Fig 5.5: Pressure distribution of glycerine at the velocity of 1.0m/sec for different gap ratios

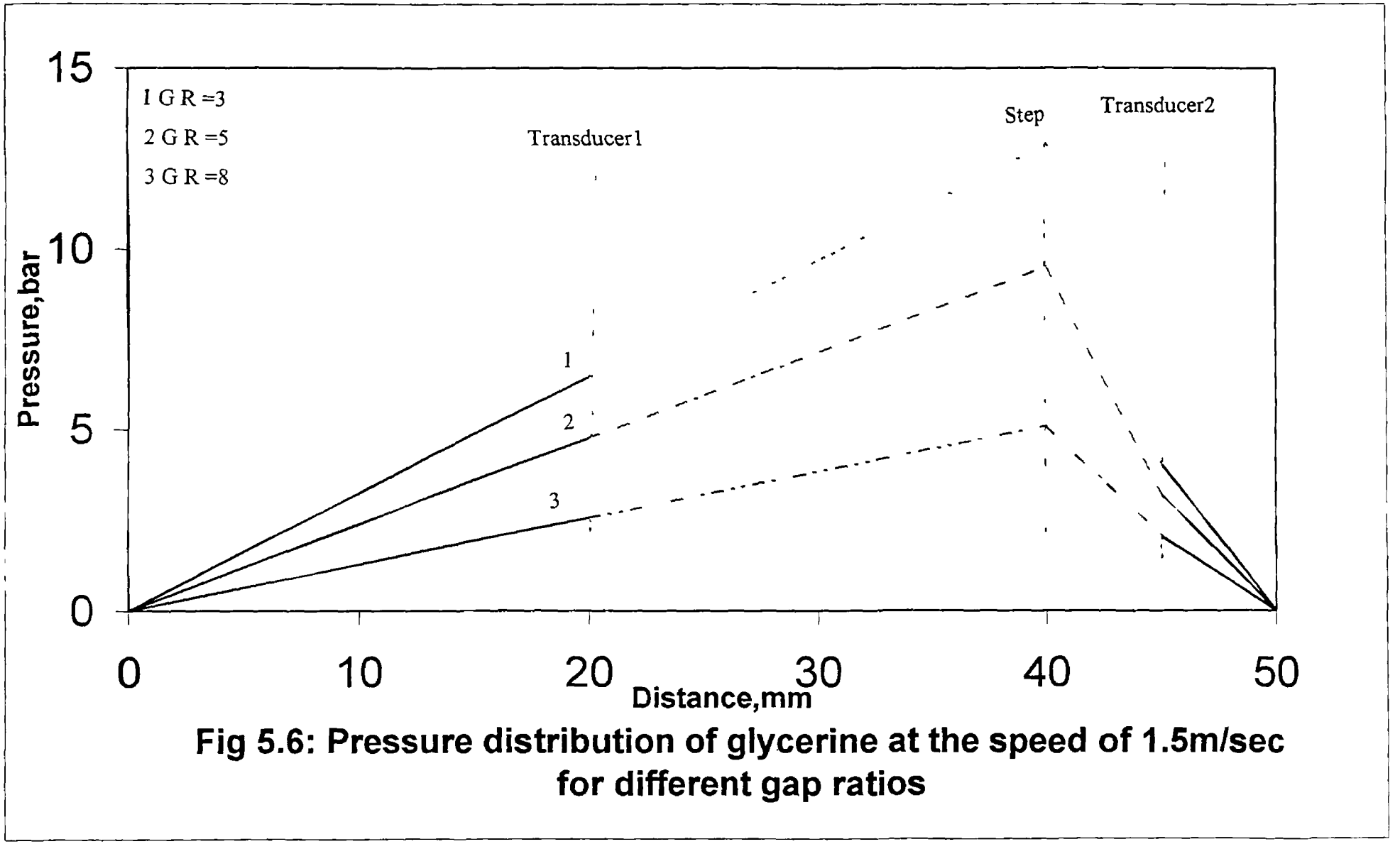

Fig 5.6: Pressure distribution of glycerine at the speed of 1.5m/sec for different gap ratios

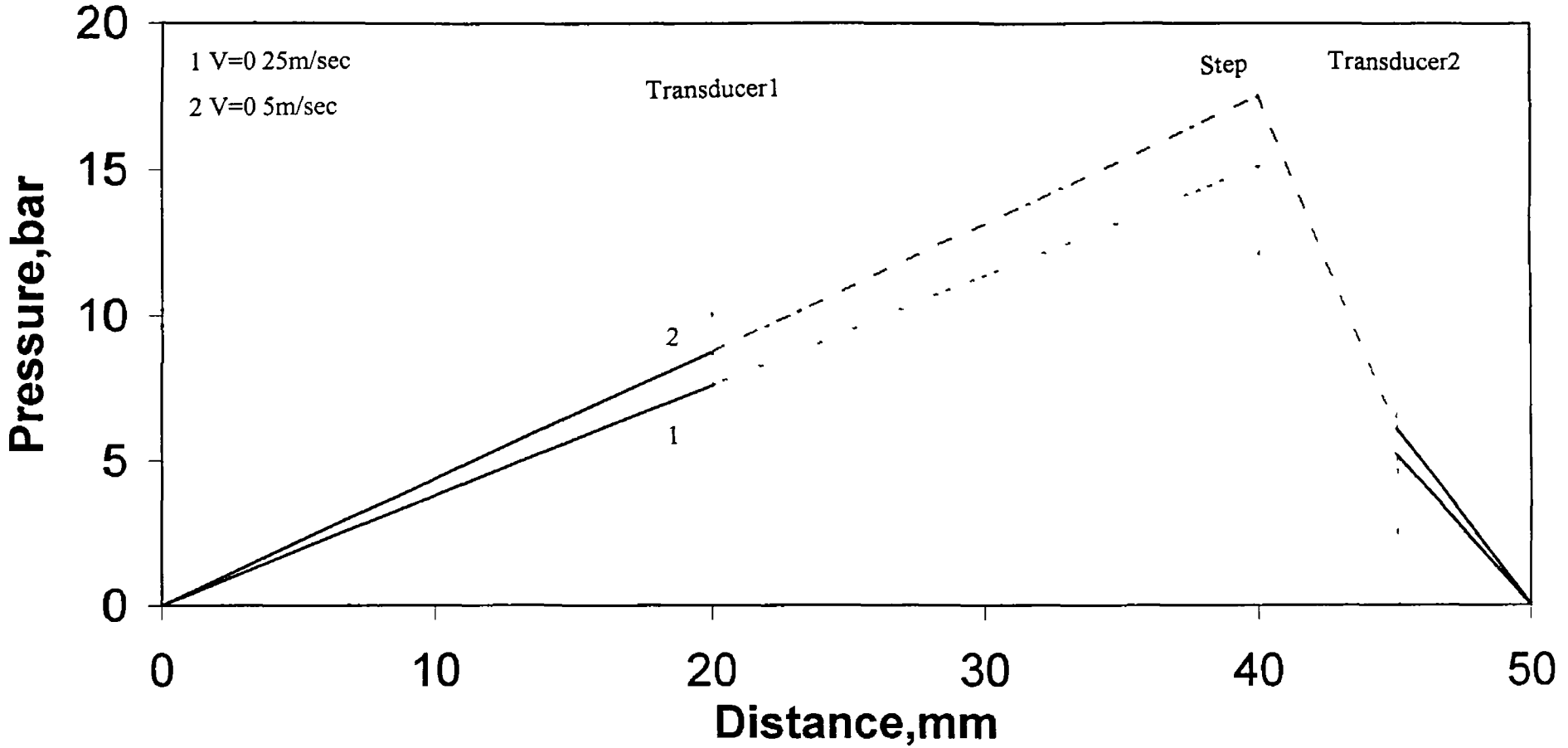

Fig 5.7: Pressure distribution of silicon 5 for different velocities at the gap ratio of 3.

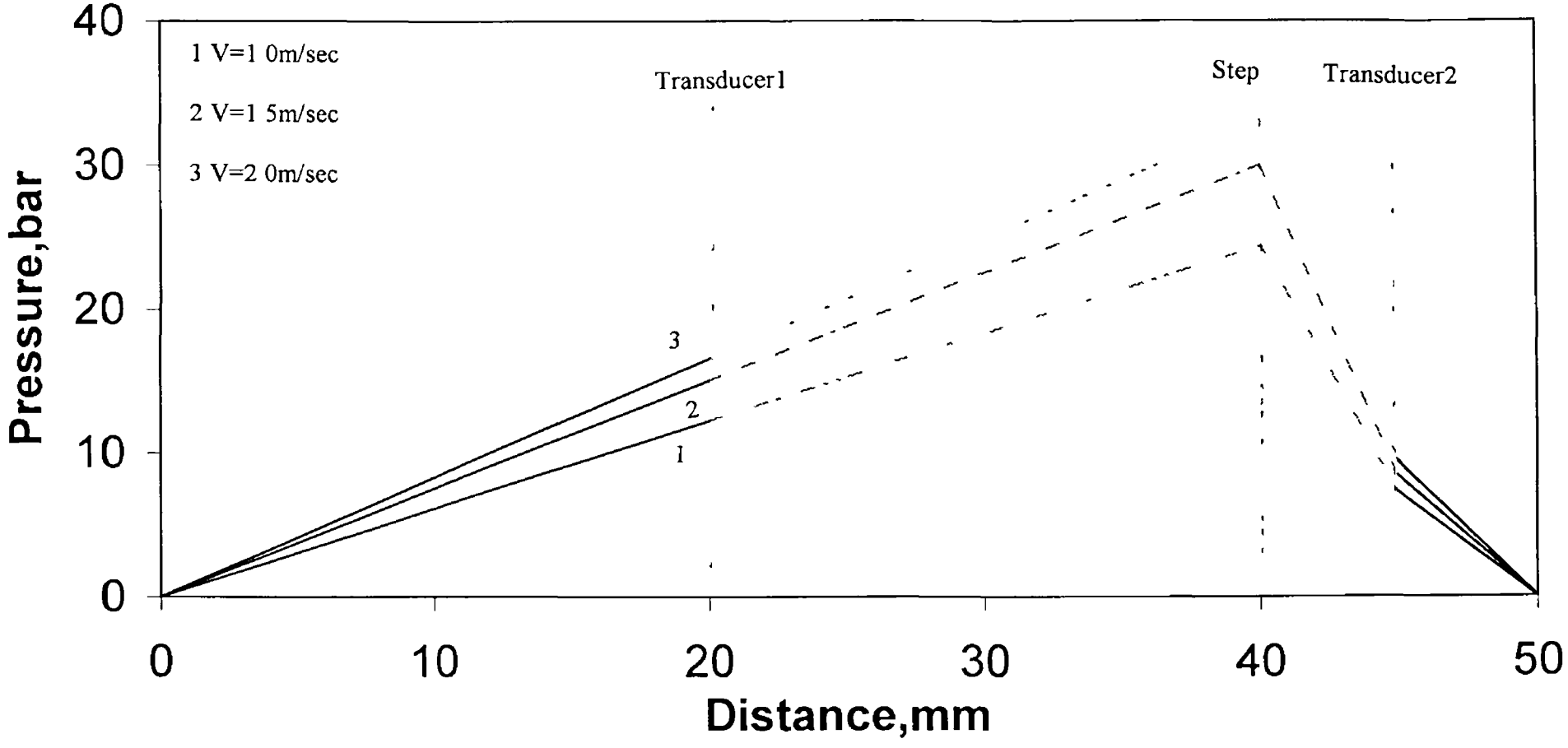

Fig 5.8: Pressure distribution of silicon 5 for different shearing speeds at the gap ratio of 3.

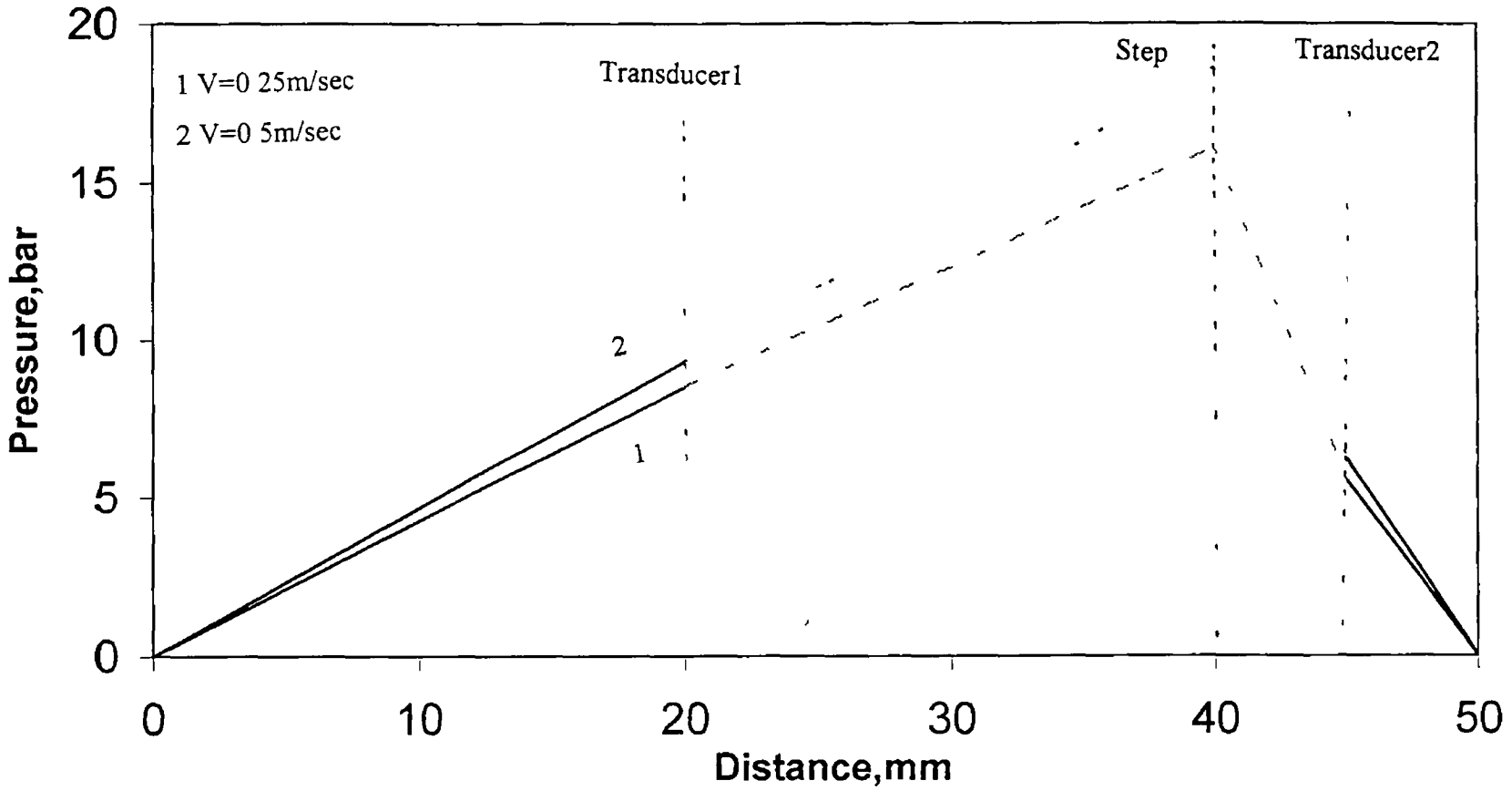

Fig 5.9: Pressure distribution of silicon 5 for the different shearing speeds at the gap ratio of 5.

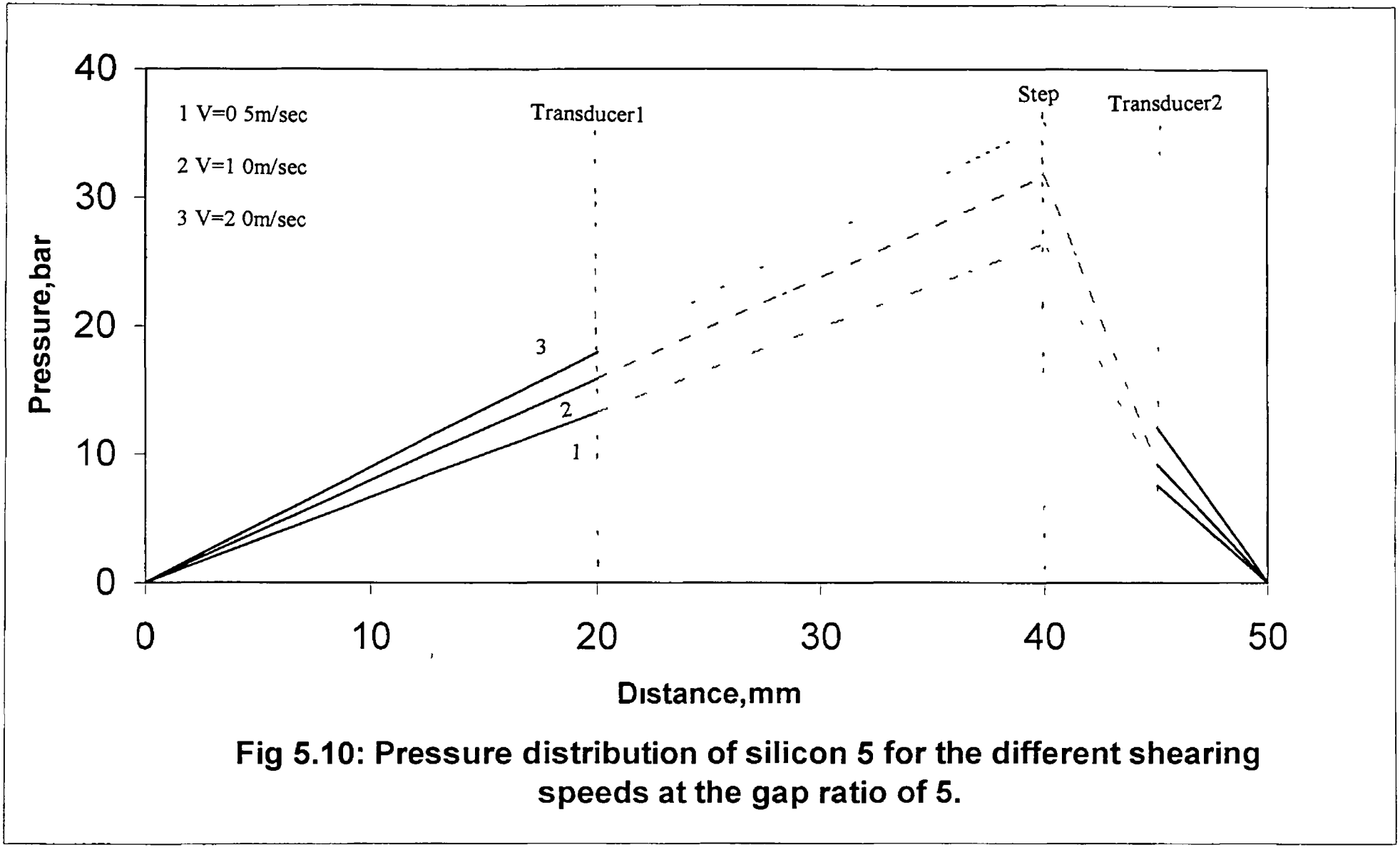

Fig 5.10: Pressure distribution of silicon 5 for the different shearing speeds at the gap ratio of 5.

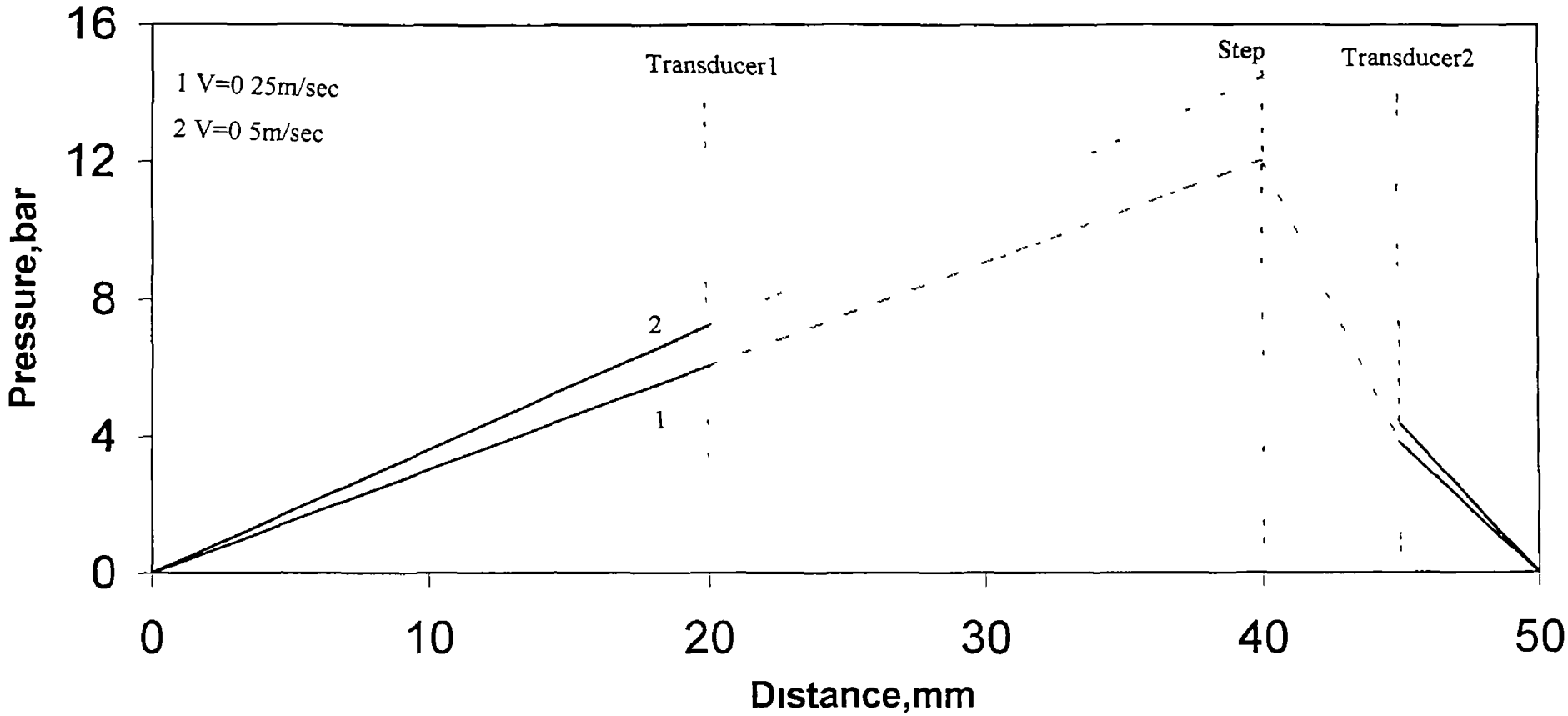

Fig 5.11: Pressure distribution of silicon 5 for different shearing speeds at the gap ratio of 8.

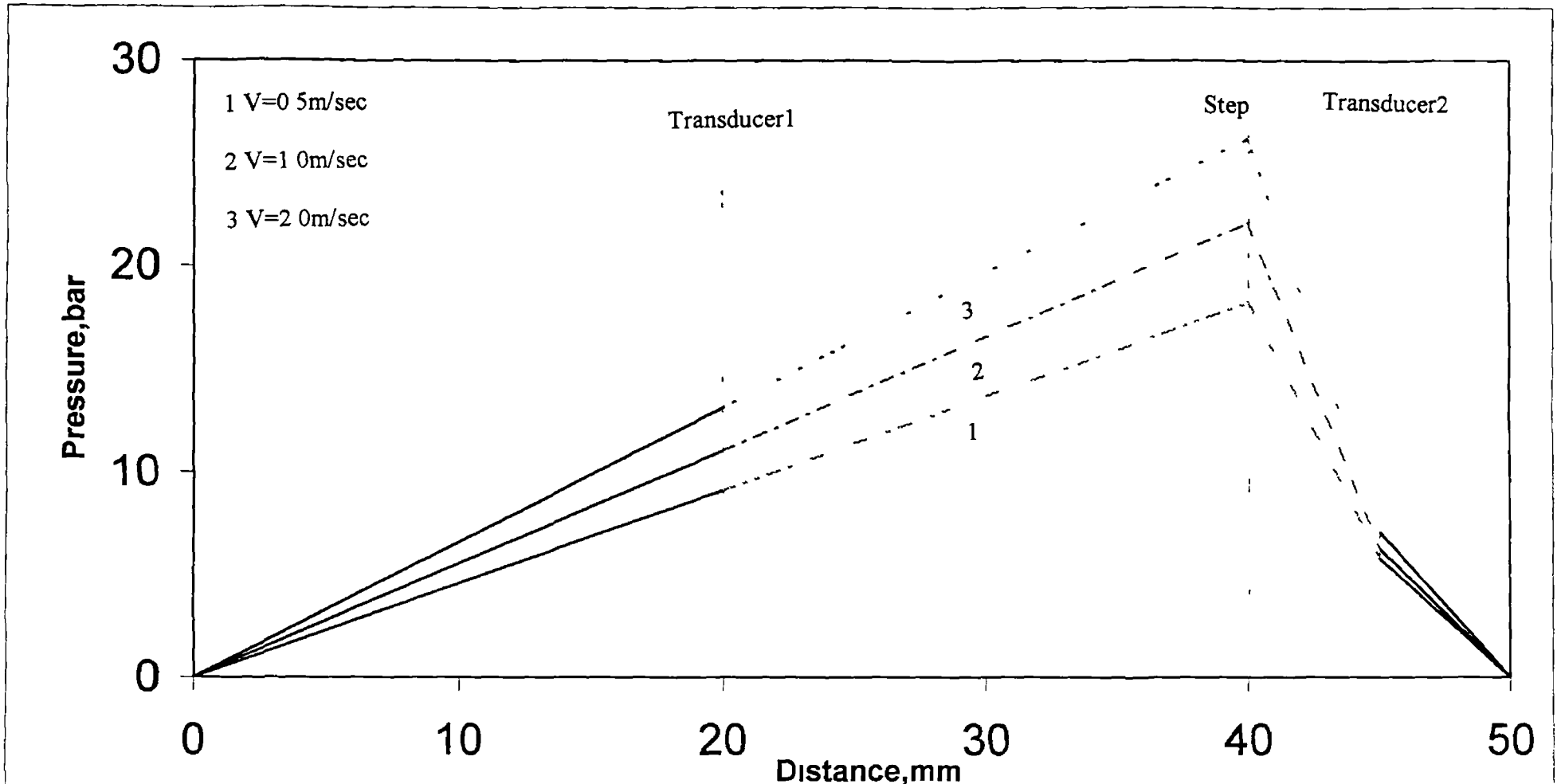

Fig 5.12: Pressure distribution of silicon 5 for different velocities at the gap ratio of 8.

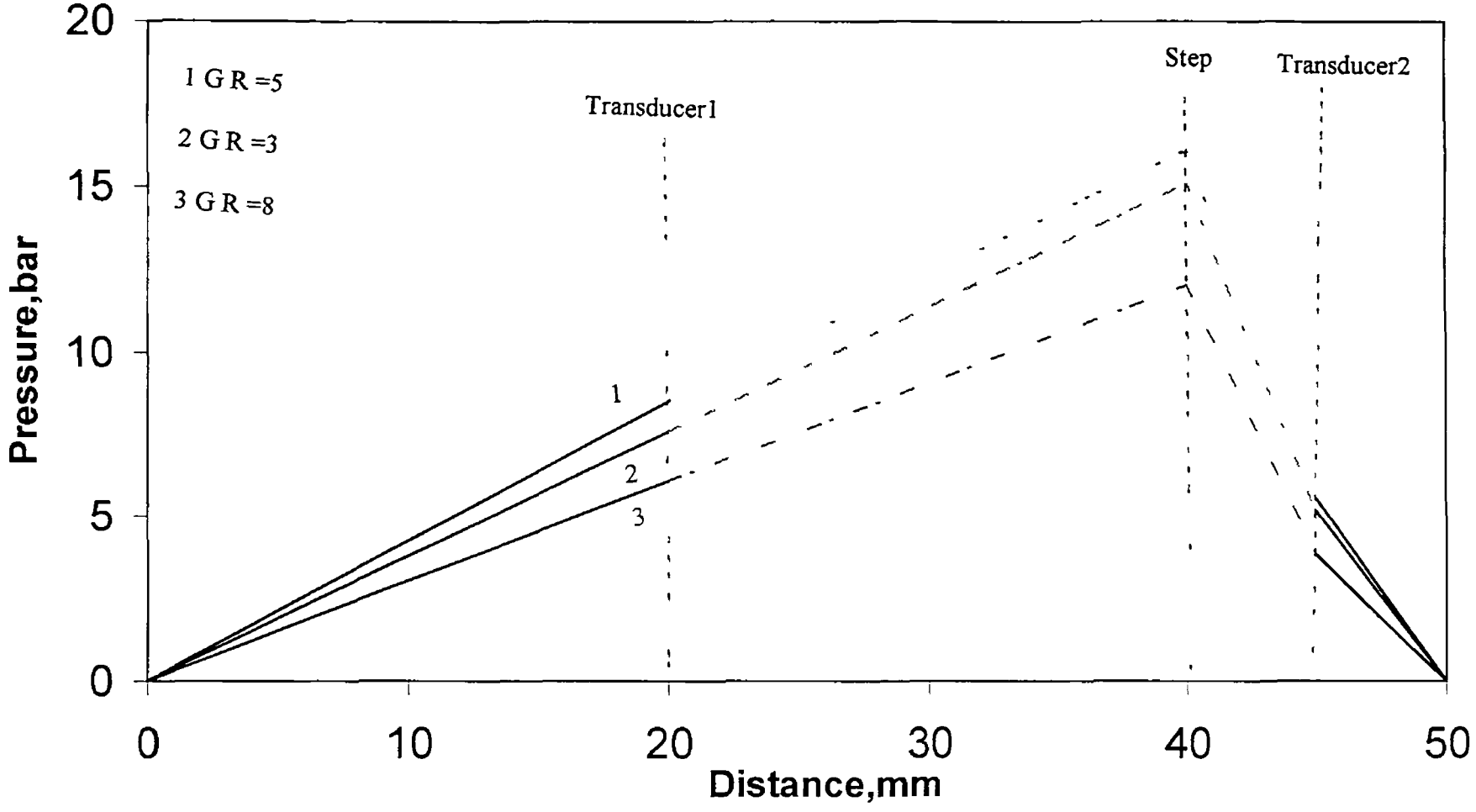

Fig 5.13: Pressure distribution of silicon 5 at the velocity of 0.25m/sec for different gap ratios.

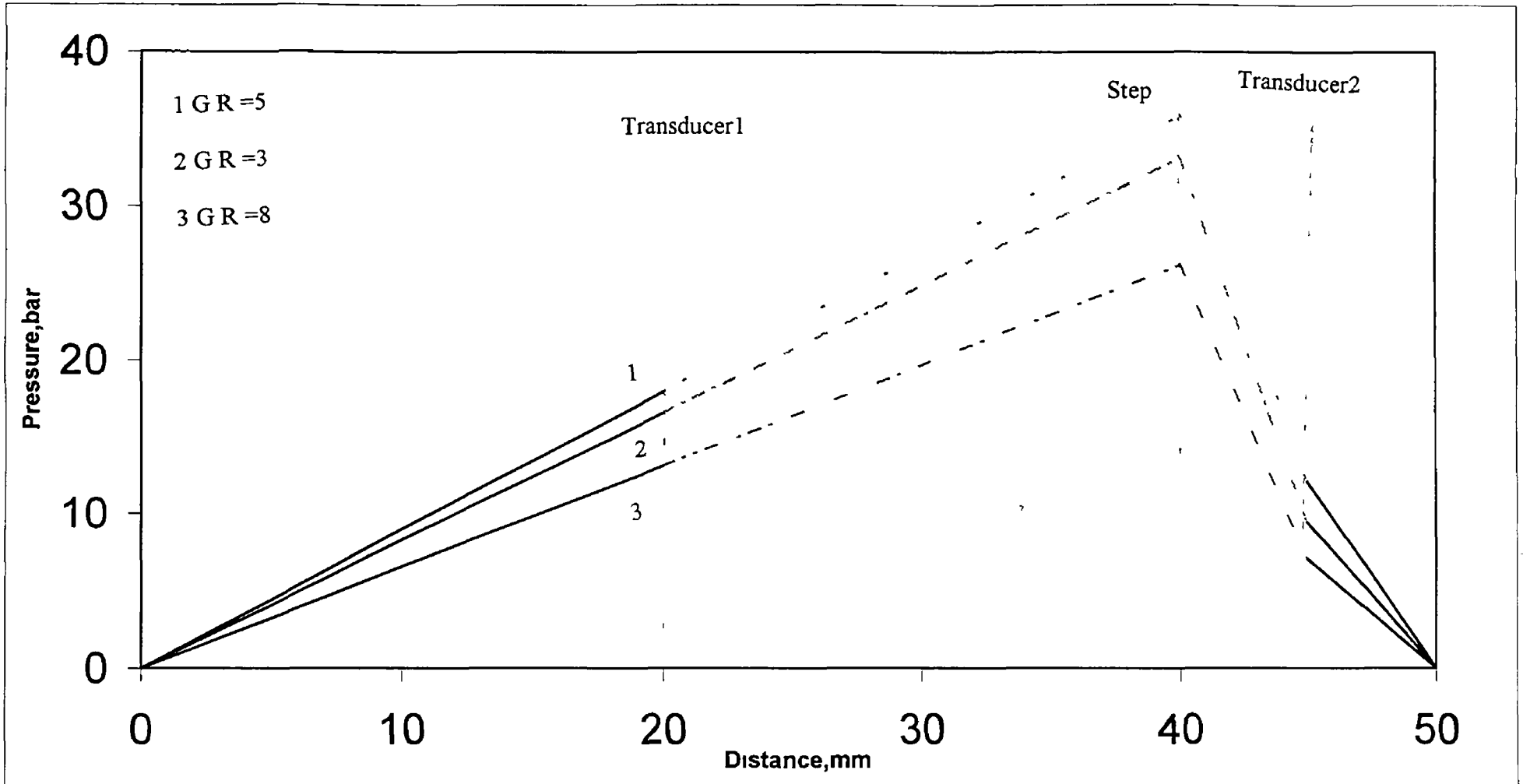

Fig 5.14· Pressure distribution of silicon 5 at the velocity of 2m/sec for different gap ratios.

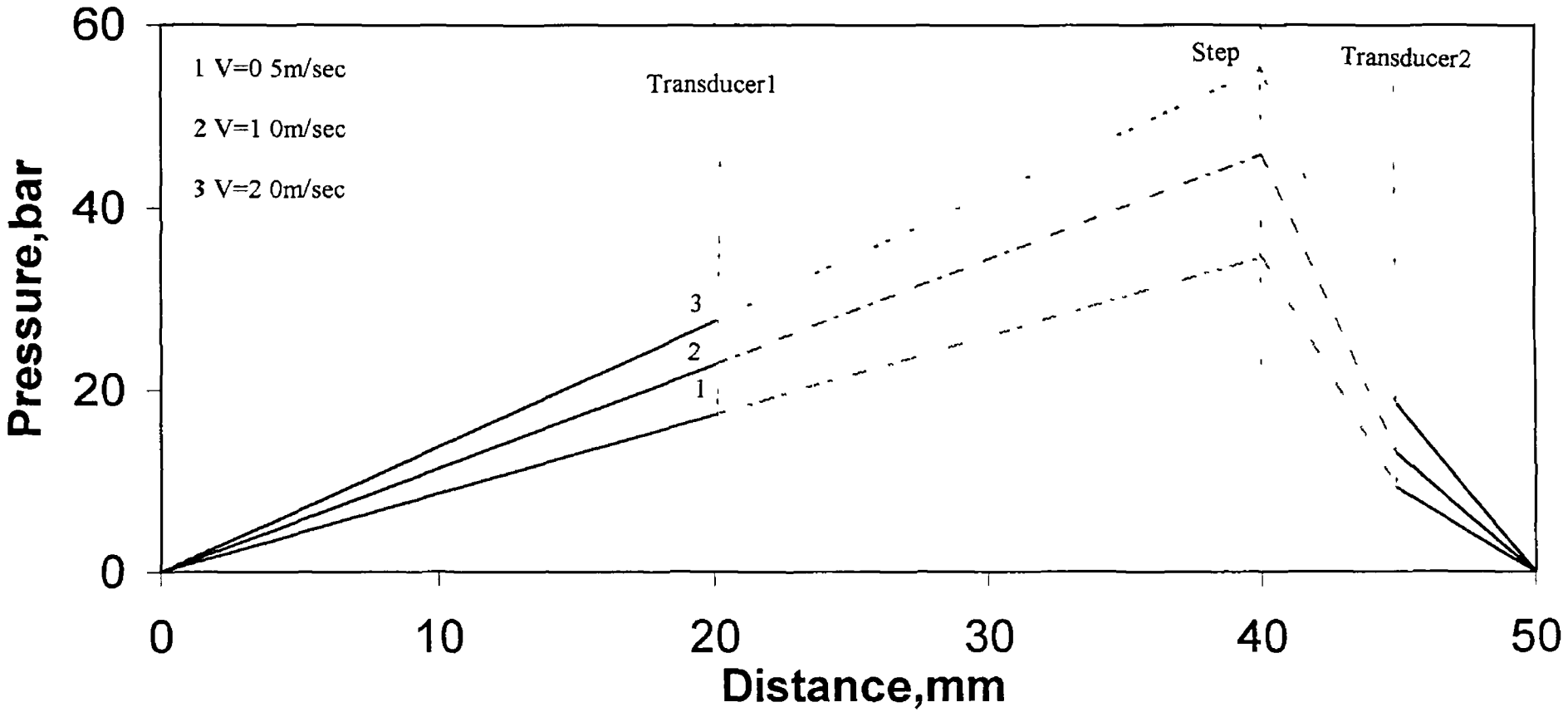

Fig 5.15: Pressure distribution of silicon 12.5 for different velocities at the gap ratio of 3.

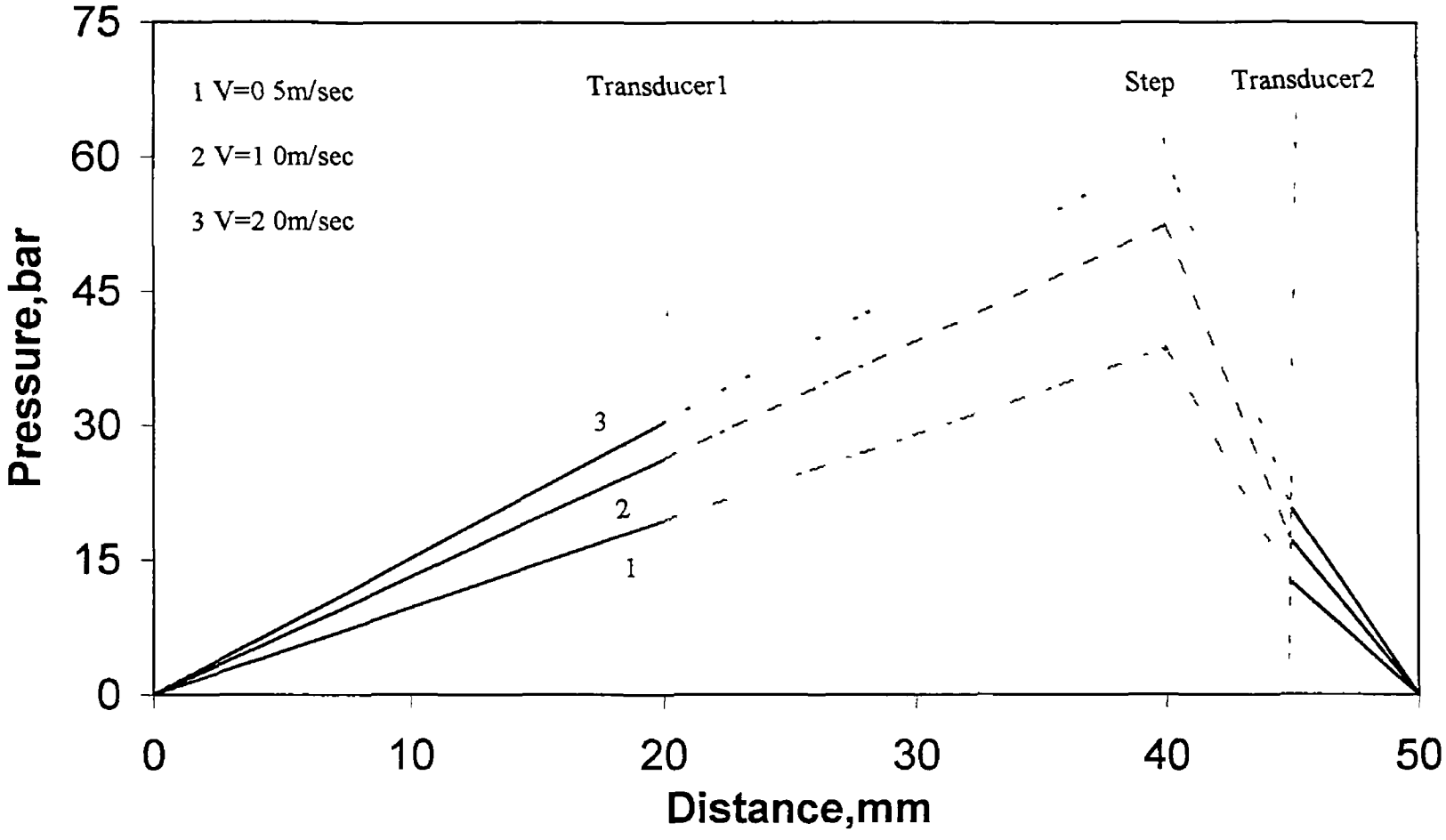

Fig 5.16: Pressure distribution of silicon 12.5 for different velocities at the gap ratio of 5.

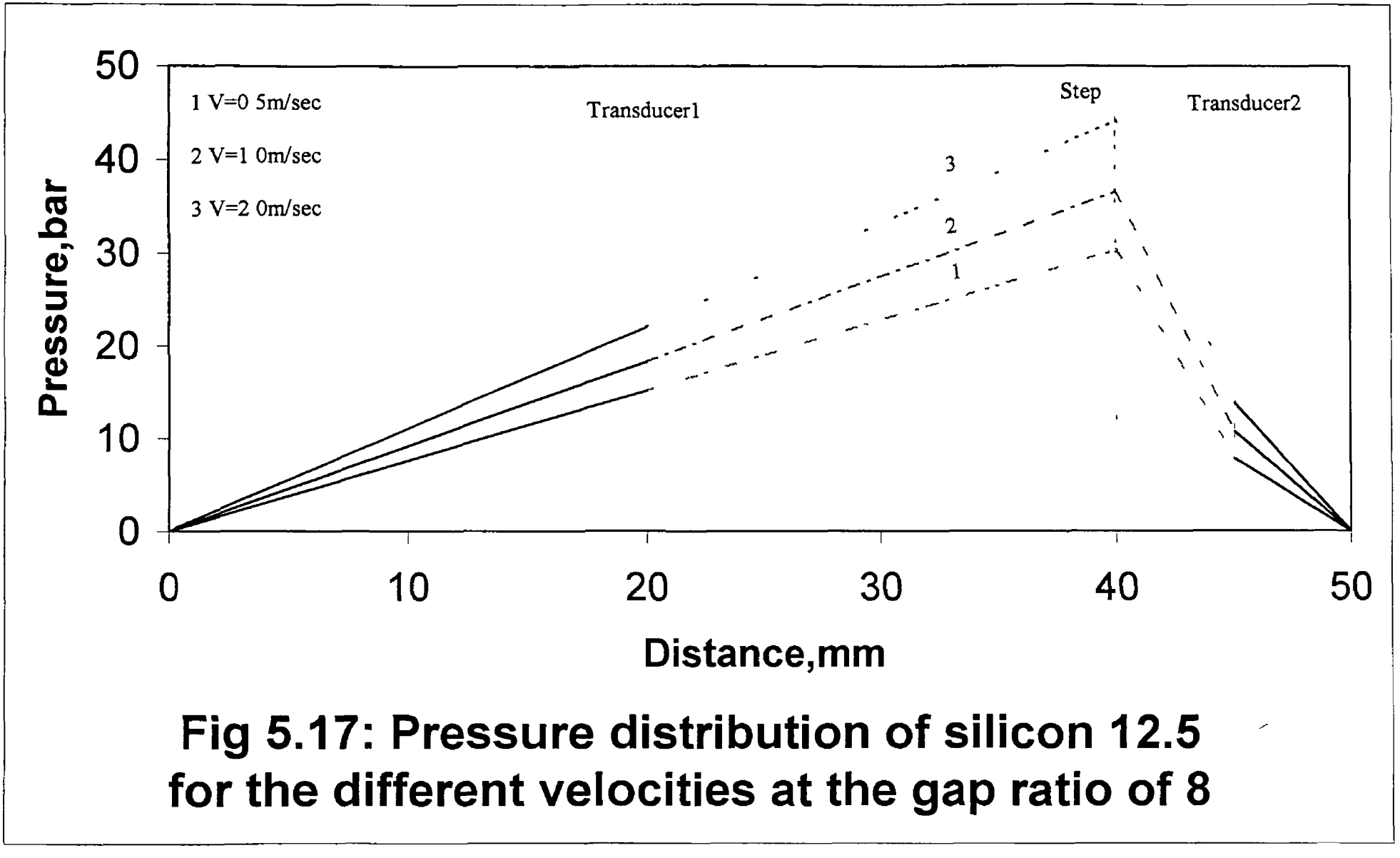

Fig 5.17: Pressure distribution of silicon 12.5 for the different velocities at the gap ratio of 8

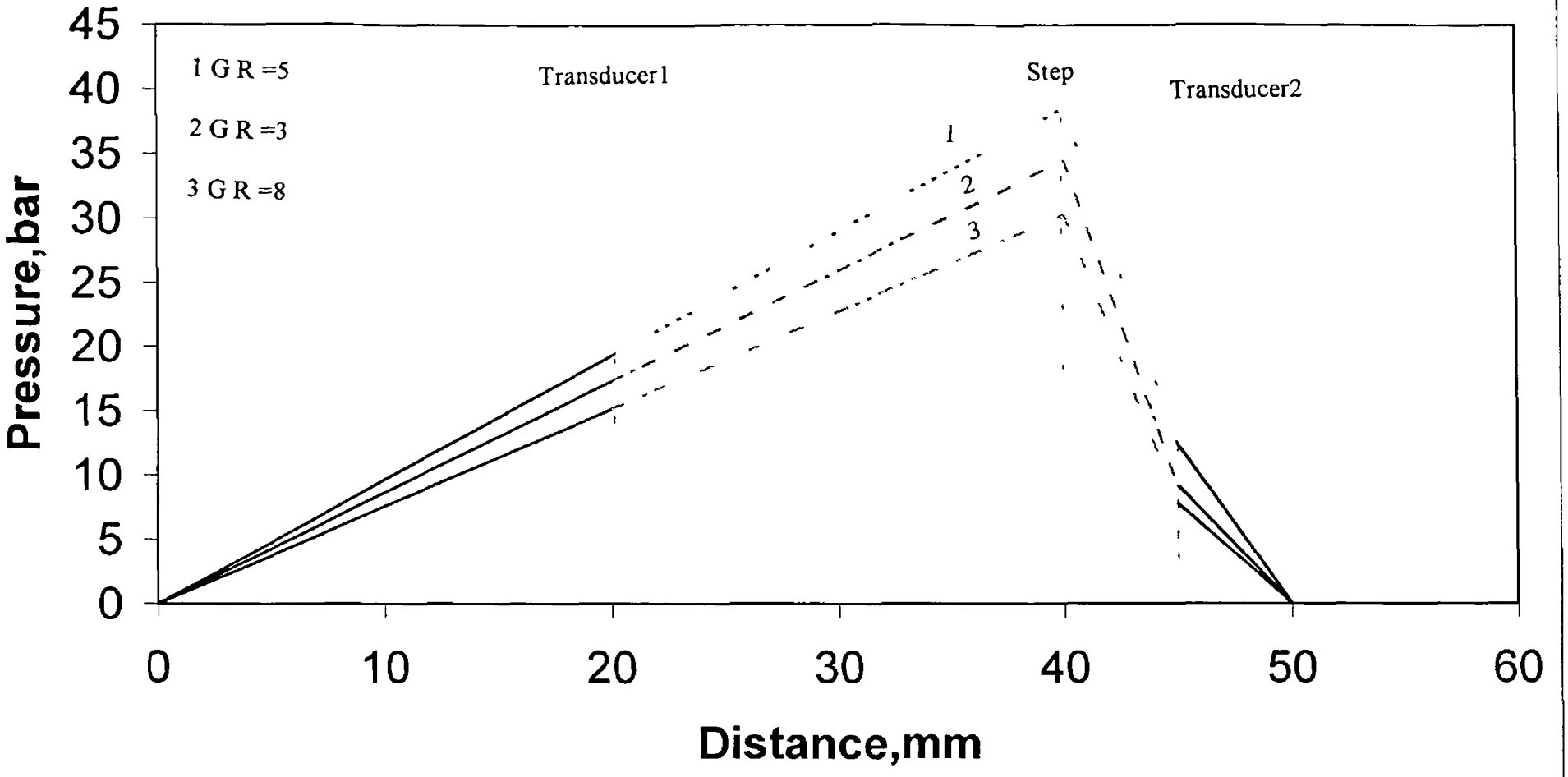

Fig 5.18: Pressure distribution of silicon 12.5 at the velocity 0f 0.5m/sec for different gap ratios

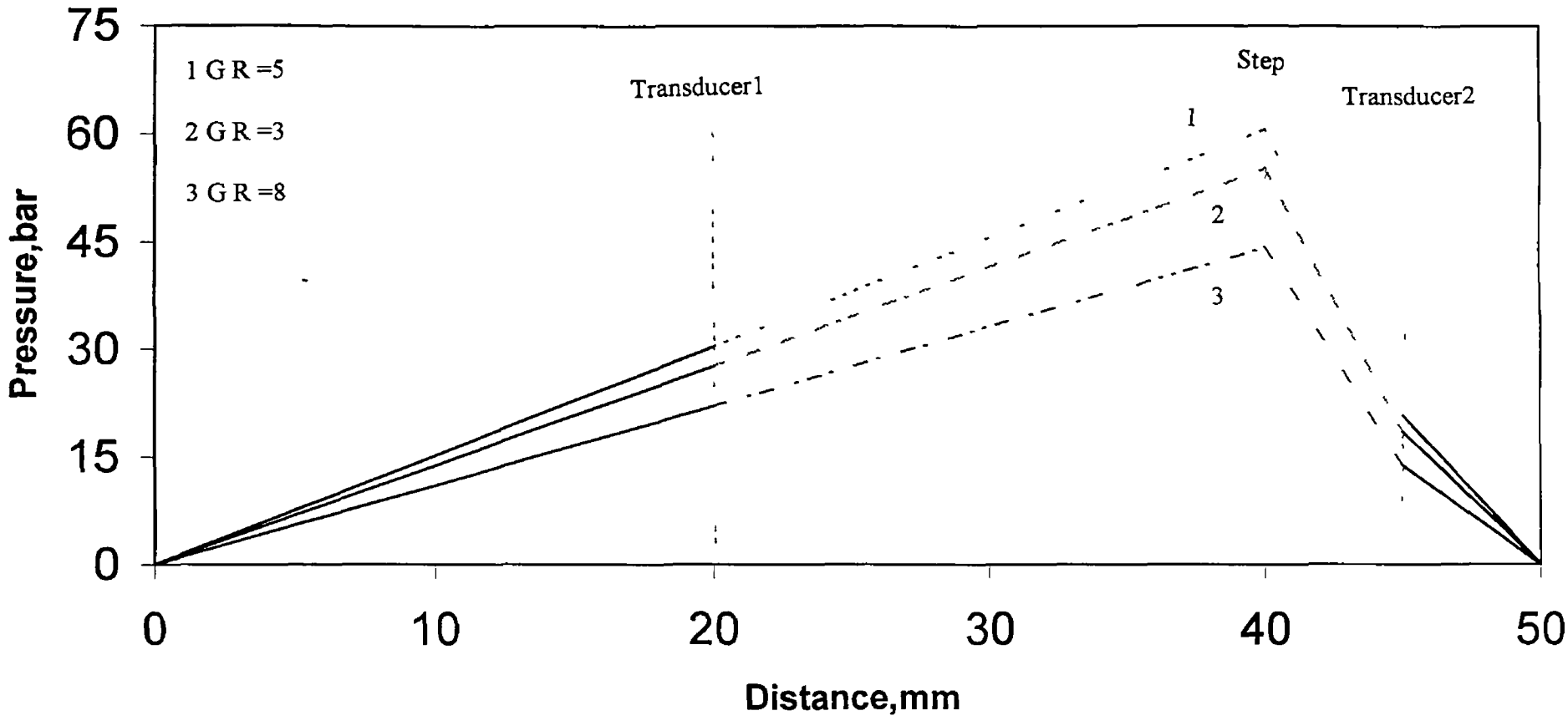

Fig 5.19: Pressure distrbution of silicon 12.5 at the velocity of 2.0m/sec for the different gap ratios.

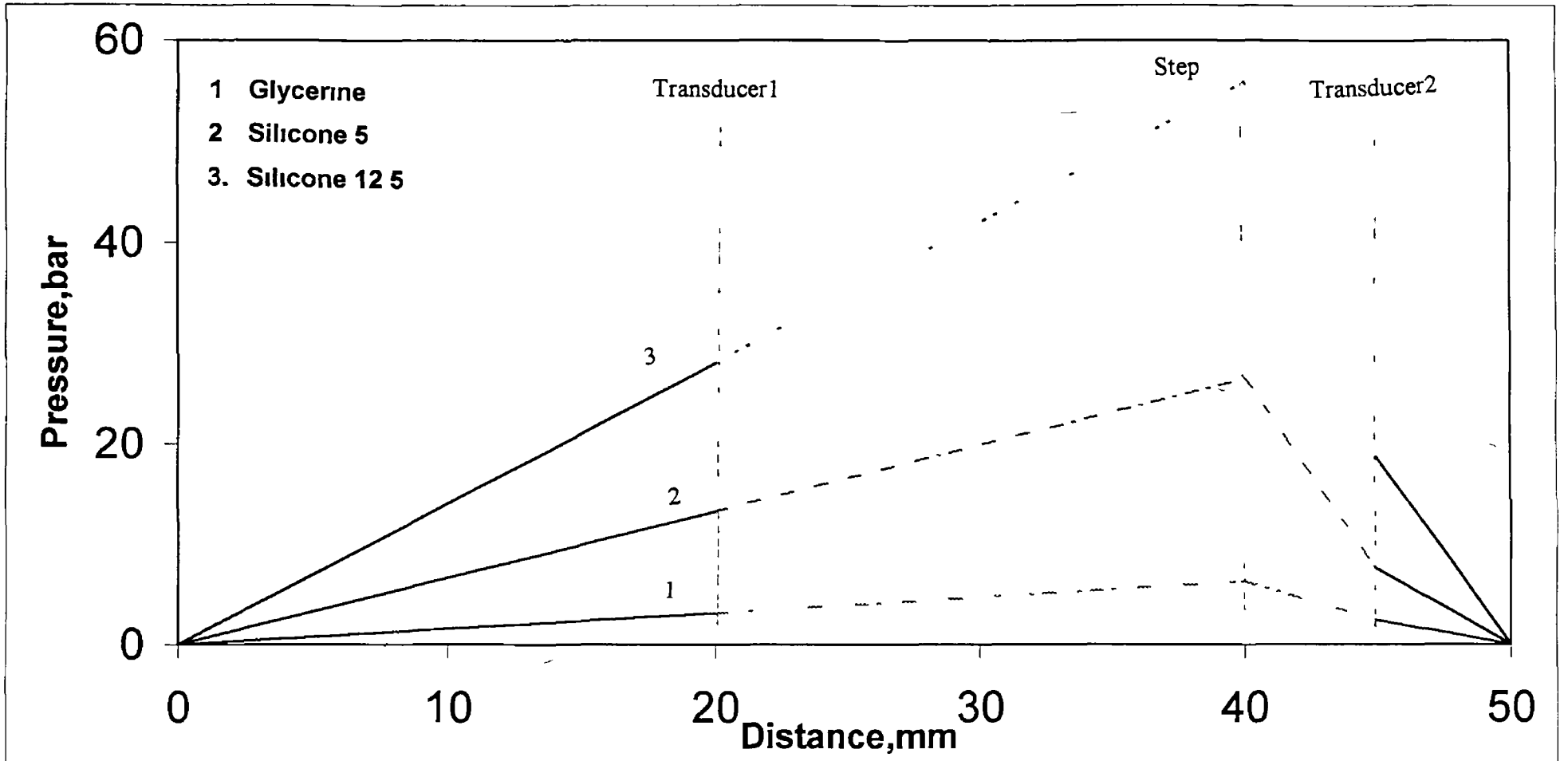

Fig 5.20: Comparison of Pressure distribution of glycerine,silicon 5,silicon 12.5 at the gap ratio of 5 and at the velocity of 1.0m/sec

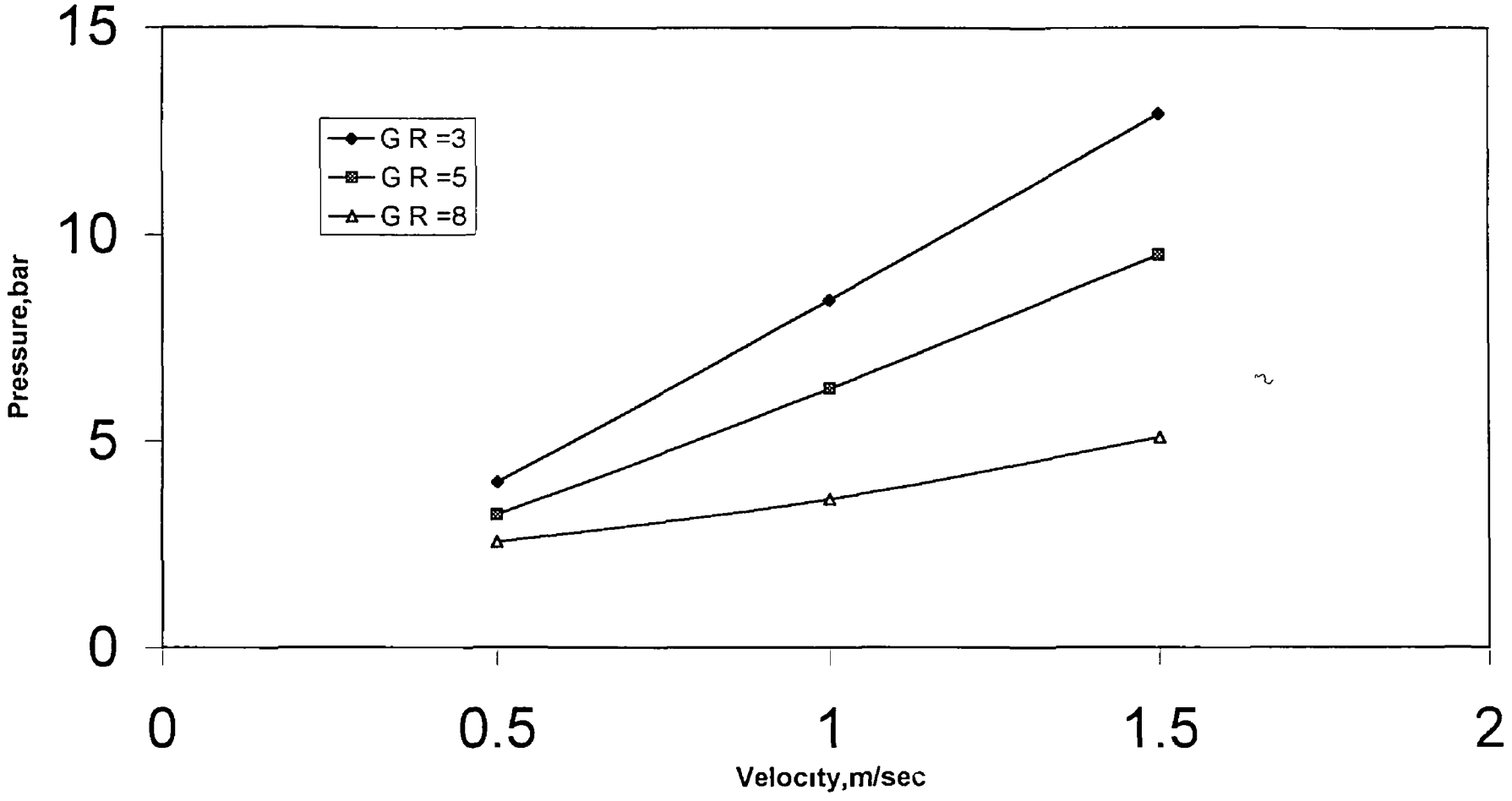

Fig 5.21: Maximum pressure vs speed of glycerine for different gap ratios.

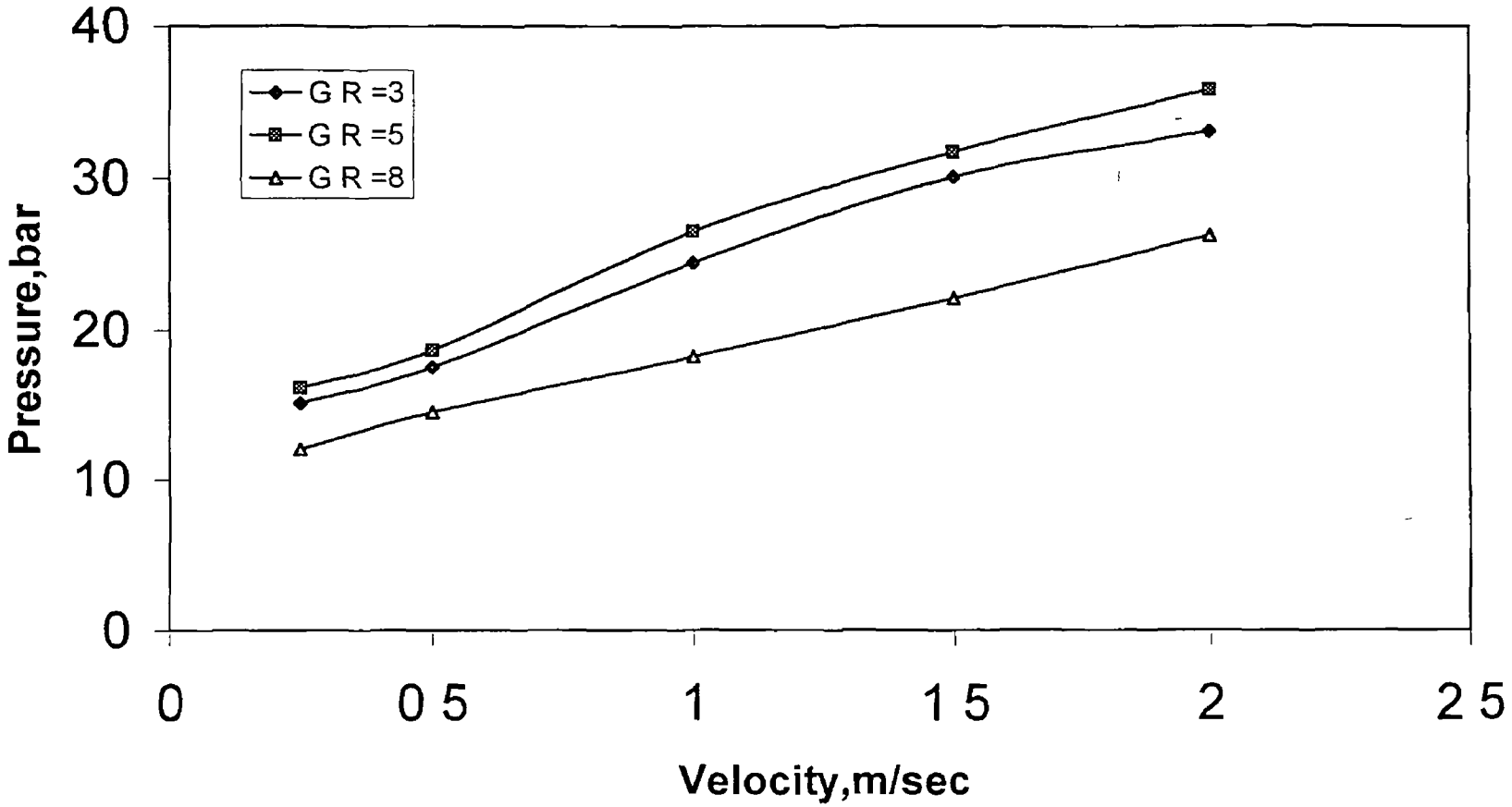

Fig 5.22: Maximum pressure vs speed of silicon 5 for different gap ratios.

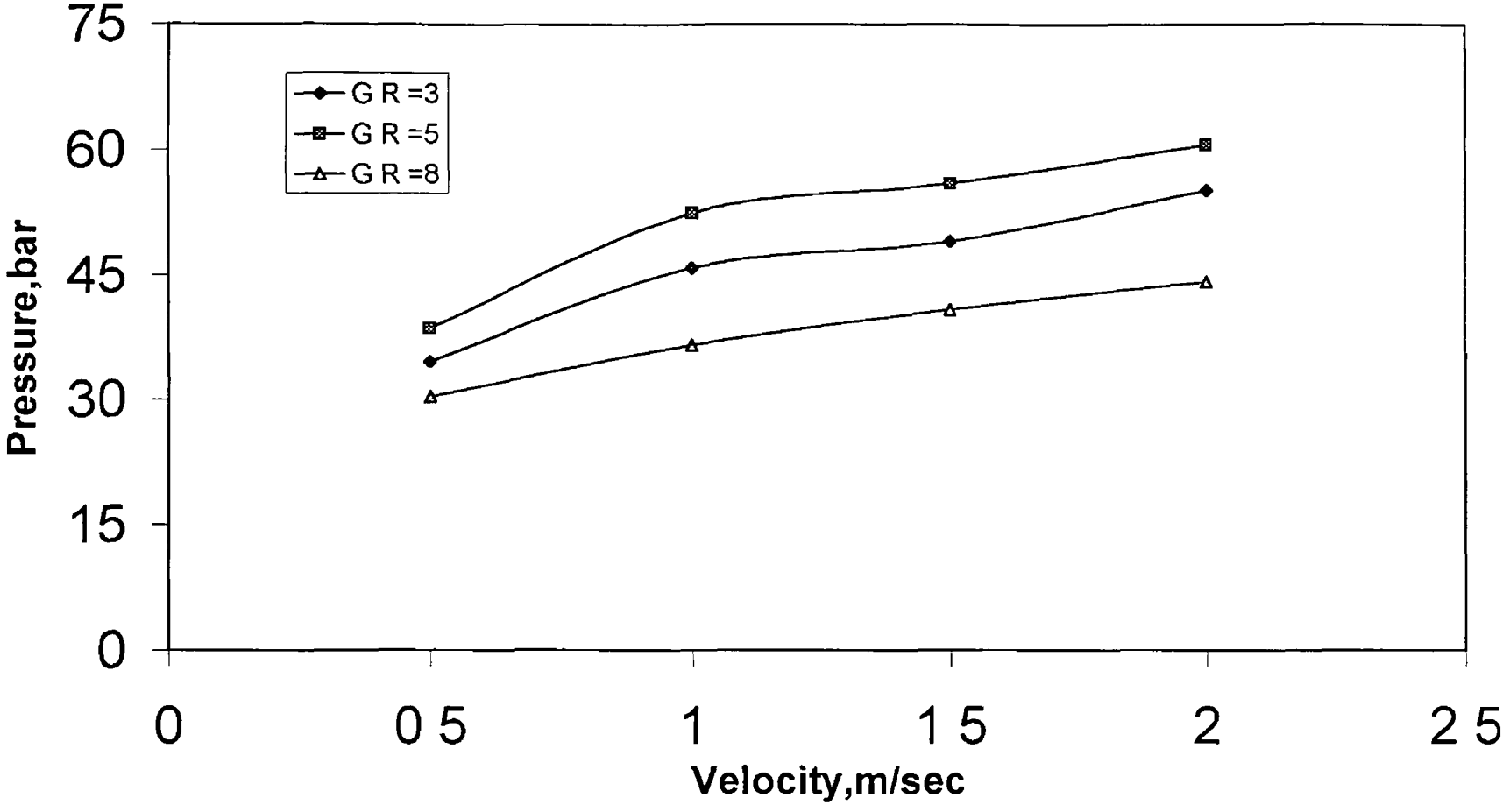

Fig 5.23: Maximum pressure vs speed of silicon 12.5 for different gap ratios.

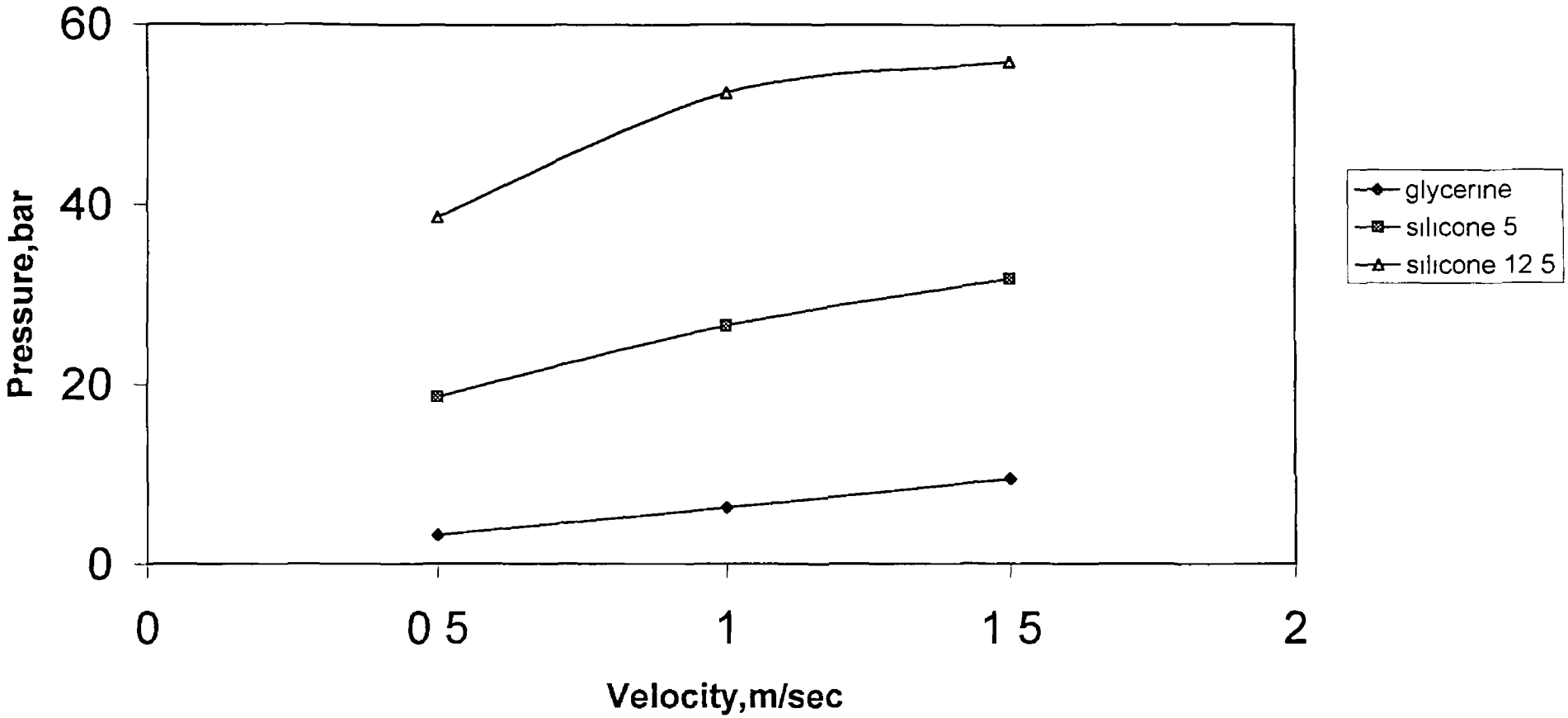

Fig.5.24: Maximum pressure vs speed of glycerine,silicon 5 and silicon 12.5 at the gap ratio of 5.

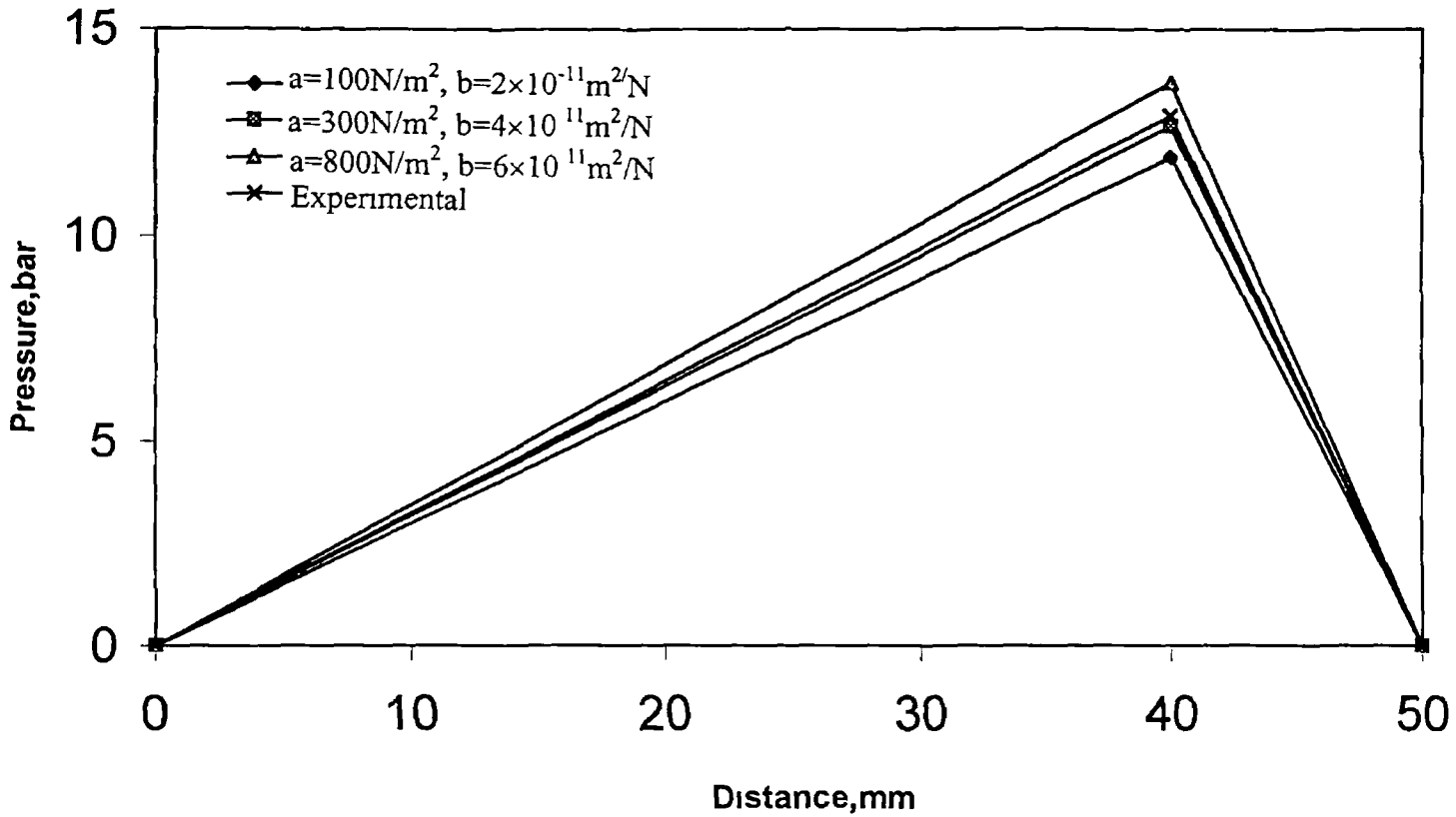

Fig 5.25: Experimental and theoratical pressure profile of glycerine for the different values of 'a' and 'b' at the velocity of 1 5m/sec

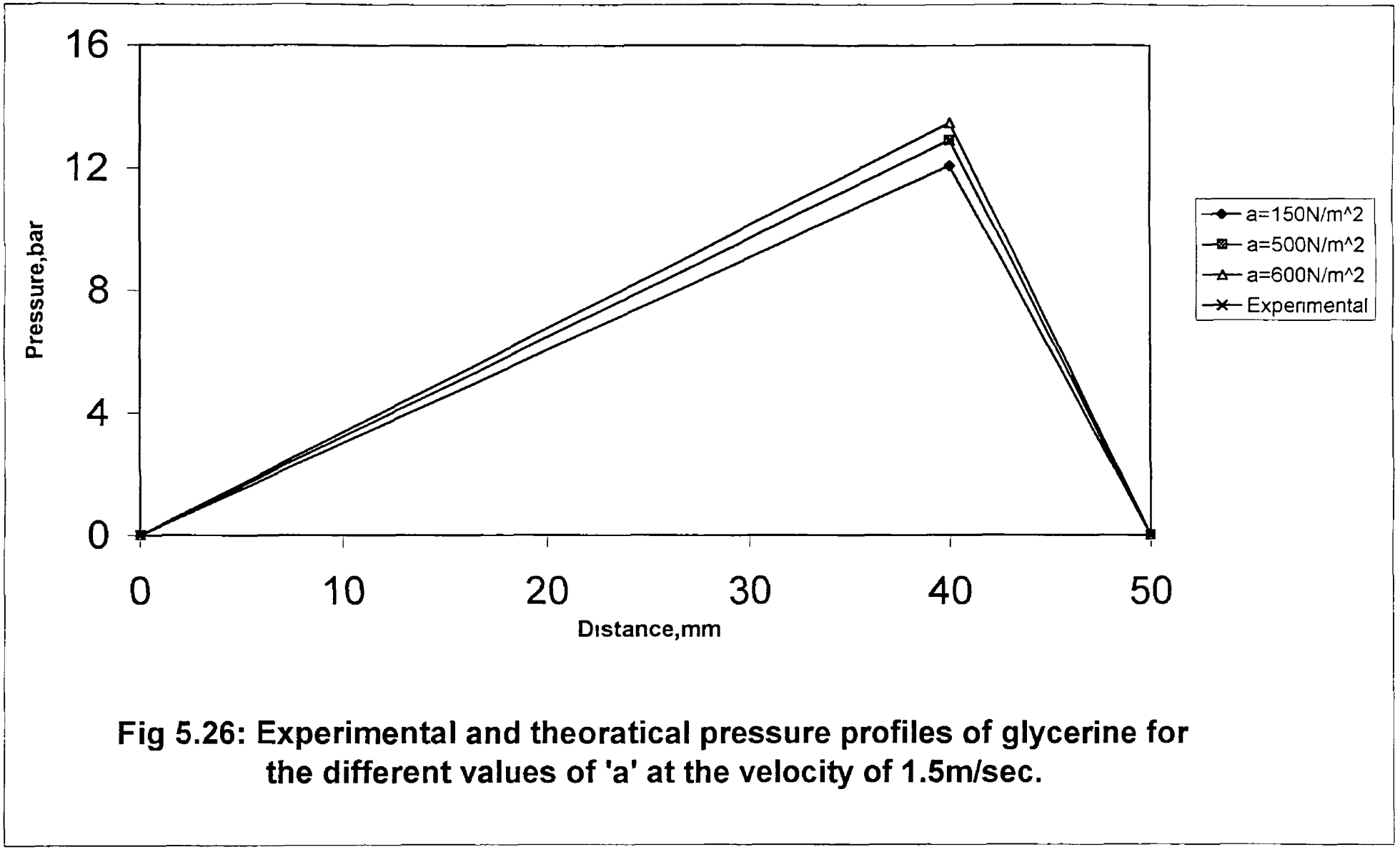

Fig 5.26: Experimental and theoratical pressure profiles of glycerine for the different values of 'a' at the velocity of 1.5m/sec.

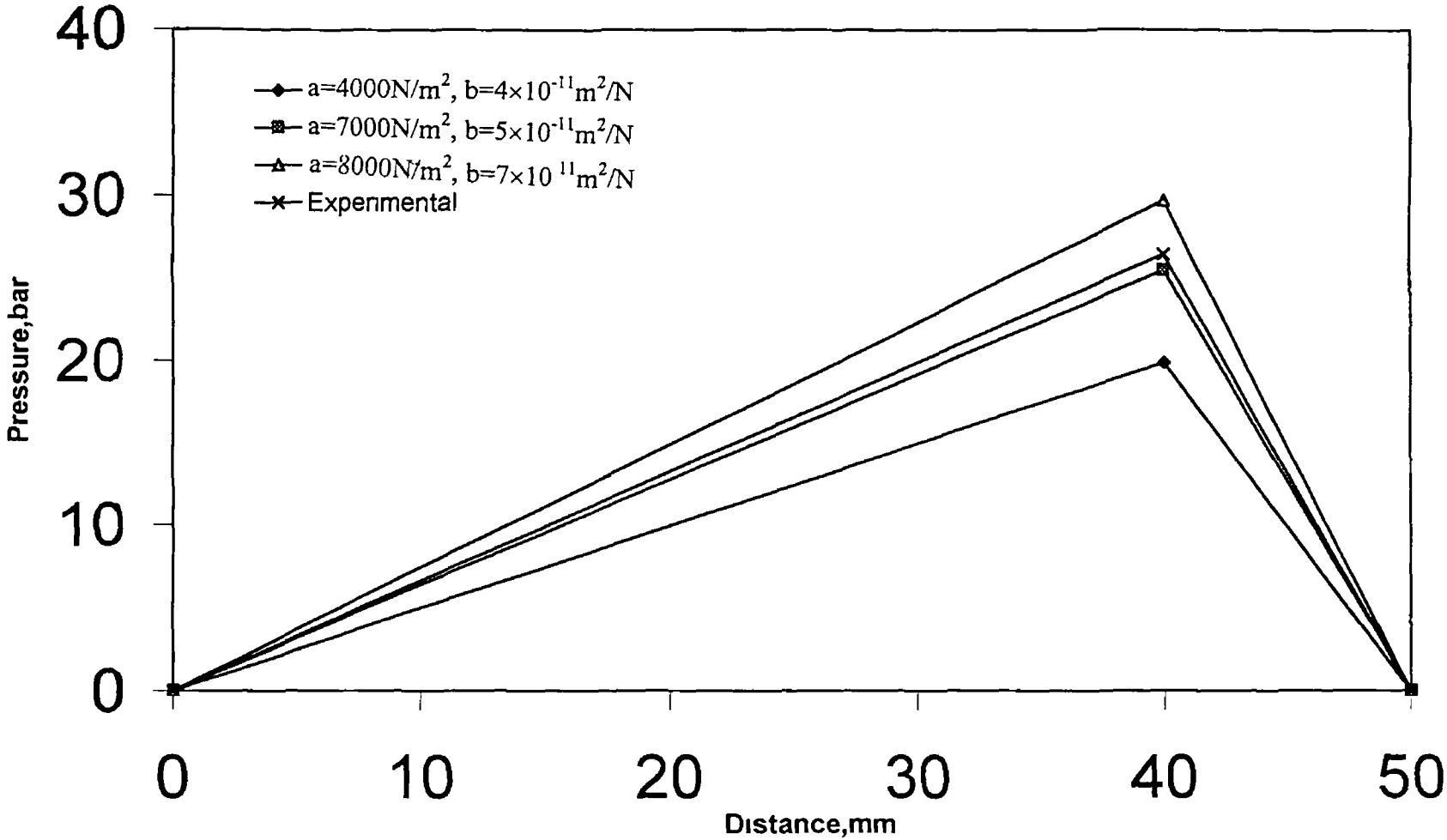

Fig 5.27: Experimental and theoratical pressure profile of silicon 5 with different values of 'a' and 'b'.

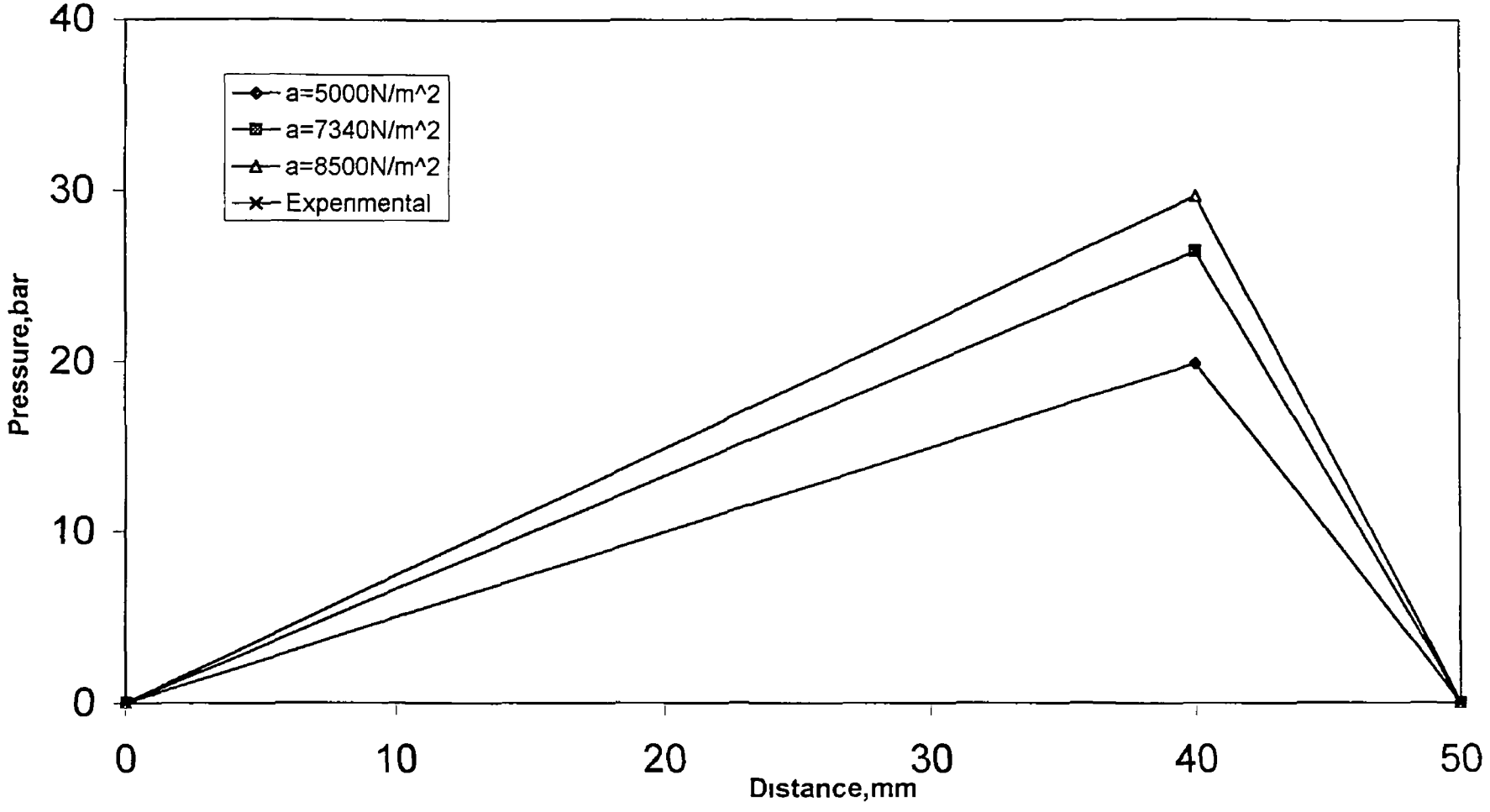

Fig 5.28: Experimental and theoratical pressure profile of silicon 5 for the different values of 'a' at the velocity of 1 0m/sec.

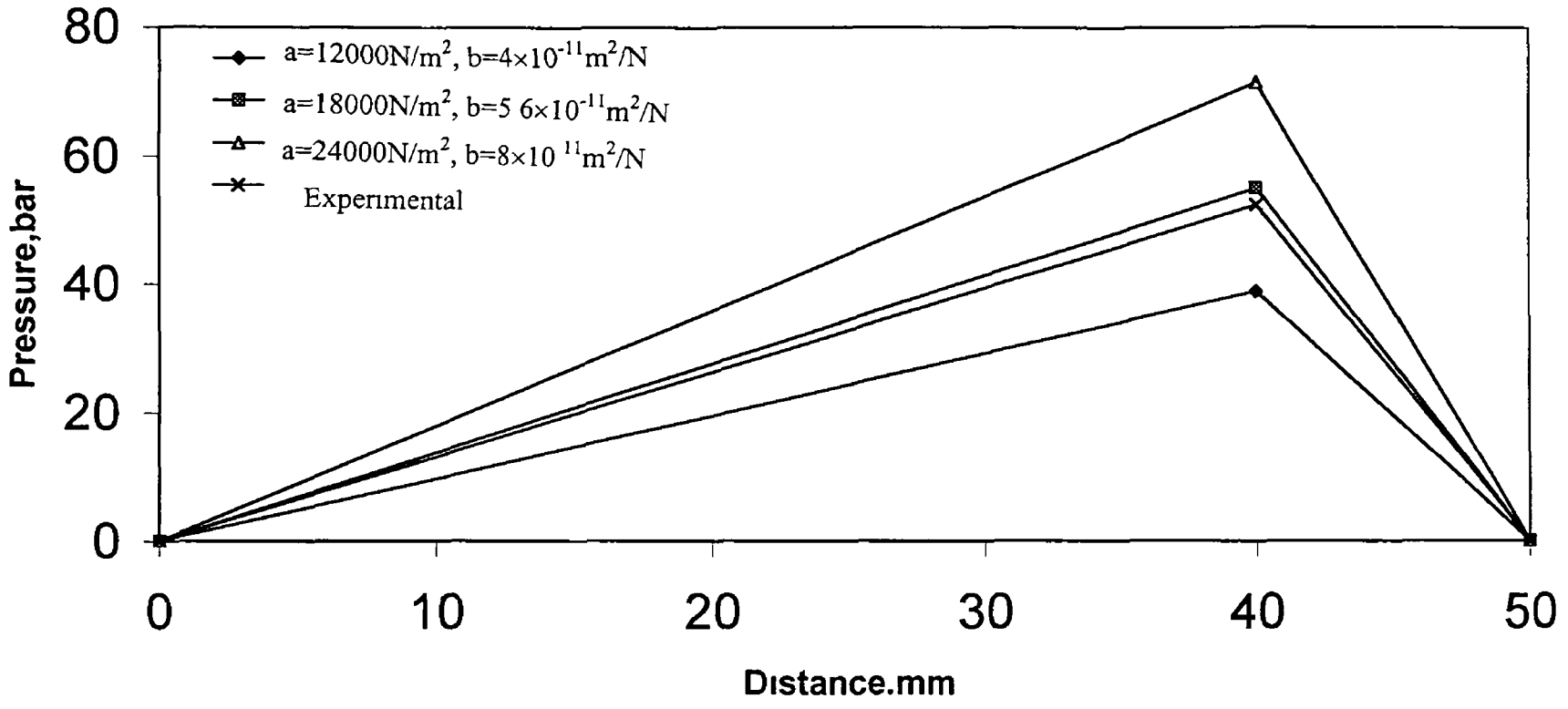

Fig 5.29: Experimental and theoratical pressure profile of silicon 12.5 for differeent values of 'a' and 'b' at the velocity of 1.0m/sec.

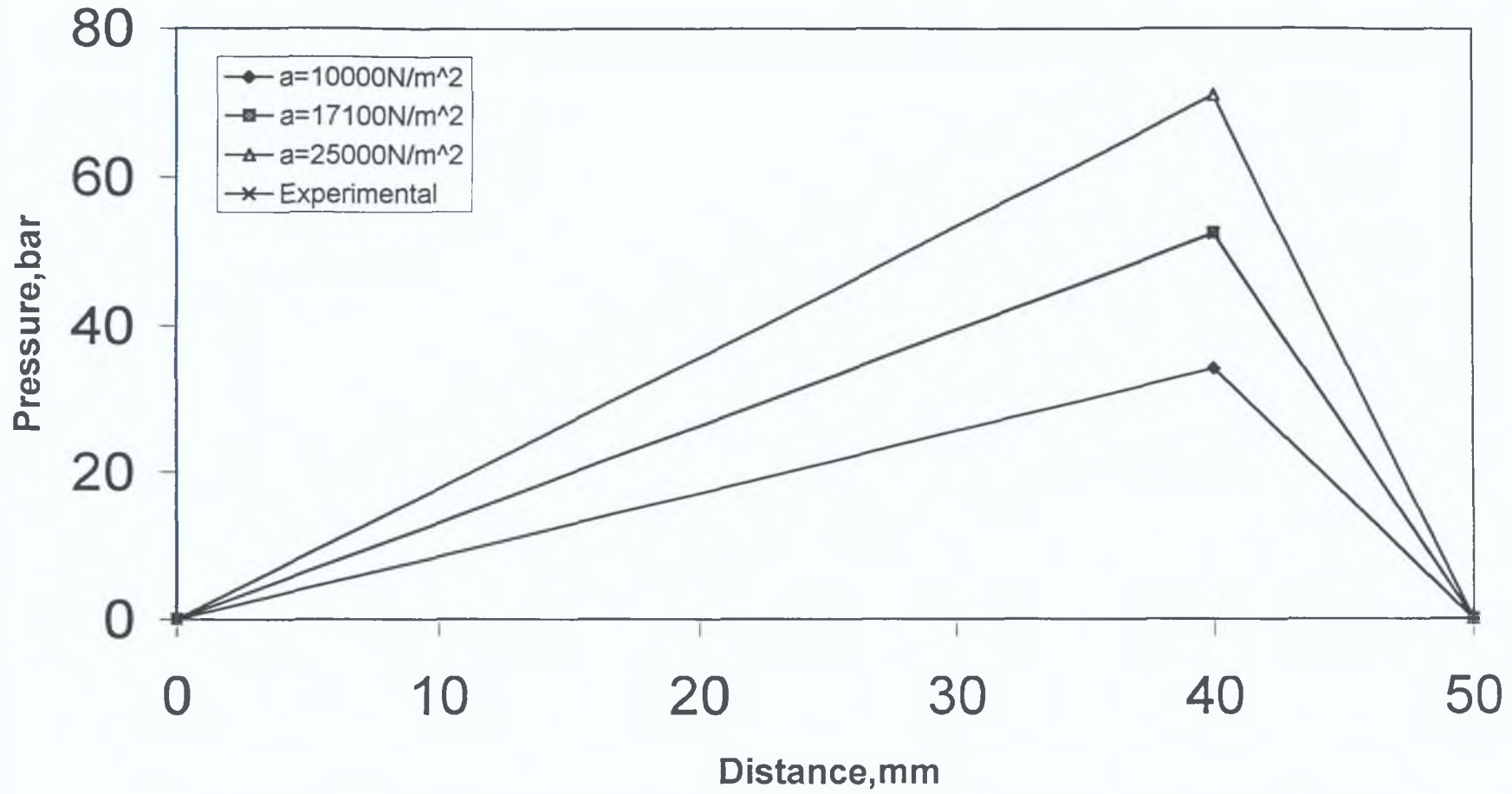

Fig 5.30: Experimental and theoratical pressure profile of silicon 12.5 with different values of 'a'.

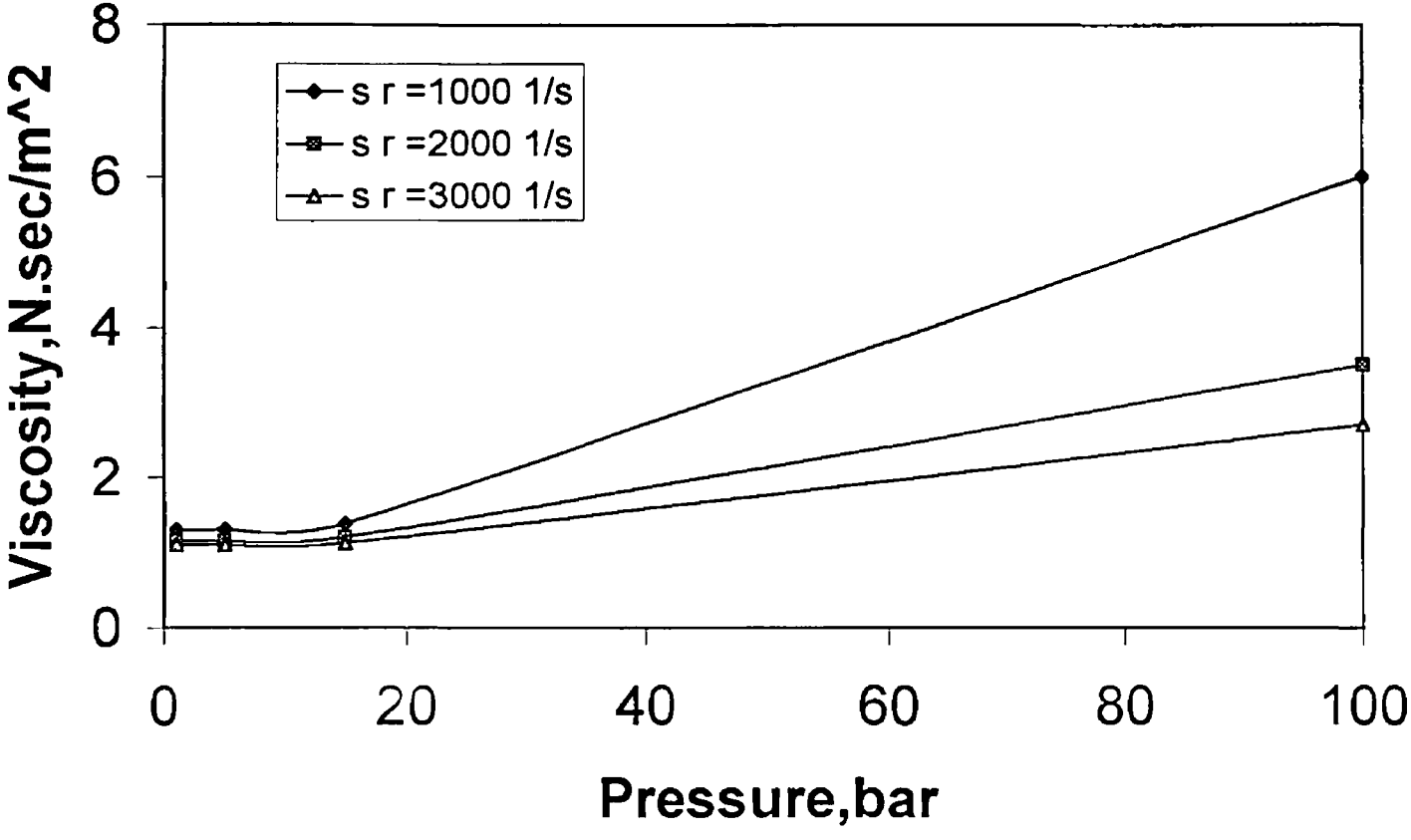

Fig 5.31: Effect of pressure on viscosity for glycerine.

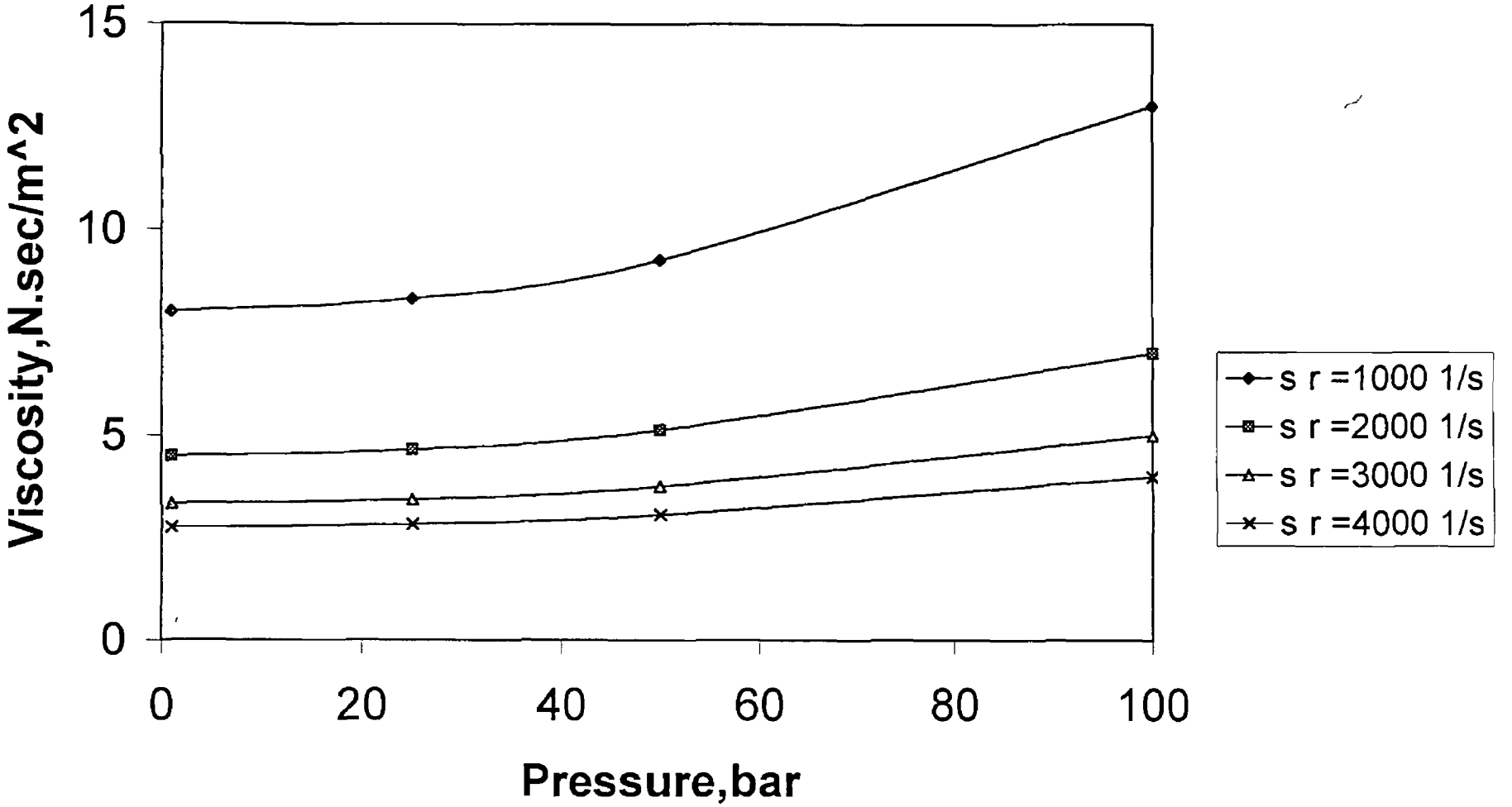

Fig 5.32: Effect of pressure on viscosity for silicon 5

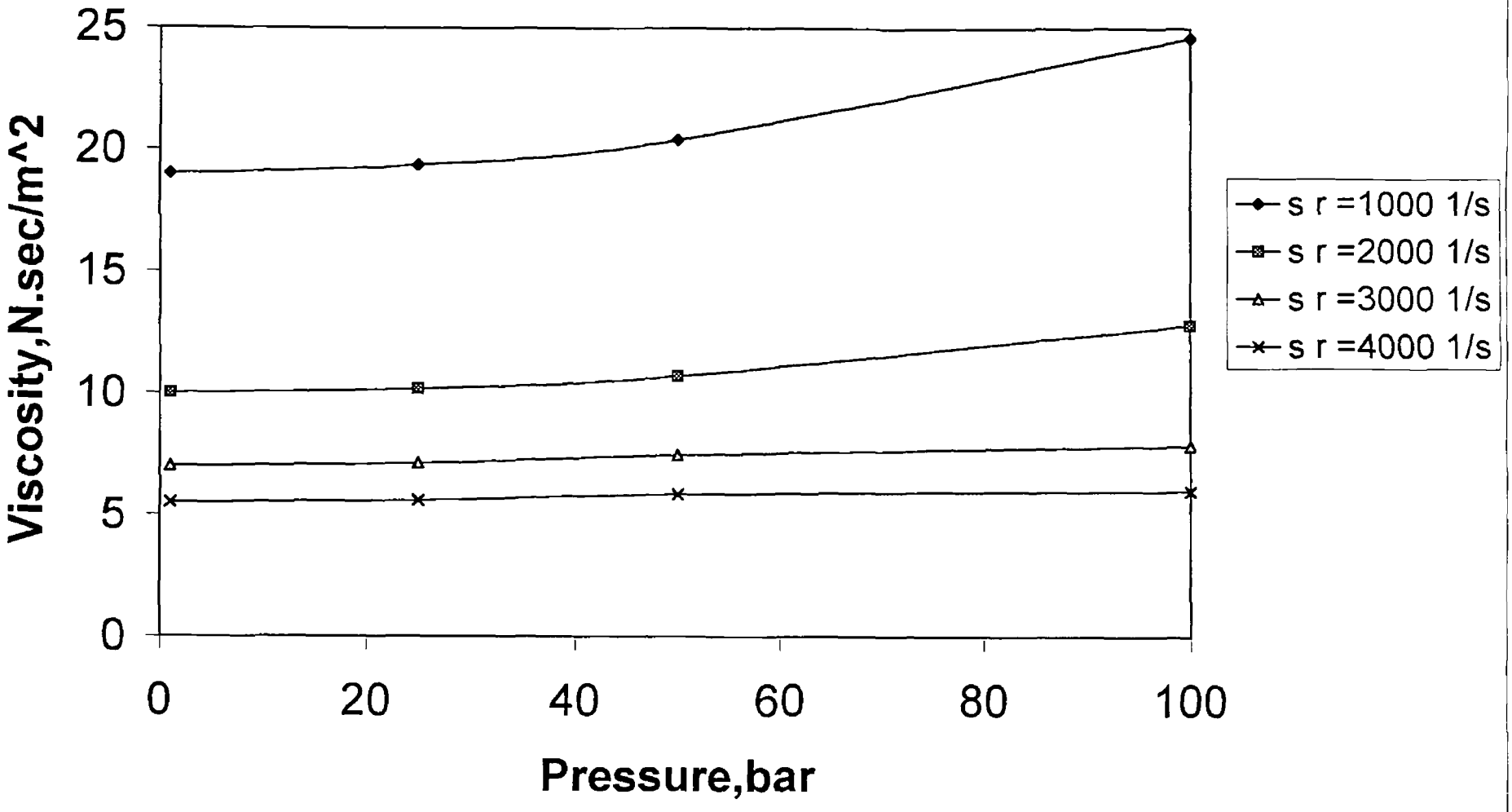

Fig 5.33: Effect of pressure on viscosity for silicon 125

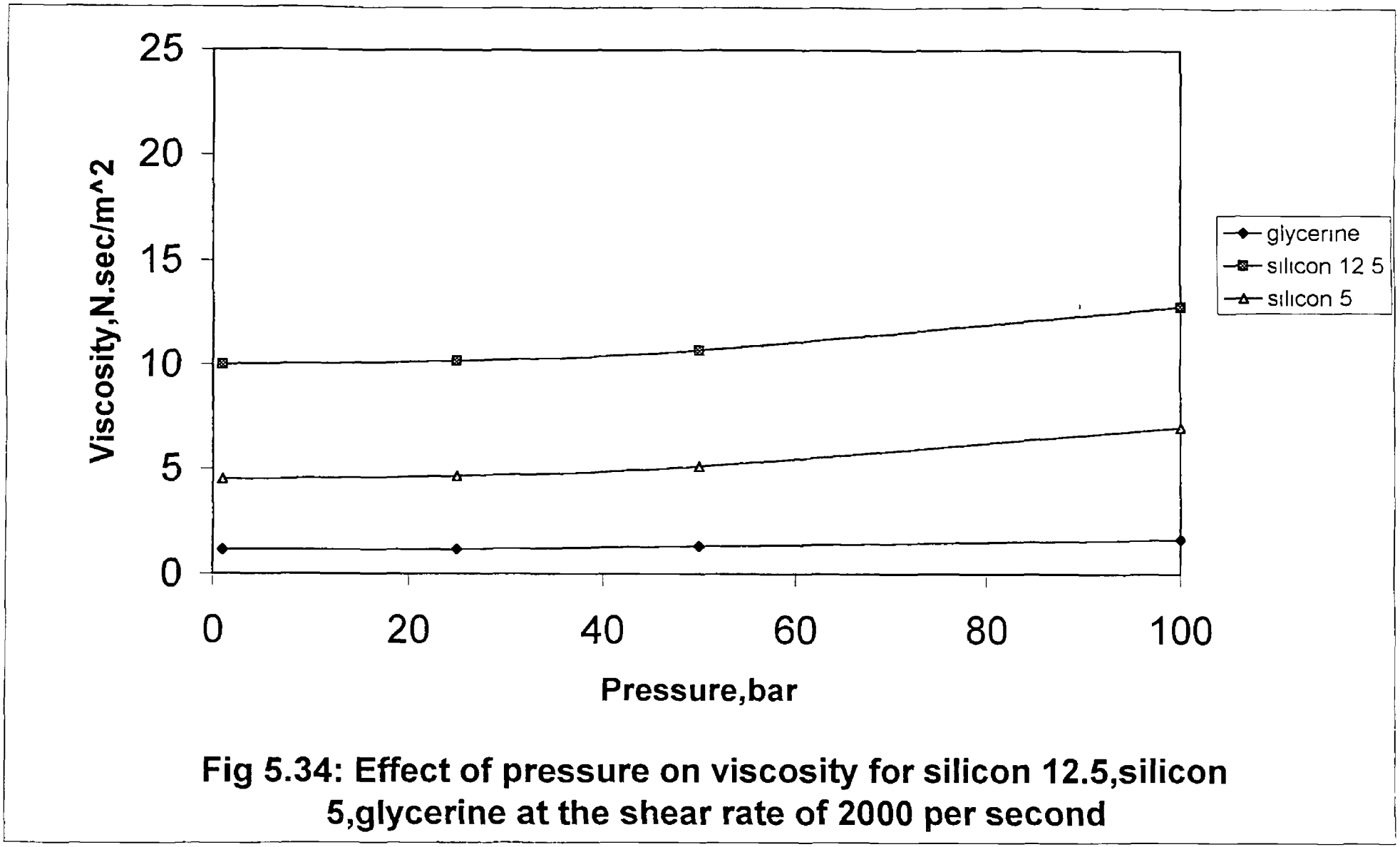

Fig 5.34: Effect of pressure on viscosity for silicon 12.5,silicon 5,glycerine at the shear rate of 2000 per second

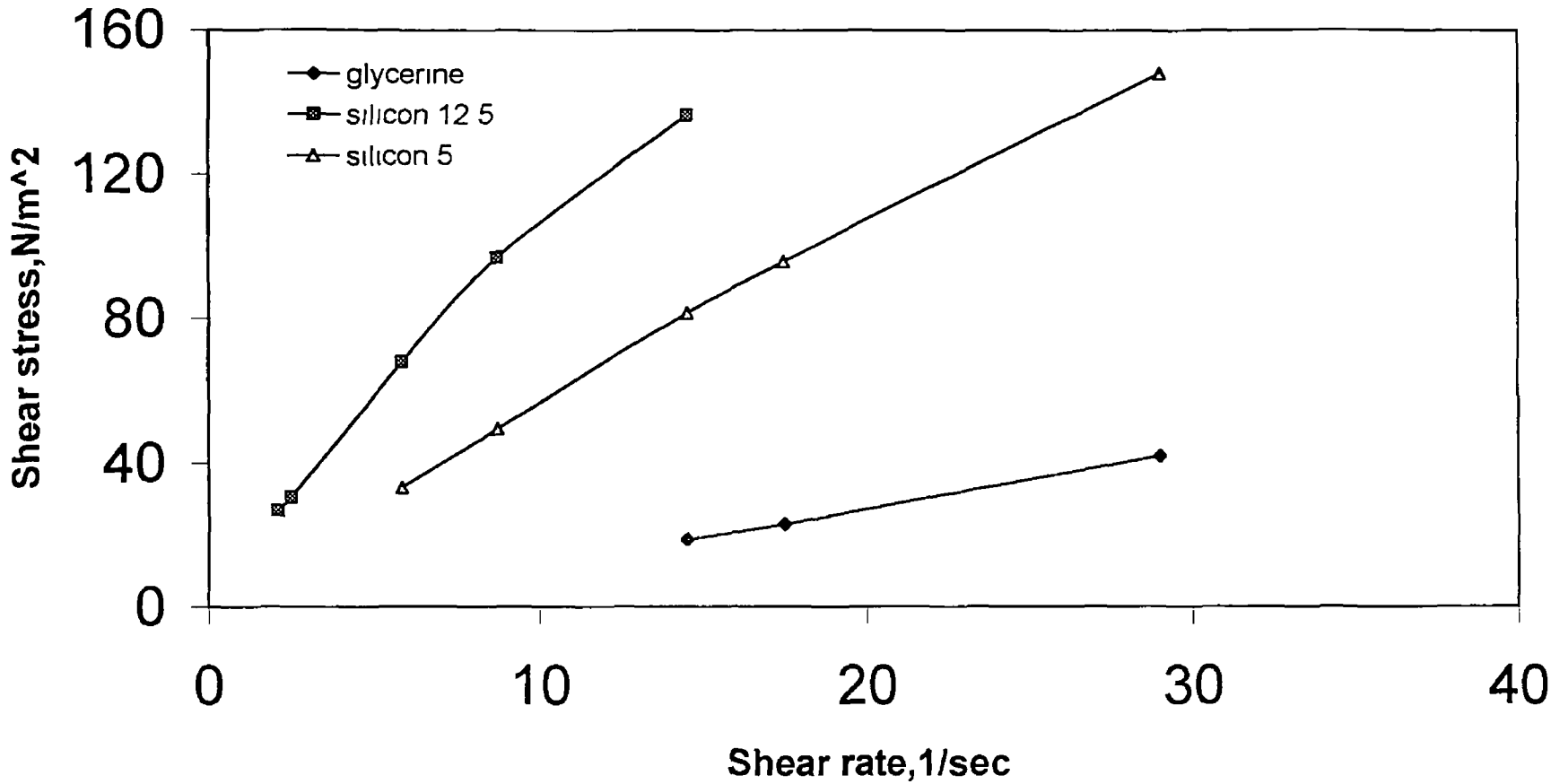

Fig 5.35: Shear rate vs Shear stress of glycerine,silicon 5,silicon 12.5 using Brookfield viscometer.

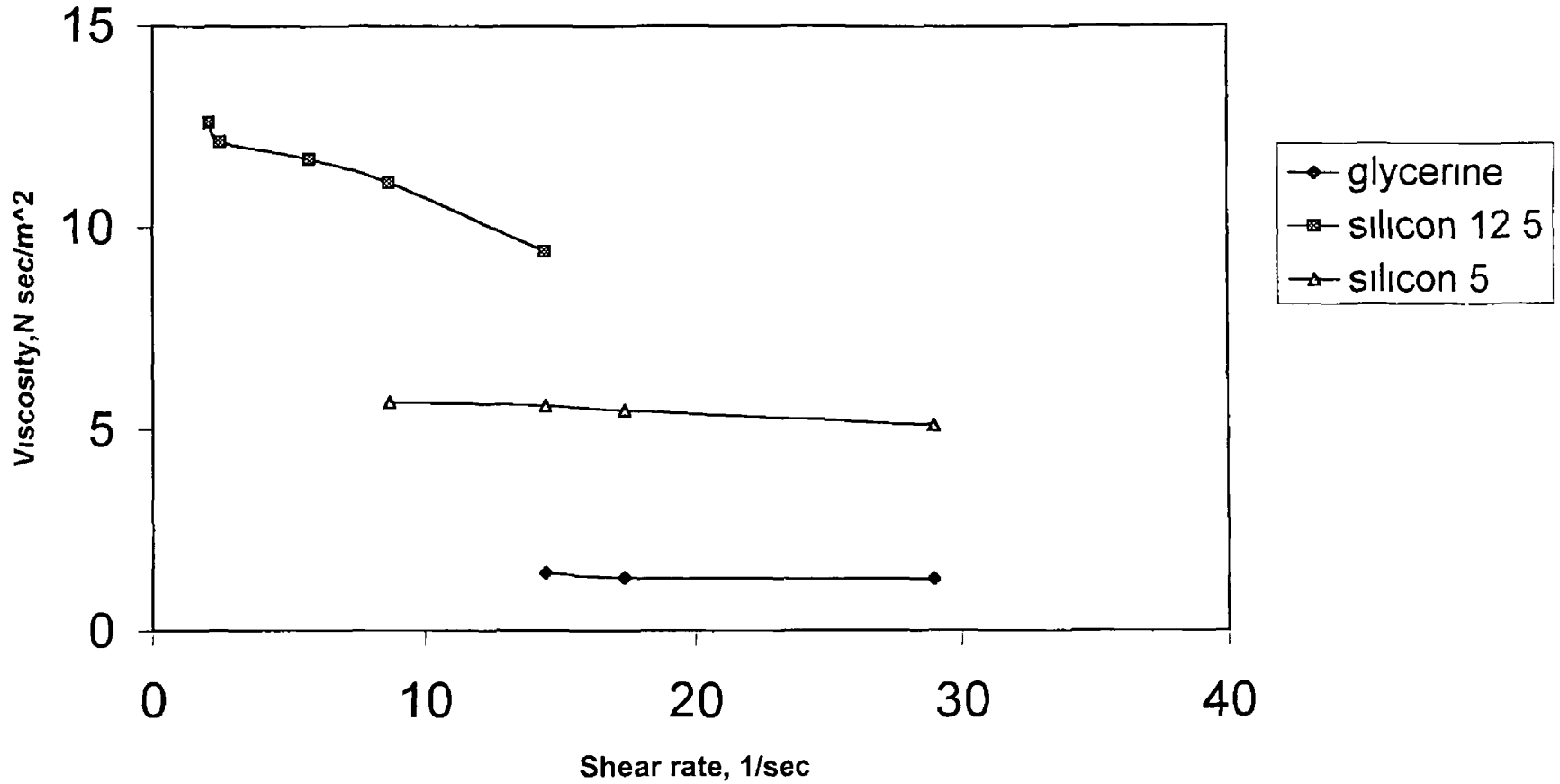

Fig 5.36: Effect of shear rate on viscosity of glycerine,silicon 5, silicon 12.5 using the Brookfield viscometer.

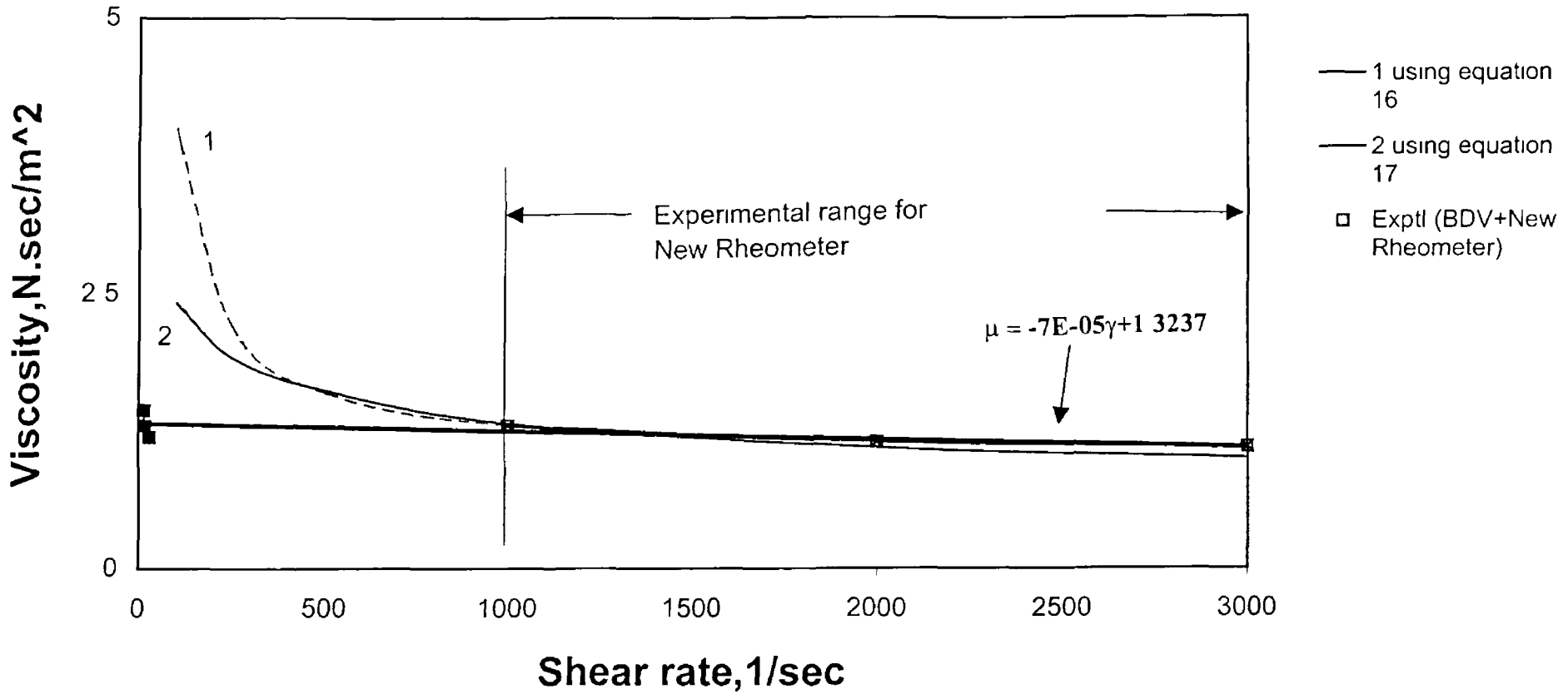

Fig 5.37: Effect of shear rate on viscosity of glycerine at atmospheric pressure.

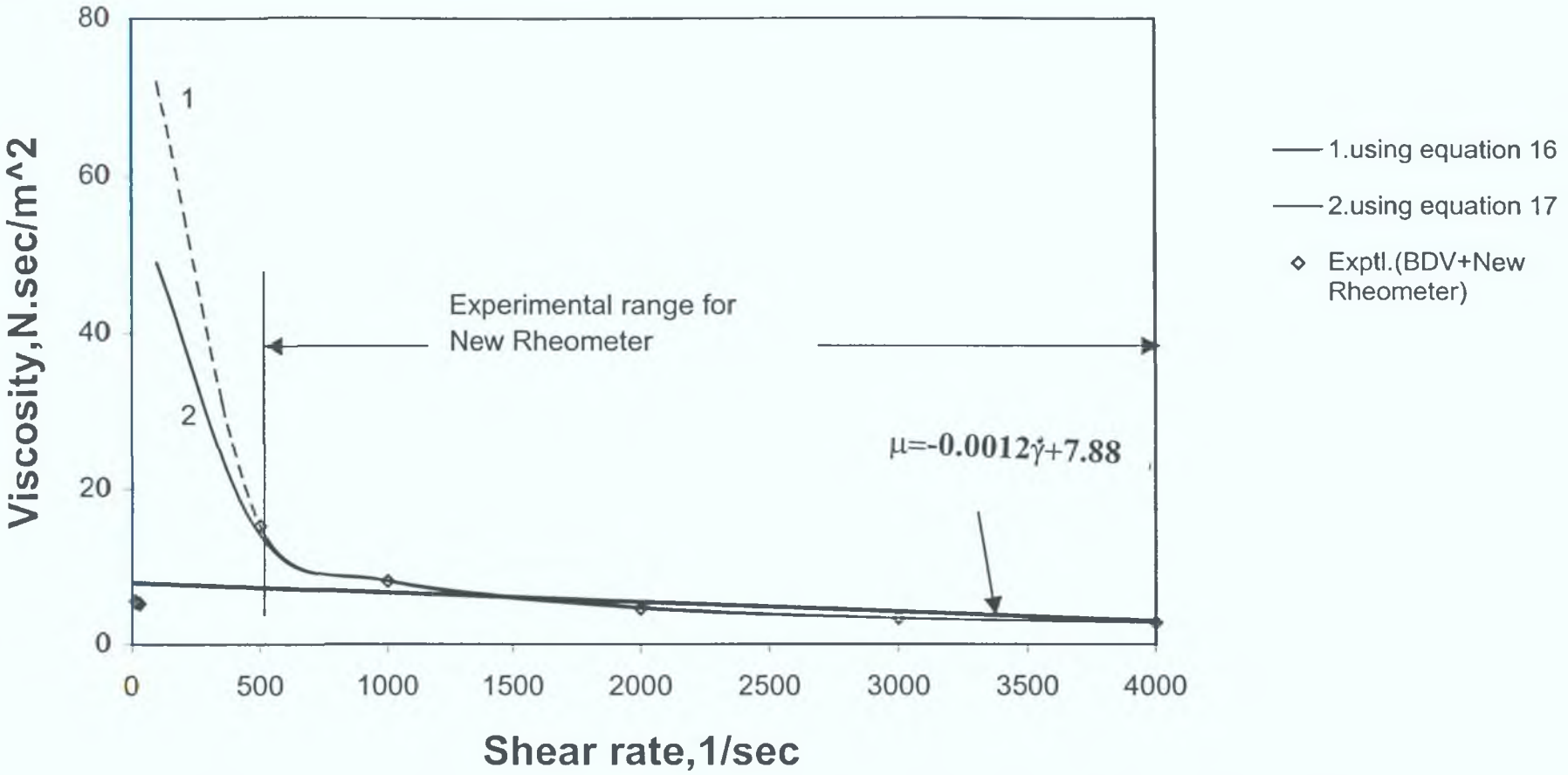

Fig 5.38: Effect of shear rate on viscosity of silicon 5 at atmospheric pressure.

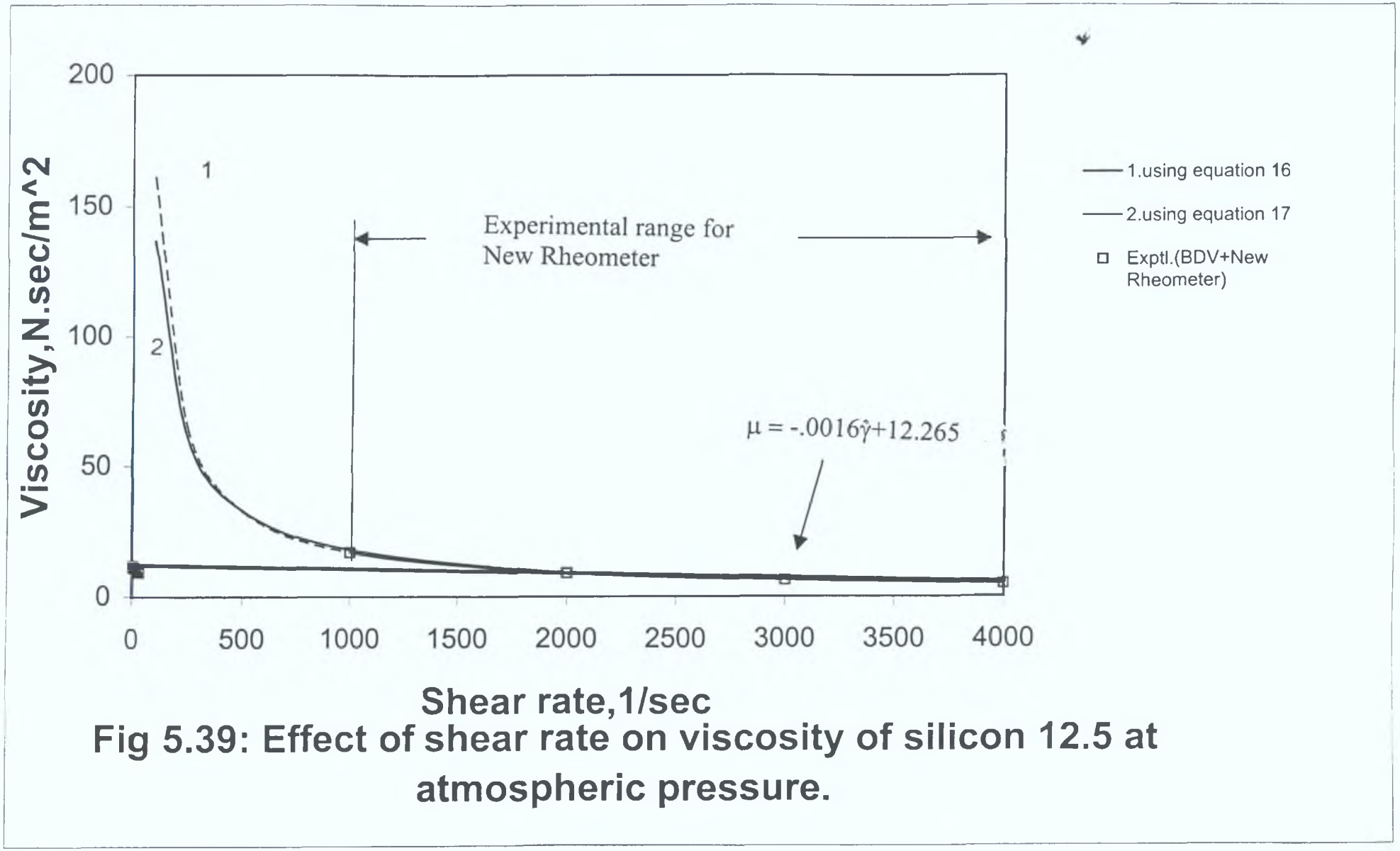

Fig 5.39: Effect of shear rate on viscosity of silicon 12.5 at atmospheric pressure.

5 6 Discussion

5 6 1 Introduction

Hydrodynamic principle has been introduced in a novel rheometric device to study the rheological behaviour of non-Newtonian fluids using glycerine and silicon as examples To investigate the performance of the device, an extensive experimental and theoretical programme was conducted during which a considerable amount of data were obtained Limited experiments were also done by using a Brookfield viscometer at atmospheric pressure only This section is aimed to highlight the important results obtained experimentally and theoretically to determine the viscosity-shear rate relationship for glycerine, silicon 5 and silicon 12 5 fluids

The discussion chapter is divided into three sections (i) test procedure and experimental work (ii) analysis and theoretical results and (iii) error analysis

5 6 2 Discussion on Test Procedure and Experimental Work

A number of interesting results have been observed while carrying out the experimental tests, using the new rheometric device and glycerine and silicon as the test fluids During the course of the experimental programme, parameters such as gap ratios, shearing speed, fluid type were varied in order to investigate their effect on the performance of the pressure unit The length and the length ratio, the outlet gap h_2 were constant throughout the tests Experimental work was first done with the two pressure transducers, their rating was 2000 bar using glycerine as the test fluid The readings were not changing with the change of the speed The pressure transducers

were over rated and hence new lower capacity 70 bar ones were selected These new transducers were found to be sensitive to the variation of pressure with changing shear velocity

The results of the pressure versus shearing speed using silicon 5, silicon 12 5 and glycerine as test fluids are shown in Fig 5 1 to 5 20 For the gap ratio of 5 the generated pressure is found to be higher As the inlet gap decreases, the fluid flow rate also decreases into the gap, which in turn is thought to be responsible for lower pressure An increase in the inlet gap without increasing the outlet gap may cause back flow of the polymer which would also reduce the pressure From Fig 5 35 it is seen that glycerine and silicon 5 show Newtonian behaviour as the shear stress and shear rate curves are almost linear for shear rate values of less than about 30 per second Silicon 12 5 shows non-Newtonin behaviour This is also confirmed from the results in Figs 36 Figs 5 37 to 5 39 show the viscosity vs shear rate curves At lower shear rate the predicted viscosity values are much higher than those measured using the Brookfield viscometer The difference in results is due to the fact that experimental work was carried using the new rheometer at higher shear rates and the coefficients were calculated according to theoretical and experimental results at higher shear rate The thermocouple was connected where the pressure reading is zero, so that the actual temperature cannot be measured With an increase of one degree centigrade at that location the temperature in the may increase by several degrees which may decrease the viscosity and hence the pressure readings

5 6 3 Discussion on the Analysis and the Theoretical Results

A model has been developed based on the assumption that the pressure medium demonstrates non-Newtonian characteristics The following assumptions were made in order to simplify the analysis

(i) The flow of the fluid medium in the present pressure unit is laminar This seems to be a reasonable assumption since the shearing speeds of the shaft are relatively low and the gaps are small

(ii) The flow of the fluid pressure medium is axial Once flow through the pressure unit has commenced, little or no back flow is expected This assumption allowed one-dimensional flow to be considered

(iii) The thickness of the fluid layer is small compared to the dimensions of the Rheometric pressure unit This assumption enabled the analysis to be conducted in cartesians rather than cylindrical co-ordinates

(iv) The pressure in the fluid medium is uniform in the thickness direction This assumption simplified calculation of the pressure in the unit and allowed the viscosity constant to be evaluated

(v) The flow of the fluid through the unit is isothermal This may introduce some error in the results since viscosity of the fluids is sensitive to the temperature change

The emperical non-Newtonian equation commonly used to represent the behaviour of the fluid, as proposed by Rabinowitch [12] takes the form,

$$\tau + K\tau^3 = \mu \frac{du}{dy}$$

This equation was used in the analysis to predict the pressure The non-Newtonian factor 'K' and the initial viscosity μ were both determined experimentally by curve

fitting the above equation over the results obtained from the flow characteristics of polymer melt

The above equation represents the effect of shear stress on the viscosity only It is known that the pressure increases the viscosity of the fluid To incorporate this effect in the analysis, the data provided by Westover for the Alkathene polymer was used to produce Fig 1 2 Which shows that the influence of pressure on the viscosity is dependent on the shear rate The accuracy of Westover's results is not known and unfortunately the polymer used for his experiments was not WVG 23 Therefore this may have introduced some discrepancy in the theoretical results in Fig1 2, A generalised equation was derived to predict the viscosity of the polymer melt at known pressure and the shear rates which is shown to take the form

$$\mu = \mu_o + \frac{a + bp^2}{\gamma}$$

where γ is the apparent shear rate in the first part of the unit and assumed to be $\frac{V}{h_1}$,

The theoretical value of μ_o and non-Newtonian factor 'K' have been taken from ref [49] in which similar fluids were used However, there were some differences in the properties, which may produce some error in the theoretical results

5 6 4 Error Analysis

Errors always occur in experimental work owing to inaccuracies of other variables, however small they may be, which the final results depend upon Investigation of the probable error is therefore necessary before results can be considered with some degree of confidence Theoretical results were predicted using

numerical techniques incorporating interation methods In conjunction to the experimental and theoretical results, the values of the pressure coefficients of viscosity have been determined using an iteration technique For different values of 'a' and 'b' different theoretical pressure values have been obtained at the same shearing speed Error has been calculated within the difference between the theoretical and the experimental pressure values Appendix C shows the error analysis for different types of fluid For glycerine ($a = 300\ N/m^2$, $b = 4 \times 10^{11}\ m^2/N$) at the gap ratio of 8, 5 and 3 at the speed of 0 5 m/sec the percentage of errors are 12,14 and 11 8 respectively On the otherhand for the same fluid for the same value of 'a' and 'b' at the gap ratio of 8,5 and 3 at the speed of 1 5m/sec, the percentage of errors are 7,5 ,5 and 2 4 A possible arithmetic error of about $\pm$ 15% were occurred in the theoretical and experimental pressure values while calculating the values of the pressure coefficients of viscosity A considerable difference has been observed between some of the experimental and the theoretical results, based on mean values of 'a' and 'b' of equation (16) This suggests that the analysis carried out for the rheometric device needs more refinement It is believed that the discrepancies may have arisen due to the value of non-Newtonian factor 'K', the absence of the parameter in the analysis which affect the flow properties of fluids

Chapter Six

CONCLUSION AND SUGGESSIONS FOR FURTHER WORK

6 1 Introduction

This chapter presents a summery of the current thesis It is divided into two sections The first section represents the investigation under consideration, the techniques to carry out this task and a brief summery of the conclusion, and the second identifies further studies that can be pursude in future works

6 2 Conclusion

This thesis outlines the author's research effort m the area of high-pressure non-Newtonian fluid rheology

- This work involved measurement of the variation of pressure with shear rate and gap ratio for glycerine and silicon using a novel rheometer designed on the basis of hydrodynamic principles The range of shear rate is 500 to 4000 per second
- A theoretical analysis based on the non-Newtonian characteristics for a new rheometric device has been presented where the effect of the hydrodynamic pressure influences the viscosity of the fluids
- The influence of the geometry of the unit and the speed on the maximum pressure generation, which affect the viscosity, has also been discussed Experimental results from the pressure distribution within the stepped

parallel gap Rheometric device have been used in conjunction with the theoretical pressure results to determine the coefficients for a viscosity shear rate

- Using these coefficients, the viscosity at different pressures was calculated and the effect of shear rate and pressure on viscosity was demonstrated
- Using the coefficients the viscosity of these fluids was predicted at lower shear rates at atmospheric pressure Using the Brookfield viscometer, viscosity values of the three different types of fluids were measured at different lower speeds and the shear rate vs viscosity curve has been plotted These values were much higher than those measured using the Brookfield viscometer
- New type of equations have been developed at the shear range 0 to 4000Sec^{-1} based on the experimental results using the BDV and New Rheometer
- The new Rheometric device is an innovative facility in high-pressure fluid rheology

Although considerable amount of work on the process was done so far, there are more avenues of work on this process in the future

6 3 Suggessions For Future Work

- In the present work the analysis was developed assuming isothermal condition It is suggested that a great deal of knowledge could be obtained about the rheology of different non-Newtonian fluids at elevated temperatures

- The viscosity of a fluid is known to be sensitive to the temperature change, hence a relationship predicting the viscosity change due to the temperature variation may improve the results
- The rheology of the fluid should be better understood with respect to the effect of pressure and temperature on viscosity So, the theoretical model should be based on both the temperature and pressure
- In the present study the temperature of the fluid was monitored out side the pressured gap where the hydrodynamic pressure is zero The temperature should be measured within the gap But it is difficult to insert a thermocouple in the step without damaging the step configuration So, finite element modelling can be used for predicting the theoretical temperature in the step
- The geometry of the pressure unit could be changed to tapered, combined or parabolic types
- The pressure transducers could be placed at the nearest position of the step
- The experimental work could be done at the lower shearing speeds modifying the thickness of the entry gap of the unit and at the lower shear rate, the coefficient values can be obtained

REFERENCES

[1] H A Barnes, J F Hutton and K Walter, "An Introduction to Rheology", published by Elsevier Science, Netherlands, 1980

[2] Carley, J F "J Modern Plastics", December, 1961

[3] Nielsen, L E "Polymer Rheology", New York, 1977

[4] Sanchez, I C "J Appl Phys ",pp 45 & 4204, 1974

[5] Westover, R F "Polymer Engg Sci ", pp 6 & 83, 1966

[6] Cohen, M and Turnbull, D "J Chem Phys ", pp 31 & 1164, 1959

[7] Jacobson,B O , Rheology and Elastohydrodynamic Lubrication,Tribology Series,19,Elsevier Science Publishers,ISBN 0-44-88146-8, 1991

[8] Westover R F, " The significance of slip in polymer melt flow, Polymer Engineering and Science, January ,pp 6, 83-89, 1960

[9] B Maxwell, and Jung, A , "Hydrostatic pressure effect on polymer melt viscosity", Modern Plastics, 35, November , pp 174, 1957

[10] Choi, S Y , "Determination of melt viscosity as a function of hydrostatic pressure in an extrusion rheometer", Journal of Polymer Science, A-2,Vol 6, pp 2043

[11] Cogswell, F N , " The influence of pressure on the viscosity of polymer melts", Plastics and polymers, February, pp 39 and 41, 1973

[12] Rabinowitsch, B , " Uber Die Viskostat and Elastizitat Von Solen", Z Phys Chem A145, pp 141, 1929

[13] M L WILLIAMS, R F LANDEL and J D FERRY, "The temperature dependence of relaxation mechanisms in amorphous polymers and other glass-forming liquids", Journal of the American Chemical Society, pp 77, 3701

[14] J A BRYDSON, "Flow properties of polymer melts", Published By Plastic Institute, London, Illiffe Books, 1970

[15] DIENES,G J Applied Phys 24,779,195

[16] Crampton R "Hydrodynamic Lubrication and Coating of Wire using a Polymer Melt During Drawing Process" , PhD Thesis, Shefield City Polytechnic, 1980

[17] E B BAGLEY, "The separation of elastic and viscous effect in polymer flow", Trans Of The Society of Rheology, pp 341-353, 1961

[18] E R HOWELLS and J J BENBOW, " Flow defects in polymer melts", ICI Publication, August 1962

[19] A B METZNER, "Fracture of non-Newtonian fluids at higher shear stresses", Industrial and eng Chemistry, Vol 50, No 10,1958

[20] Christopherson, D G and P B Naylor, "Promotion of fluid lubrication in wire drawing", Proceeding of Institute of Mechanical of Engineering,, pp 169 and 643-653, 1955

[21] Wistreich,J G , "Lubrication in wireing drawing", *Wear*, March (1997), pp 505-511, 1997

[22] TATTERSALL, G H "Hydrodynamic Lubrication In Wire Drawing" J Mech Engg Sc , Vol 3, No 4, pp 378, 1961

[23] CHU, P S "Theory of lubrication applied to pressure nozzle design in wire drawing" Proc Inst Mech Engg , Vol 181, pp-3, 1967

[24] Bedi D S " A hydrodynamic model for wire drawing" The inter national J production and Research, Vol 6, No 4 ,1968

[25] Bloor M, DAWSON D, and PARSON B , "An elasto-plast-hydrodynamic lubrication analysis of the plane strain drawing process ", J-Mech Sc , Vol 12, No 3, 1970

[26] OSTERLE J F and DIXON J R , " Viscous lubricaation in wire drawing", ASLE Transactions, vol 5, pp 233-241,1962

[27] MIDDLEMISS A , "Hydrostatic lubrication for drawing steel wire," Tribology in iron and steel works, ISI, Publication 125

[28] KALMOGROV, V L AND SELISHCHEV, K P "Cold drawing tubes with improved lubrication" stall in english pp 830-831, 1962

[29] Orlov, S I , Kolmogrov, V L , Ural, Skll, V I And Stukalov, V T , "Intregated Development and Introduction of New High-Speed Mill and Hydrodynamic Lubrication System for Drawing Wires", Steel In The USSR, Vol 10, pp 953-956, 1974

[30] Swamy, S T N Prabhu, B S and Rao, B V A " Calculated Load Capacity of Non-Newtonian lubrication inFinite Width Bearings", EAR, Vol 3(1975), pp 277-285

[31] Thompson, P J and Symmons, G R , " A Plasto Hydrodynamic analysis of the Lubrication and Coating using Polymer Melt During Drawing", Proc Inst Mech Eng Vol 191, pp 13, 1977

[32] Slevens, A T , "A plasto-Hydrodynamic Investigation of the Lubrication and Coating of Wire Using a Polymer Melt During Drawing", M Phil Thesis, Shefield City Polytechnic, 1979

[33] Crampton, R Symmons, G R , and Hashmi, M S J "A non-Newtonian Plasto-hydrodynamic analysis of the lubrication and coating of wire using a polymer melt during drawing", Int Symposium, metal working lubrication, San Fransisco, USA, pp 107-115, August 1980

[34] M I PANWHER, R CRAMPTON AND M S J HASHMI "Dieless tube sinking pasto-hydrodynamic analysis based on Newtonian fluid characteristics" Proceedings of 1st Conference on Manufacturing technology, Irish Manufacturing Committee, pp 153-172, Dublin, March 1984

[35] M S J HASHMI, R CRAMPTON and M I PANWHER ,"Plasto-hydrodynamic tube sinking Experimental evidence and numerical solution" Proceeding of 3rd International Conference on Numerical methods for non-linear problems, Dubrovnik, Yugoslavia, September, pp 115-129, 1986

[36] M S J HASHMI, R CRAMPTON and] M I PANWHER "Mathematical modelling of dieless tube sinking based on non-linear deformation profile Proceeding of 6th Conference of the Irish Manufacturing Committee,pp 248-254, Dublin, August 1989

[37] M I PANWHER "A novel technique for tube sinking" PhD Thesis SHEFIELD City Polytechnic,1986

[38] M I PANWHER , R CRAMPTON and] M S J HASHMI," Analysis of the die-less tube sinking process based on non-Newtonian characteristics of the fluid medium", Journal of Material Processing Technology, vol 21, pp 155-175, 1990

[39] G R Symmons, Hashmi , M S J and YD XIE, " The optimisation of Plasto-hydrodynamic wire drawing process", Proceeding of 6th International Conference on Modelling, Paris, France, June, pp 362-366, 1987

[40] G R Symmons, YD XIE and Hashmi , M S J "Thermal effect on a plasto-hydrodynamic wire drawing using a polymer melt" Proceedings of Xth International Conference on Rheology, Vol 2, pp 295-297, Sydney, Australia, August 1988

[41] G R SYMMONS, A H MEMON and M S J HASHMI " A mathematical model of a plasto-hydrodynamic drawing of narrow strip" Mathematical computation modelling, Vol 11 pp 926-931, 1988

[42] G R SYMMONS, A H MEMON and M S J HASHMI, " A Newtonian model of a plasto-hydrodynamic drawing process of a rectangular cross sectional continuum", Proceeding of 7th International Conference on modelling identification and control , pp 67-70, Grindlwald, Switzerland, February 1988

[43] G R SYMMONS, A H MEMON, R CRAMPTON and M S J HASHMI, "An experimental study of a plasto-hydrodynamic strip drawing process of rigid non-linearly strain hardening strip through a stepped rectangular slot", Journal of process mechanical engineering, Proceeding of ImechE, Part E, Vol 203, pp 57-65, 1989

[44] G R SYMMONS, A H MEMON, R CRAMPTON and M S J HASHMI,"A numerical solution for plasto-hydrodynamic drawing of rigid non-linearly strain

hardening strips through a stepped rectangular slot", Proceeding of 3rd International Conference on Numerical methods in Id Forming Process, pp 575-580, Colorado, U S A , June, 1989

[45] H Parvinmehr, G R Symmons, and M S J Hashmi, " A non-Newtonian plasto-hydrodynamic analysis of dieless wire-drawing process using a stepped bore unit" International Journal of Mechanical Science Vol 29 no 4, pp 54-62, London, May 1982

[46] M S J Hashmi, G R Symmons, and H Parvinmehr," A novel technique of wire drawing", Journal of Mechanical Engineering Sci, Inst Mech Negro 24, 1982

[47] G R Symmons, M S J Hashmi and H Parvinmehr" Plasto- hydrodynamic dieless wire drawingtheoratical treatment and experimental results," Proceedings of Interntional Conference on Development in Drawing Metals, Metals Soceity, pp 54-62, London, May 1983

[48] G R Symmons, M S J Hashmi and H Parvinmehr " Aspects of product quality and process control in plasto-hydrodynamic dieless wire drawing", Proceeding of 1st Conference on Manufacturing technology, Irish Manufacturing Committee, pp 153-172, Dublin, March 1984

[49] H parvinmehr, "Optimisation of plasto-hydrodynamic system of wire drawing using polymer melts", Ph D Thesis, Shiefield City Polytechnic, UK, (1983)

[50] HASHMI M S J and SYMMONS G R " A numerical solution for the plastohydrodynamic drawing of rigid non-linearly strain hardening continum through a conical orifice" 2nd Int Conf on numerical Methods for non-linear problems, Spain 1984

[51] I AL-NATOUR and M HASHMI, "Development of a complex geometry pressure unit for hydrodynamic coating applications" Proceeding of 6th Conference of the

Irish Manufacturing committee, Dublin City University, pp 280-297, August 1989

[52] I AL-NATOUR, "Plastohydrodynamic pressure due to the flow of viscous fluid through a confined passage", M Engg Thesis, Dublin city University, 1989

[53] M A NWIR and M S J HASHMI, "Optimization of pressure and drawing stress in a simple tapered pressure unit using Borosiloxane as a pressure fluid",Proceedings of Twelfth Conference of the Irish Manufacturing Committee, pp 253-258,1995

[54] M A NWIR and M S J HASHMI, "Hydrodynamic pressure distribution in a tapered ,stepped parallel bore and Complex geometry pressure units experimental results",Proceedings of Advances in Materials and Processing technologies, pp 1431-1437,1995

[55] M A NWIR, "Plastohydrodynamic pressure in a simple tapered and combined geometry unit or drawing and coating of wires", Ph D Thesis, Dublin City University, 1994

[56] M A Nwir, "Plastohydrodynamic pressure in a simple tappered and combined geometry unit for drawing and coating of wires, Ph D Thesis, Dublin City University, Dublin, IRELAND, 1994

[57] Akhter, S , " Study of viscous flow during their film polymer coating and drawing of continuum", Ph D Thesis, Dublin City University, Dublin, IRELAND, 1997

[58] J R VAN WAZER, J W LYONS, K Y KIM and R E COLWEL "Viscosity and Flow Measurement, A Laboratory Handbook of Rheology "Published by

INTERSCIENCE PUBLISHERS, 1963

[59] J D NOVAK and W O WINER, "The effect of Pressure on the non-Newtonian Behaviour of Polymer Blended Petroleum Oils" ASME Trans JOLT, Vol 91,NO 3, 1969

[60] M M COUETTE, Ann chim et phys , pp 21& 433 1890

[61] E M BARBER, J R MUENGE and F J VILLFORTH, " A high rate of shear Rotational Viscometer, Analytical Chemistry, Vol 27, No3, pp 425,1955

[62] G D GALVIN, J F HUTTON and B JONES "Develoment of a High-Pressure, High-shear Rate Capillary Viscometer" Journal non-Newtonian Fluid Mech Vol 8, pp 11-28, 1981

[63] D M KALYON, H GKTRUK and I BOZ "An Adjustable Gap in-line Rheometer" Proc Of the 1997 55th Annual Technical Conference, ANTEC Part3, Canada,1997

[64] Y I CHO , E CHOI, and W H KIRKLAND, JR " The Rheology and Hydrodynamic Analysis of Grease Flows in a Circular Pipe" STLE TRIBIOLOGY TRANSACTIONS, Vol 36, No 4, pp 545-554, 1993

[65] S BAIR " The High- Pressure Rheology of a soap Thikened Grease" STLE TRIBIOLOGY TRANSACTIONS, Vol 37, No3 p646-650, 1994

[66] H K NASON "A High Temperature,High Pressure Rheometer for Plastics" Journal of Applied Physics, Vol 16, pp 338-34, 1945

[67] D M KALYON, H GKTRUK and I BOZ "An Adjustable Gap in-line Rheometer" Proc Of the 1997 55th Annual Technical Conference, ANTEC Part3, Canada 1997

[68] JAGADISH SORAB and WILLIAM E VANARSDALE "A Correlation for the

Pressure and Temperature Dependence of Viscosity" Tribology Trans, Vol 34, PT 4, pp 604-610, 1991

[69] T Mamdouh, Ghannam and M Nabil Esmail " Rheological properties of poly(dimethylsiloxane)" Ind Engg Chem Res 1998,Vol 37, pp 1335-1340,1998

[70] J Companik, S Bidstrup,"The viscosity and ion conductivity of polydimethylsiloxane systems 1 Cham length and ion size effects Polymer 1994, 25(22), pp 4823

[71] D Graebling, D Froelich, R Muller, " Viscoelastic properties of polydimethylsiloxane-polyoxyethylene blends in the melt emulsion model" J Rheol 1989, 33(8), pp 1283, 1989

[72] H Allock, F Lampe, " Contemporary polymer chemistry,Prentice-Hall Inc Englewood Cliffs, NJ, 1981

[73] C S Miner, N Dalton (eds),Glycerol, Rheinhold, NewYork, 1953

[74] A Fiechter, " Advances in Biochemical Engmeering/Biotechnology", Published By Spring-Verlag, Berlin, pp 95-97, 1990

[75] Jr Fred W Bill Meyer, " Text Book of Polymer Science", Third Edition, A Wiley Interscience Publication, John Wiley and Sons, New York, 1984

[76] G Moore D Kline, "Properties and Polymers for Engineers, Prentice-Hall Inc Engle Wood Cliffs, 1984

[77] Hand Book of Brook Digital Viscometer, Model DV-1+Version 2 0, Operating Instrumentations, Manual No M/92-021-0593

Publications Arising From the Present Work

1 S A Iqbal, Hashmi, M S J , "High Pressure Viscosity Rheometry Based on Hydrodynamic Principle", Proceedings of the International Conference on Advances in Materials and Processing Technologies (AMPT 98), University Putra Malaysia, Kuala Lampur, Malaysia, August, 1998, eds Hamouda A M S , Sulaiman S and Ahmadun M , Vol II pp 338 -348, 1998

2 S A Iqbal, Hashmi, M S J , "Determination of the Pressure Dependent Viscosity of non-Newtonian Fluid using a New Rheometrical Device", Proceedings of the International Conferences on Advances in Materials and Processing Technologies (AMPT 99) & 16th Annual Conference of the Irish Manufacturing Committee, IMC-16, Dublin City University, Dublin, Ireland, August 1999, eds Hashmi, M S J , and Looney, L ,Vol III pp 1139-1148, 1999

APPENDIX A

Listing of Computer Programme for the analysis based on non-Newtonian Fluid Characterstics

Listing of Computer Programme for the analysis based on non-Newtonian Fluid Characterstics

```
10 DIM P(500),H(50),V(50),A(100),B(100)
20 PRINT "THIS PROGRAMME CALCULATES THEORATICALLY THE MAXIMUM PRESSURE, VISCOSITY, COEFFICIENTS OF VISCOSITY"
30 PRINT
40 AL1= 04  AL2= 01
50 H1= 0008  H2= 0001
60 AVIS=1  PC=5 6E-11
70 V=4
80 V=V+1
90 VEL=V/10
100 PRINT "THE VALUE OF B"
110 INPUT B
120 PRINT "THE VALUE OF A"
130 INPUT A
140 SRT=VEL/H1
150 PSTEP=1000000
160 REM1=1E-9
170 PEX=479613
180 P1=100
190 P1=P1+PSTEP
200 VIS=AVIS+((((P1^2)*(B))+A)/SRT)
210 DP1=PI/AL1
220 POIS1=(4+(PC*(DP1^2)*(H1^2)))/(12*PC)
230 QUET1=(VIS*VEL)/(2*PC*H1)
240 T11=-QUET1+(SQR((POIS1^3)+(QUET1^2)))
250 T12=QUET1+(SQR((POIS1^3)+(QUET1^2)))
260 PHY1=(T11^ 3333)-(T12^ 3333)
270 TC1=PHY1-(DP1*H1* 5)
280Q1=((DP1*(H1^3))/(6*VIS))+(TC1*(H1^2)/(2*VIS))+(VEL*H1)+(PC/VIS))*
(((DP1^3)*(H1^5)/20)+((TC1^3)*(H1^2)/2)+((DP1^2)*(H1^4)*TC1* 25)+( 5*(TC1^2)*
DP1*(H1^3)))
290 DP2=P1/AL2
300 POIS2=(4+(PC*(DP2^2)))/(12*PC)
```

```
310 QUET2=(VIS*VEL)/(2*PC*H2)
320 T21=-QUET2+(SQR((POIS2^3)+(QUET2^2)))
330 T22=QUET2+(SQR((POIS2^3)+(QUET2^2)))
340 PHY2=(T21^ 3333)-(T22^ 3333)
350 TC2=PHY2+(DP2*H2* 5)
360 Q2=-((DP2*(H2^3))/(6*VIS))+(TC2*(H2^2)/(2*VIS))+(VEL*H2)+(PC/VIS)*
(-((DP2^3)*(H2^5)/20)+((TC2^3)*(H2^2)* 5)+((DP2^2)*(H2^4)*TC2* 25)-
( 5*(TC2^2)*DP2*(H2^3)))
370 RES1=Q1-Q2
380 IF (ABS(RES1)<=REM1) THEN GO TO 450
390 IF RES1<0 THEN GO TO 410
400 IF RES1>0 THEN GOTO 190
410 P1=P1-PSTEP
420 PSTEP= PSTEP/10
430 GO TO 190
440 ER=P1-PEX
450 PRINT "VEL=", VEL, "PM=", P1, "TC1=", TC1,"TC2=", TC2, "Q1=",Q1,"Q2=", Q2,
"Q1-Q2=", Q1-Q2
500 END
```

APPENIDX B

SOLUTION OF THE CUBIC EQUATION

In chapter 2, Equation (10) is a cubic equation which can be solved by applying Cardens formula This equation however, is shown to have two imaginary roots and one real root

The cubic equation is of the form,

$$\phi_1^3+3p\phi_1+2q=0$$

Where $3p=A_1$ so that $p=A_1/3$,

And

$2q=B_1$ such that $q=B_1/2$,

The discriminant of the equation $(A_1\text{-}1)$ in the number

$$J_1=-p^3-q^3$$

Substiting the value of p and q in the above equation gives,

$$J_1=-(A_1^{\ 3}/27)-(b_1^{\ 2}/4)$$

According to Carden's formula the real root of equation $(A_2\text{-}1)$ is

$$\phi_1=U_1+V_1$$

Where $U_1 = [-q+ (q^3 + p^3)^{1/2}]^{1/3}$ and $V_1 = [-q-q^2 + p^3)^{1/2}]^{1/3}$

Appendix C

Error Analysis

Comparison of experimental pressure with the theoratical pressure for different values of 'a' and 'b' (Error analysis)

Table C 1: For Glycerine

Speed m/sec	Values of Pressure Coefficients	Gap ratio H_1/H_2	Experimental Pressure (Pex) bar	Theoretical Pressure (Pth) bar	Percentage of error =(Pex-Pth)/Pex
0.5	a = 300 m^2/N b = $4x10^{-11}$ N/m^2	8	2.54	2.07178	15
0.5	a = 150 m^2/N b = $2x10^{-11}$ N/m^2	8	2.54	1.73412	31.7
0.5	a = 600 m^2/N b = $7x10^{-11}$ N/m^2	8	2.54	2.7498	10
1.0	a = 300 m^2/N b = $4x10^{-11}N/m^2$	8	3.58	3.47	3.07
1.0	a = 150 m^2/N b = $2x10^{-11}$ N/m^2	8	3.58	3.133	12.4
1.0	a = 600 m^2/N b = $7x10^{-11}$ N/m^2	8	3.58	4.1593	16.1
1.5	a = 300 m^2/N b = $4x10^{-11}$ N/m^2	8	5.09	4.9	3.7
1.5	a = 150 m^2/N b = $2x10^{-11}$ N/m^2	8	5.09	4.531	10.9
1.5	a = 600 m^2/N b = $7x10^{-11}$ N/m^2	8	5.09	5.57	9.4
0.5	a = 300 m^2/N b = $4x10^{-11}$ N/m^2	5	3.2	3.64	13.75
0.5	a = 150 m^2/N b = $2x10^{-11}$ N/m^2	5	3.2	3.2206	0.63

1 0	a = 300 m^2/N b = 4x10 ^{11} N/m^2	5	6 27	6 46	3 03
1 0	a = 600 m^2/N b = 7x10 ^{11} N/m^2	5	6 27	7 36	17 38
1 5	a = 300 m^2/N b = 4x10 ^{11} N/m^2	5	9 5	9 3	2 11
1 5	a = 300 m^2/N b = 4x10^{-11} N/m^2	5	9 5	10 2	7 36
0 5	a = 300 m^2/N b = 4x10 ^{11} N/m^2	3	4	4 6	15
0 5	a = 150 m^2/N b = 2x10^{-11} N/m^2	3	4	4 24	6
1 0	a = 300 m^2/N b = 4x10 ^{11} N/m^2	3	8 4	8 51	1 3
1 0	a = 600 m^2/N b = 7x10 ^{11} N/m^2	3	8 4	9 29	10 6
1 5	a = 300 m^2/N b = 4x10 ^{11} N/m^2	3	12 9	12 63	2 1
1 5	a = 600 m^2/N b = 7x10 ^{11} N/m^2	3	12 9	13 46	4 34
0 5	a = 100 m^2/N b = 4x10 ^{11} N/m^2	3	4	4	0
0 5	a = 140 m^2/N b = 4x10^{-11} N/m^2	5	3 2	3 2	0
0 5	a = 270 m^2/N b = 4x10 ^{11} N/m^2	8	2 50	2 4	4
1 0	a = 250 m^2/N b = 4x10 ^{11} N/m^2	3	8 4	8 4	0
1 0	a = 230 m^2/N b = 4x10 ^{11} N/m^2	5	6 27	6 27	0
1 0	a = 360 m^2/N b = 4x10 ^{11} N/m^2	8	3 58	3 58	0

1 5	$a = 500\ m^2/N$ $b = 4x10^{11}\ N/m^2$	3	12 9	12 9	0
1 5	$a = 390\ m^2/N$ $b = 4x10^{-11}\ N/m^2$	5	9 5	9 55	
1 5	$a = 430\ m^2/N$ $b = 4x10^{11}\ N/m^2$	8	5 09	5 1	

Results For Glycerine

Speed m/sec	Values of Pressure Coefficients	Gap ratio H_1/H_2	Experimental Pressure (P+h) bar	Theoretical Pressure (p+h) bar	Percentage of error =
0 5	a = 295 m^2/N b = $4x10^{11}$	3	4	4 6	15
0 5	a = 300 m^2/N b = $4x10^{11}$	5	3 2	3 69	13 75
0 5	a = 300 m^2/N b = $4x10^{11}$	8			
1 0	a = 300 m^2/N b = $4x10^{11}$	3	8 4	8 5	1 3
1 0	a = 300 m^2/N b = $4x10^{11}$	5	3 58	6 46	3 03
1 0	a = 300 m^2/N b = $4x10^{11}$	3	12 9	12 53	2 6
1 5	a = 300 m^2/N b = $4x10^{11}$	5	9 5	9 3	2 1
1 5	a = 300 m^2/N b = $4x10^{11}$	8	5 09	4 9	3 7

DATA FOR SILICON 5

Speed m/sec	Values of Pressure Coefficients	Gap ratio H_1/H_2	Experimental Pressure (P+h) bar	Theoretical Pressure (p+h) bar	Percentage of error =
2	a = 5000 m^2/N b = 5x10 ^{11} N/m^2	5	35 83	19 86	44 57
2	a = 8500 m^2/N b = 5x10 ^{11} N/m^2	5	35 83	29 7	17 1
2	a = 4000 m^2/N b = 4x10 ^{11} N/m^2	5	35 83	16 93	52
2	a = 8000 m^2/N b = 4x10 ^{11} N/m^2	5	35 83	28 77	19 70
1 5	a = 7500 m^2/N b = 5x10 ^{11} N/m^2	5	31 69	29 7	2 4
1 5	a = 295 m^2/N b = 5x10 ^{11} N/m^2	3	30 04	29 31	2 4
1 5	a = 7500 m^2/N b = 5x10 ^{11} N/m^2	8	22 05	20 84	5 6
1 0	a = 8000 m^2/N b = 5x10 ^{11} N/m^2	5	26 46	28 31	6 9
1 0	a = 8000 m^2/N b = 5x10 ^{11} N/m^2	3	24 4	26 63	9 1
1 0	a = 295 m^2/N b = 4x10 ^{11} N/m^2	8	18 19	20 57	13

0 5	a = 7500 m^2/N b = 5x10 ^{11} N/m^2	5	18 5	24 1	29 5
0 5	a =7500 m^2/N b = 5x10 ^{11} N/m^2	3	17 5	21 58	23
0 5	a = 7500 m^2/N b = 5x10 ^{11} N/m^2	8	14 47	18 13	25
0 25	a = 7500 m^2/N b = 5x10 ^{11} N/m^2	5	17 1	22 69	31 9
0 25	a = 7500 m^2/N b = 5x10 ^{11} N/m^2	3	15 1	19 63	30
0 25	a = 7500 m^2/N b = 5x10 ^{11} N/m^2	8	12 028	17 45	45
0 25	a = 10,000 m^2/N b = 8x10 ^{11} N/m^2	5	17 1	30 48	78
0 25	a = 10,000 m^2/N b = 8x10 ^{11} N/m^2	3	15 1	25 94	71
0 25	a = 10,000 m^2/N b = 8x10 ^{11} N/m^2	8	12 028	23 19	92
0 5	a = 10,000 m^2/N b = 8x10 ^{11} N/m^2	5	18 6	31 93	71
0 5	a = 10,000 m^2/N b = 8x10 ^{11} N/m^2	3	17 5	27 94	61
0 5	a = 10,000 m^2/N b = 8x10 ^{11} N/m^2	8	14 47	23 80	64
1 0	a = 10,000 m^2/N b = 8x10 ^{11} N/m^2	5	26 46	34 83	31 6

1 0	a = 10,000 m^2/N b = 8x10 ^{11} N/m^2	3	24 4	31 91	30 7
1 0	a = 10,000 m^2/N b = 8x10 ^{11} N/m^2	8	18 19	25 2	38
1 5	a = 10,000 m^2/N b = 8x10 ^{11} N/m^2	5	31 69	37 7	18
1 5	a = 10,000 m^2/N b = 8x10 ^{11} N/m^2	3	30 04	35 84	19 4
1 5	a = 10,000 m^2/N b = 8x10 ^{11} N/m^2	8	22 05	26 56	20
2 0	a = 10,000 m^2/N b = 8x10 ^{11} N/m^2	5	35 89	40 55	12
2 0	a = 10,000 m^2/N b = 8x10 ^{11} N/m^2	3	33 07	39 71	20
2 0	a = 10,000 m^2/N b = 8x10 ^{11} N/m^2	8	26 18	27 89	6 9
2 0	a = 8700 m^2/N b = 5x10 ^{11} N/m^2	5	35 84	35 74	0 27
1 5	a = 8200 m^2/N b = 8x10 ^{11} N/m^2	5	31 69	31 69	0
1 0	a = 7340 m^2/N b = 8x10 ^{11} N/m^2	5	26 97	26 47	0
0 5	a = 6000 m^2/N b = 8x10 ^{11} N/m^2	5	16 44	16 50	0 36